Studies of dynamics and automatic steering systems of combines(Dissertation_全文)

AUTHOR(S):

Ikeda, Yoshio

STUDIES OF DYNAMICS AND AUTOMATIC STEERING SYSTEMS OF COMBINES

YOSHIO IKEDA

KYOTO UNIVERSITY
FACULTY OF AGRICULTURE
APRIL 1975

STUDIES
OF
DYNAMICS AND AUTOMATIC STEERING SYSTEMS
OF
COMBINES

YOSHIO IKEDA

KYOTO UNIVERSITY
FACULTY OF AGRICULTURE
APRIL 1975

TABLE OF CONTENTS

FOREWARD

The mechanization of rice harvesting in Japan had not been done for long time, because of the small-scale and intensive farming.

Since a combine was used tentatively in 1960 for the first time in Japan, many attempts to use the combines in Japanese paddy fields have been made with the purpose of minimum labor requirement and maximum performance. Most of these combines, however, were foreign-made (and in this paper these combines are called the Western-type combines, from now on), and some combines made in Japan were developed and tried to use. When these Western-type combines were used to harvest rice grown in Japan, which is usually more difficult to thresh than rice grown in other countries, the grain losses (unthreshed and damaged grain) were high. In addition, most of these foreign-made combines are too large (about 3 meter or more cutting width) to use in the small individual paddy fields in our country. The attempts to adopt the combines developed in USA and European countries are very significant. On the other hand, considering these peculiarities of rice and fields in Japan, small rice combines (0.5 to 1.2 meter cutting width) were recently investigated and manufactured in our country. These small combines were called self-feeding (or head-feeding) type combines in Japan, because these consisted of Japanes self-feeding (or head-feeding) thresher which threshed only the head of rice plant fed to the thresher by the chain conveyer,

the cutting and travelling assemblies. A feature of the combine of this type is that grain damage and loss are very low.

PURPOSE AND SCOPE OF STUDY

In this paper the characteristics of power distribution and consumption and the dynamic behaviors of the functional elements of the Western-type and head-feeding type combines will be discussed and the difference between these two types of combines be observed. The travelling characteristics of combines such as contact pressure distribution pattern and fluctuation of travelling torque as well as vibration characteristics of the small combines will be also discussed. The automatic steering system of the head-feeding type combine and its response paths to the artificial and actual input row of rice plant will be investigated.And, introducing the mathematical model for the combine and using the digital simulation technique, the applicability of the automatic steering system to the actual paddy field and the reliability of the mathematical model will be considered.

ACKNOWLEDGEMENT

The author wishes to express his gratitude to the guidances and encouragement received from Dr., Prof. Noboru KAWAMURA and Dr., Prof. Ryoichi MATSUDA, and also wishes to express his thanks to the members of his groupe, especially Dr., Prof. Ritsuya YAMASHITA, Kiyoshi NAMIKAWA, Makoto YUKUEDA and Masakazu NAKATANI, who carried out much of the experimental and constructional.

CHAPTER 1

Introduction

The historical reviews of the studies of combine during resent twenty years are given below.

The characteristics of power requirements of each functional element of the combine which harvested wheat and soybeans were discussed by D. E. Burrough[1]. He used two machines for the experiments, one of which was self-propelled and equipped with 8-ft. cutter bar and the threshing cylinder of the flail or rub-bar type. Most of his experiments on this combine were conducted to determine the maximum conditions which the machine would be expected to encounter. The other machine was a pull-type combine, equipped with an auxiliary engine and employed with a rasp-bar cylinder and a 6-ft. cutter bar. The experiments of this combine were conducted to determine the change in power requirement with increasing feed rate.

The power requirements with increasing travelling velocity of four combines of pull-type and a self-propelled combine were studied by C. Dolling[2), 3)]. The combines which were used for the experiments were equipped with 4, 5.5, 7, 6 and 8 ft. cutter bar, respectively, and they harvested rye and wheat. He discussed the tractive forces for the pull-type combines and the fluctuations of power requirements of the engine and the threshing cylinders.

The threshing and separation characteristics of the combine were presented by D. Frenzel[4)]. He displayed the relationships between the header-length and grain loss,

between cylinder speed and threshing loss as well as grain separation ratio, and between concave clearance and the threshing loss as well as grain ratio.

N. A. Lazebnyj discussed the motion of the grain on the combine sieve[5]. According to his discussion, the conditions for the grain motion on the sieve of the travelling combine were determined not only by the kinematic factor, sieve slope and friction between grain and sieve surface, but also by the design date of combine suspension, elastic characteristics of sieve suspension, field profile and travelling velocity of the machine.

N. V. Filatov et al developed increasing grain separation efficiency on the straw sieve[6]. He used for the experiments with separation of chaff and small straw, normal straw sieve of the combine SK-4 and the double-bottom experimental straw sieve.

The statistical characteristics of the threshing force of the combine SK-4 were discussed by Tudel' et al[7].

The discussions of the statistical indices for evaluation, such as an autocorrelation function and power spectral density function, of the combine operation were presented by A. F. Kononenko[8] and A. B. Lur'e et al[9]. A. F. Kononenko reported the normalized autocorrelation functions and power spectral densities of field profile, straw layer thickness and threshing torque. A. B. Lur'e et al reported the above-mentioned functions of the fluctuations of the power requirement, planting density and crop field profile.

The rice combines with the wide threshing cylinder (

width of 1280 mm and 972 mm, respectively) were reported by Z. Undirbaev[10].

In Japan, the experiments of a trially manufactured rice combine were conducted, the functions of elements of the combine were observed and discussed by I. Yokoyama et al[11]. They revealed the threshing and separating characteristics, and measured the power requirement for threshing and operating efficiency in the field.

For a small header combine which had a rotating disc cutter and cut only the head of rice plant and conveyed it pneumatically, power requirements and grain separation characteristics were discussed by S. Umeda et al[12), 13].

The experiments of the Western-type small rice combine which was equipped a 2.3 meter cutter bar and the threshing cylinder of 73 cm width were conducted for harvesting rice by N. Kawamura et al[14), 15]. They reported the power requirements of the functional elements and the dynamic characteristics of the torques. The similar experiments of the Western-type rice combine which was equipped a 1.3 meter cutter bar and the threshing cylinder of 67 cm width were conducted for harvesting rice and barley by H. Ezaki et al[16]. They reported the power requirements of the functional elements of the combine and the statistical characteristics of the fluctuating torque of the threshing cylinder.

For head-feeding type thresher, the power requirements of each functional element and the statistical characteristics of the fluctuating torques of the elements were discussed by N. Kawamura[17), 18] et al.

For the head-feeding type combines, the similar studies as the above-mentioned thresher were conducted by N. Kawamura et al[19] and by H. Ezaki et al[20].

About the travelling performances of the agricultural machinery, there are many papers, and the power requirements of the combines for travelling were discussed in the above-mentioned references.

The pressure distribution patterns under a track-laying vehicle and the forces on the shoes were discussed by I. F. Reed[21], A. P. Sofiyan et al[22] and A. I. Brusencev[23]. However, they were about the track-type tractors upon which the traction or propulsion forces acted.

N. Kawamura et al studied the pressure distribution patterns under the track-type small rice combine on the paddy fields[15), 19]. Y. Yasuda et al also discussed the pressure distribution patterns under the track-type combine on sand[24]. They determined the pressure distribution pattern theoretically and confirmed experimentally using soil pressure transducers buried in sand.

Many studies of vibration of agricultural machinery were conducted and W. Sönne displayed the statistical method for vibration analysis of agricultural machinery and discussed the vibration characteristics of the tractor[25]. On vibratin of combine, Ju. V. Grin'kov discussed the influence of the operation of the functional elements to vibration of the combine SK-4 and isolation of vibration[26]. For the Western-type small rice combine, the vibration characterictics were discussed in connection with the fluctuation of the travelling

torque by N. Kawamura et al[15]. L. M. Grosev discussed the random vibration of combine under operation and obtained the correlation functions and power spectral densities of the road and field profiles and the acceleration of the frame on the steering axle of the combine SK-4, and the change in root mean square deviation with the combine velocity[27]. For the head-feeding type combine, the vibration characteristics were studied by N. Kawamura et al[19].

The automatic steering system for the tractor was reported by L. A. Liljedahl et al[28], M. A. Gravum et al[29], Lal. N. Shukla et al[30], A. P. Julian[31], M. G. R. Warner et al[32] and M. B. Widden et al[33]. Many methods for detecting the input and automatic steering system were given in these papers. R. L. Parish et al experimented the automatic steering system of the windrower with hydro-static transmissions[34] and discussed the tracking accuracy by means of the experiments and digital simulation techniques[35]. For the head-feeding type small rice combine, the experiments and digital simulation of the automatic steering system were conducted by N. Kawamura et al[36),37),38),39] and by Y. Yasuda et al[40].

CHAPTER 2

Power Distribution Characteristics of the Individual Functional Element of the Combine

2-1 Power Distribution of the Western-type Small Rice Combine*

Because a combine has cutting, threshing, conveying, separating, cleaning and travelling functions at the same time, its power transmission system is very complicated. So, it is necessary for the future improvement to make clear the characteristics of the torque at each element and the power distribution to each element.

In Europe and America, for the combines used to harvest wheat, barley, rye and soybean their power requirements of the functional elements had been measured and their characteristics had been discussed[1), 2), 3)]. In Japan, however, the characteristics of the torques and the power distribution of a half-tracked combine for harvesting rice plant had not yet been measured and discussed.

Some experiments were conducted with a Western-type small rice combine manufactured in Japan which had spike-tooth threshing cylinder and concave for threshing rice and of which travelling device was full-tracked. And the torques as well as rotating speeds of its main functional elements were measured under some different operating conditions. Namely, for the records of the torques obtained under each operating condition, their average values were measured and the relationships between the operating conditions and average power requirements were discussed.

2-1-1 Principal Description of the Experiments

The principal specifications of the combine used for the experiments are given in Table 2-1.

Table 2-1 Specifications of Experimented Combine

Type of Combine	Full-tracked and Self-propelled Small Rice Combine
Engine	Water-cooled Gasoline Engine with Four Cylinders
Rated Power	35 PS / 2100 rpm
Maximum Power	40 PS / 2100 rpm
Cutting Device	Reciprocating Cutter Bar
Frequency	400 cpm
Stroke	75 mm
Threshing Device	Spike-tooth Cylinder and Concave
	Variable-speed V-belt Drive
Cylinder width	730 mm
Cylinder Diameter	540 mm
Cylinder Speed	700 - 1000 rpm
Concave Width	725 mm
Concave Clearance	3 - 25 mm
Travelling Device	Variable-speed V-belt Drive
Forward	1st 0.208 - 0.416 m/sec
	2nd 0.398 - 0.796 m/sec
	3rd 0.800 - 1.600 m/sec
Reverse	0.346 - 0.692 m/sec
Tare	4200 kg
Contact area under Track	2.00×10^4 cm^2
Average Value of Ground Contact Pressure	0.21 kg/cm^2

The power transmission system of this combine is shown in Fig. 2-1. The engine power was transmitted with V-belts and pulleys to the threshing cylinder, travelling

shaft, chain conveyor and other shafts through the cylinder beater.

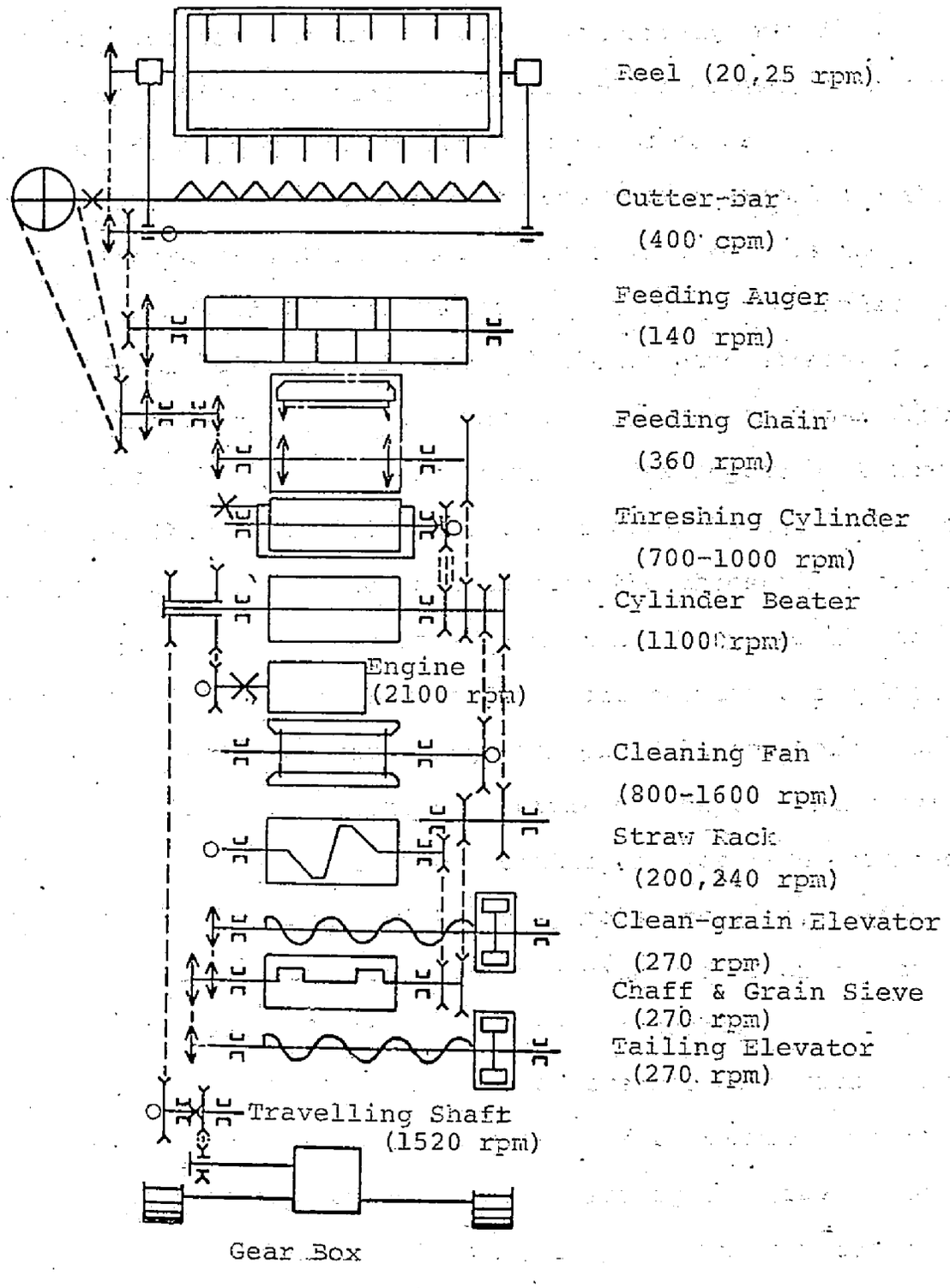

Fig. 2-1 Power Transmission System of the Small Rice Combine used for the Experiments

The variable-speed V-belts were used between the cylinder beater and the threshing cylinder as well as the travelling shaft and the gear box input shaft for changing travelling speed steplessly. The latter variable V-belt transmission device could be adjusted by the operator on the combine.

The elements of which torques were measured are shown in this figure with X's symbols, that is, the torques and rotating speeds of (1) the engine, (2) threshing cylinder shaft, (3) travelling shaft and (4) the bending strain of the bell crank driving the cutter bar and (5) the torsional force of the wheel shaft of the worm gear box for adjusting concave clearance. This torsional force was produced by the force which was transmitted to the concave through the threshed straws by the spike-teeth of the cylinder and varied most rapidly and accurately with change in rice flow rate between the cylinder and concave, although the change in the cylinder torque was affected by the mass moment of inertia of the threshing cylinder.

The elements of which rotating speeds were measured are shown in this figure with O's symbols, that is, besides the above-mentioned elements the rotating speeds of the cylinder beater, fan, reel and straw rack were measured.

The higher rotating speeds were measured with cutting a magnetic field and the lower speeds, for example, speeds of reel, straw rack and the drum for measuring the travelling velocity, were measured with cut-off of the microswitches.

The travelling velocity was measured as follows. A rotating drum, on which the nylon thread was wound, was fixed on the experimented combine. When the end of this thread was

fixed on the ground, then this drum was rotated at the speed proportional to the travelling velocity of the combine harvesting rice plant. In this experiment this rotational speed was recorded.

The experiments were conducted on October 20 th to 23rd, 1965 at the east reclaimed land of the lake of Biwa-ko and neighboring fields. The experimental conditions are shown in Table 2-2. The variable parameters of the experiment were variety of rice plant, travelling velocity and cutter bar height and cutting width. The concave clearance was adjusted to the optimum conditions and kept almost constant during all the experiments.

The torques recorded as time functions were fluctuated by the various factors. The characteristics of these fluctuating torques were discussed with the techniques as follows. In order to find the relationships between the operating conditions and the average values of the torques, the mean values of the fluctuating torques were taken. By this method, the relationships between the operating conditions (especially, feed rates of paddy and/or straw) and the average power requirements of the functional elements of the combine could be found, but the characteristics such as amplitude and frequency distributions of the torques which fluctuated with time by the other than operating conditions could not be found. These dynamic characteristics of the fluctuating torques of the functional elements of the Western-type combine will be discussed in CHAPTER 3.

Table 2-2 Experimental Condition

		1	2	3	4	5	6	7
Travelling Speed	(m/sec)	0.188	0.278	0.321	0.264	0.253	0.192	0.191
Cutter-bar Height	(cm)	9-11	10-11	9-10	8-9	20-21	7-35(16*)	
Cutting Width	(row)	9	10	10	7	10	230cm	180cm
Feed Rate of Paddy	(kg/min)	15.5	24.0	26.5	15.3	21.2		
Feed Rate of Straw	(kg/min)	34.1	53.1	58.6	33.6	37.4		
Total Feed Rate	(kg/min)	49.6	77.1	85.1	48.9	58.6	59.8	41.3
Cylinder Speed	(rpm)	793	772	744	737	740	773	797
Concave Clearance	(mm)	5.5					5.0	
Variety of rice		SATIKAZE					MANRYO	
Height of Rice Plant	(cm)	95.9					129.0	
Growing State of Rice Plant		Standing at 62 deg.					Perfectly Lodged	
Planting Method of Rice Plant		Transplanting (328 stalks/m^2)					Aerial Sowing With a Copter	
Paddy Weight	(g/m^2)	670**					610(510***, 97****)	
Paddy-straw Ratio	(%)	27.8					29.4	
Moist.Cont. of Paddy	(%)	19.4 (D.B.)					26.1 (D.B.)	
Moist.Cont. of Straw	(%)	68.4 (D.B.)					69.9 (D.B.)	
Moist.Cont. of Soil	(%)	29.1 (D.B.)					29.6 (D.B.)	

* Average Value

** Moist.Cont. were 14 %.

*** Paddy Weight

**** Unriped Grain Weight

2-1-2 Experimental Results and Their Discussions

a) Operating Performances

The operating performances were measured for Test 1, 2, 3 and 7, and the results are shown in Table 2-3.

Table 2-3 Operating Performances

Test No.		1	2	3	7
Rate of Net Yield of Grain	(%)	95.5	85.9	90.5	80.0
Specifications of Losses					
Header Loss	(%)	0.1	0.1	0.1	0.1
Cylinder Loss	(%)	2.1	3.3	2.2	12.7
Free Seed Over Rack	(%)	2.1	10.0	7.0	5.5
Free Seed Over Chaffer Sieve	(%)	0.2	0.7	0.2	1.7
Total loss	(%)	4.5	14.1	9.5	20.0

The total losses in Tests 2 and 3 were larger than the other tests, this was due to many separating loss(the grain lost out the rear of the combine in the form of threshed grain), the ratios of which were 10.0 and 7.0 percent, respectively. Besides, these higher losses might be due to insufficient adjustment of the threshing element and the errors of measurement. In Test 7, rice plant was perfectly lodged and therefore grain losses increased. The greater parts of these losses were cylinder loss (un-threshed grain) of 12.7 percent and separating loss of 5.5 percent. According to yield test per unit area at Test 7, unripened grains were 16.0 percent, therefore threshing was difficult and un-threshed

grains incresed.

b) Power Distrbutions to the Functional Elements and Their Power Requirements

As shown in Fig. 2-2, the torque of the threshing

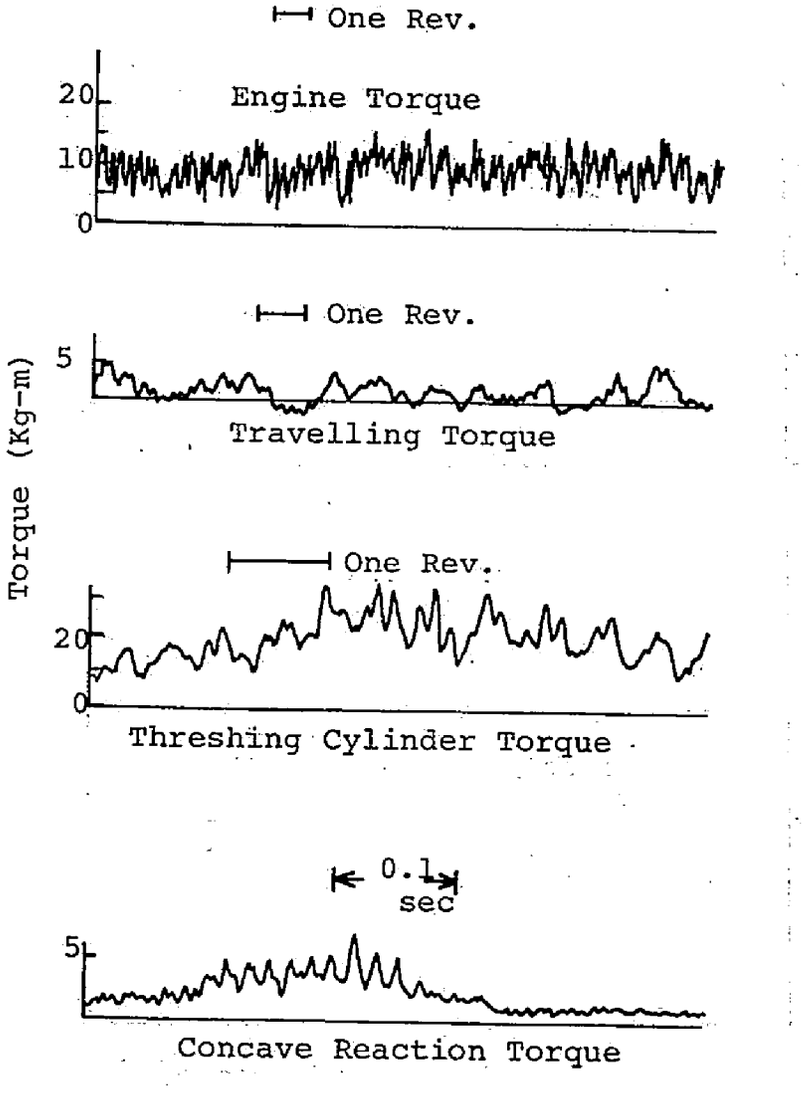

Fig. 2-2 Oscillogram Trace in Test 3

elements of the combine fluctuated with time as the same manner as the fluctuation in the force of the concave from the cylinder. This phenomenon was due to the uneven flow of rice which was fed into the threshing device. The power

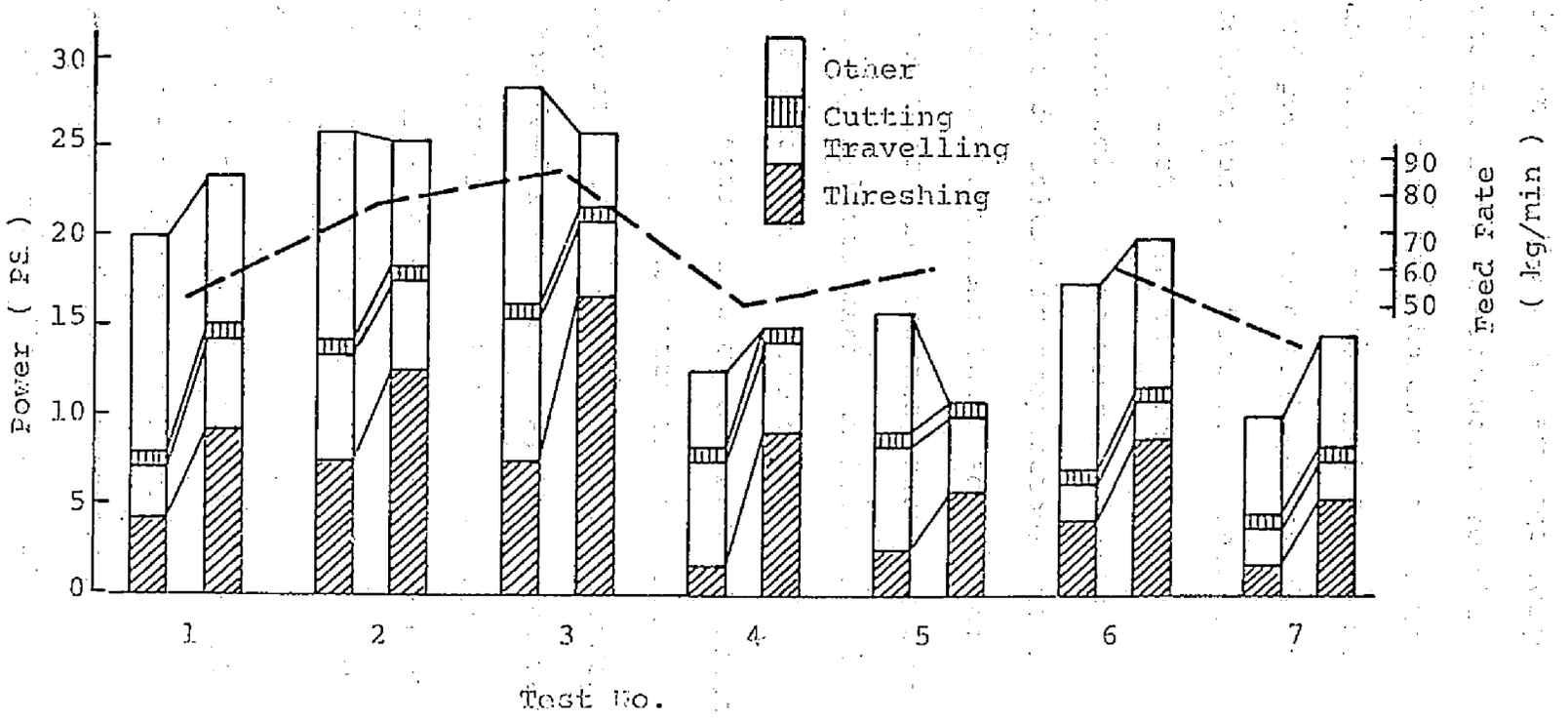

Fig. 2-3 Power Distribution and Requirement

distributions to each functional element were discussed with regard to this fluctuation in rice flow. The average torques and rotating speeds of the elements corresponding to the interval of the increased and decreased concave forces in such a length as shown in Fig. 2-2 were measured from oscillogram charts and averaged powers were calculated as shown in Fig. 2-3. The right column for each test represents the average power requirement of each element when the concave force increased and the left column when decreased, respectively. The whole area of each column is proportional to the engine power. The broken lines represent the feed rate of rice plant (kg/min), from which the average power requirements of combine were closely related with the feed rate of rice plant. Furthermore, the followings were concluded.

i) The average power of the engine in each experiment varied from 13.5 to 26.5 according to the feed rate of rice plant. Especially, the power requirements of the threshing cylinder were closely related to the feed rate, that is, the power was 2 to 9 PS (4.7 PS on the average) when the feed rate was 49 kg/min, and 7 to 16 PS (11.6 PS on the average) when the feed rate was 85.1 kg/min. According to Burrough[1)], for the similar operating efficiency as Test 4 (feed rate of 33.6 kg/min) the power requirement of the threshing cylinder of the combine, which had a rasp-bar cylinder and harvested wheats and soy-beans, were 4.1 and 6.0 PS, respectively.

The relations between the feed rate and average threshing power are shown in Fig. 2-4. In this figure, A and B represent the relations between the power and the feed

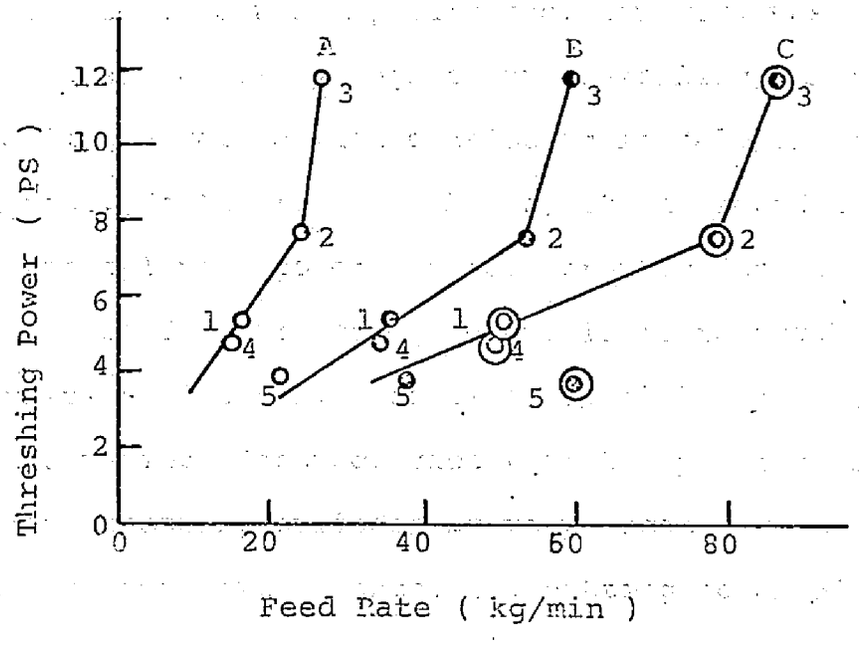

Fig. 2-4 Relations between Feed Rate and Threshing Power

rate of grain and straw, respectively. And C represents the relation between the power and the total feed rate of grain and straw. In Test 5, the extra values of the threshing powers were obtained because the cutting height was higher than others by 20 cm.

ii) In our experiments, the ratio of the average power of the cylinder to the average power of the engine was 34.8 percent in Test 4, 43.8 percent in Test 3 and 27.9 percent in Test 7. And the range of the varying ratios of the powers of the cylinder were from 14 to 60, 25.4 to 60 and 15.3 to 36.6 percent, respectively. According to Burrough[1)], for harvesting wheats at the straw feed rate of 33.6 kg/min the ratio of the cylinder power 45.5 percent, and according to Kanafojski[4)] it was 28 percent for a self-propelled combine with a rasp-bar cylinder harvesting wheats at the travelling velocity of 1.25 m/sec and the feed rate of 138 kg/min.

The combine used by Burrough, however, was a pull-type and had an auxiliary engine for travelling, therefore the travelling power was not considered in calculating power distributions. In the final analysis, it was found that the ratio of the cylinder power was much greater for harvesting rice plant than for harvesting wheat. It is remarkable characteristics of the rice combine especially used to harvest the variety Japonica rice that the power requirement of the threshing cylinder is very great.

iii) During every experiments, the cutting power did not change so much and their values were not greater than 1 PS. In harvesting wheat, they were about 1 PS according to Burrough[1)]. Therefore, so far as the cutting power there was not great difference between rice and wheats.

iv) It owed to the very low travelling velocities of 0.19 to 0.32 m/sec that the average travelling powers of the full-tracked combine were low, of 4 to 8 PS. It is very difficult to run faster than these velocities in Japanese rice field, because of the large feed rate of rice, and high moisture content of straw and grain. And their ratios to the average powers of the engine were low, that is, their values were 19 percent in Test 1 and 22.6 percent in Test 3, respectively. It had been also reported by Kanafojski that the ratio of the travelling power to the engine power of a wheel-type combine was 42 percent. This high percentage, however, might be due to the high travelling velocity (about 1.25 m/sec) of this combine.

2-2 Power Distribution of the Self-feeding Type Thresher**

The small combine of self-feeding (or head-feeding) type thresher is constructed with mounting the head-feeding thresher used in Japan to the small combine frame with the cutting, conveying and travelling devices. Because this type of combine threshes only the head fed into the threshing elements, it is of small size, light weight, low price and good operating performance to rice plant in Japan, then it may be suitable for the Japanese agricultural pursuits.

The function of the head-feeding type thresher has been reported by Shozi et al.[5),6)] In order to make clear the function of each element of the small combine with head-feeding type thresher, the power requirements of the elements of this type of thresher were measured and in this section the characteristics of the load at the elements due to the change in the feeding mode, feed rate and moisture content were discussed.

2-2-1 Principal Description of the Experiments

To drive the experimented thresher at constant velocity, the induction motor which had ample power 10 PS was used. In Fig.2-5 the schematic diagram of the power transmission system of the experimented thresher is shown. Power was transmitted with the V-belts to each element, except the feed chain conveyer which restrained straw and fed it parallel to the cylinder axis was driven with the worm and worm gear through the threshing cylinder shaft.

The shafts of which torques were measured are shown in this figure with O'symbols and the shafts of which rotating speeds

were measured are shown with X's symbols.

In order to find the relative position of the binded sheaf fed to the cylinder, the displacements of the plates which pressed the sheaf under the chain conveyer were recorded on the oscillograph.

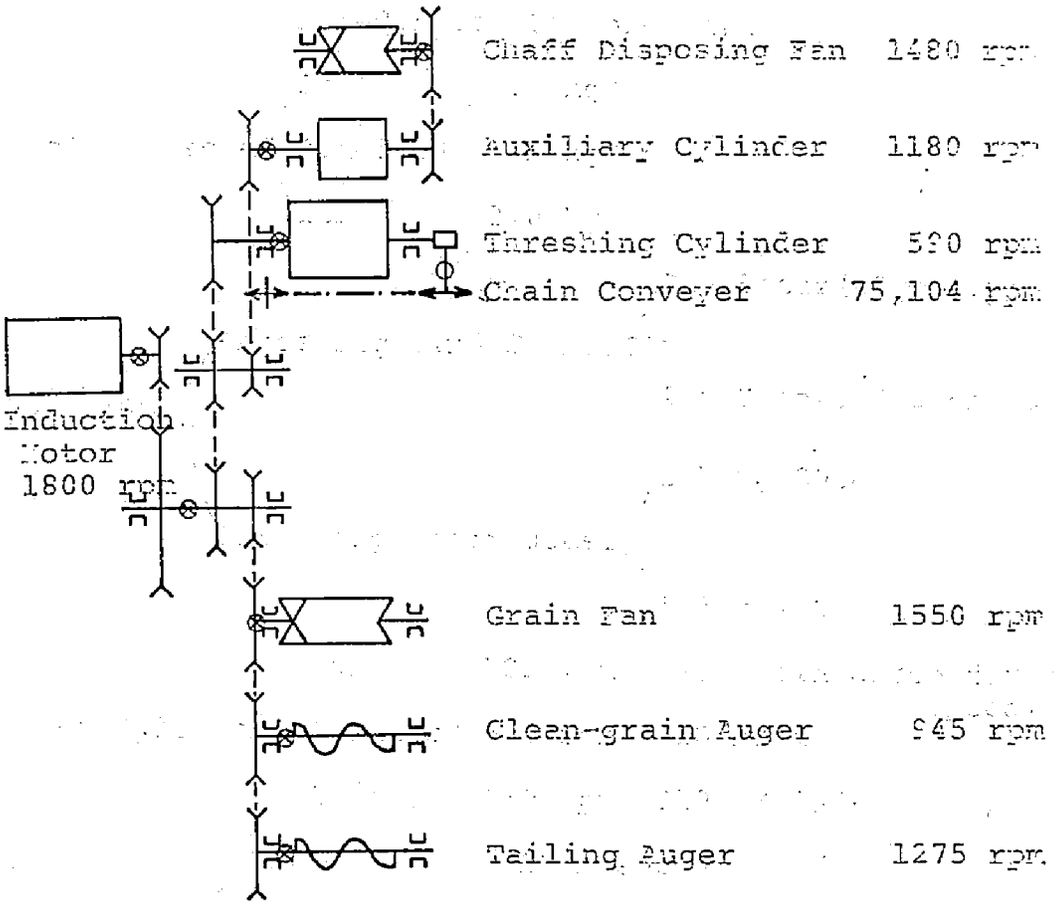

Fig. 2-5 Schematic Diagram of Power Transmission System of Experimented Thresher

The stational head-feeding thresher is originally designed for threshing the binded dried rice intermittently, but by the small combine it threshes green rice continuously. Then the experiments were produced to find the differences of the responses of the thresher due to these various feeding modes and rice conditions. The variables of the experiments were the moisture

contents of rice, sizes of sheaves, feeding mode and rotating speeds of the threshing cylinder. These experimental conditions are tabulated as follows.

1) Moisture Content
   - Green Rice (just after reaping)
   - Dried Rice (for one week)

2) Size of one sheaf
   - Small 1.0 kg*
   - Standard 1.5 kg*
   - Large 2.0 kg*

3) Feeding Mode
   - Threshing Binded Sheaf**
     - One Sheaf (80 cm interval)***
     - Two Sheaves (40 cm ")***
   - Threshing Continuously
     - 1.5 kg/80cm
     - 1.5 kg/40cm

4) Speed of Cylinder
   - Low 520 rpm 710 m/min (circumferential speed)
   - Standard 590 rpm 810 m/min (")
   - High 660 rpm 910 m/min (")

5) Feeding Speed
   - Low 0.22 m/sec
   - High 0.30 m/min

* These weights of one-sheaf were measured just after reaping and those of dried are shown in Table 2-4.

** The size of one-sheaf was standard.

*** The width of the threshing cylinder was about 53 cm.

In Table 2-4, the conditions of the rice used for experiments are shown.

The methods of feeding rice plant are as follows.

Table 2-4 Conditions of Rice

Variety of Rice		NAKATE-SHIN-SENBON		
Plant Height (cm)		86.7		
Length of Panicle (cm)		19.7		
Moisture Content of Rice and Grain-straw Ratio		Green	Dried	
Moisture Content (%)	Straw	71.3	34.5	
	Grain	24.0	15.9	
Grain-straw Ratio		33.5	43.5	
Size of One-sheaf		Small	Standard	Large
Weight of One-sheaf (kg)	Green	1.0	1.5	2.0
	Dried	0.57	0.85	1.13
Diameter of One-sheaf (cm)	Green	8.8	11.1	12.8
	Dried	8.1	9.7	11.0

When the binded sheaf was threshed, in order to keep the distance between each sheaf, the straws near the roots were fixed by two iron holding-bars. For threshing with continuous feeding, 1.5 kg of rice plant was distributed uniformly and fixed in each 80 cm or 40 cm distance on above-mentioned holding-bars. Thus, this feeding mode was similar to the feeding mode of the small combine with the head-feeding type thresher. The total feed rate corresponding feeding one-sheaf of 1.5 kg at speeds of 220 mm/sec and 300 mm/sec were corresponding to 49.5 kg/min and 67.5 kg/min (16.6 kg/min and 22.6 kg/min calculated in terms of rough rice weight, grain-straw ratio was 1:2), respectively. The ordinary feed rate of the small rice combine with the head-feeding type thresher is

about 30 kg/min and that of the head-feeding thresher is about 35 - 50 kg/min.

2-2-2 Experimental Results and their Discussions

a) Operating Performances

The operating performances of the thresher were fairly superior. In Table 2-5 the cleaning performances of the thresher at fine grain outlet for various speeds of the cylinder are shown. As the speed increased, mixing of straw and unripened

Table 2-5 Unripened Grain and Straw Contents in Fine Grain Outlet

Cylinder Speed (rpm)		520	590	660
Ratios of Unripened Grain and Straw* (%)	Green	2.6	1.6	1.2
	Dried	1.7	1.1	0.9

* At the grain outlet

grain in fine grain decreased. The husked grains which were damaged by threshing were merely found at higher speed, but not found at standard and lower speeds.

b) Distribution of the Power to Each Element and Its Change due to the Various Feeding Mode

In order to improve the operating performances of the combine, it may be useful to find the power requirements at each element of the head-feeding thresher. Especially, to control the combine automatically, it is necessary to study the smoothed wave form of the fluctuating torque to identify the input characteristics. The power requirements of the main elements and the change in power requirements due to the feeding mode are as follows. For continuous feeding, the smoothed torque at the cylinder, did not fluctuate so much. For threshing the binded sheaf,

however, the smoothed torque changed according to the relative position of the sheaf to the threshing cylinder. Therefore the average torque of the cylinder was calculated in the interval where the torque was relatively large and constant. In Fig. 2-6, the power requirements of each element for threshing the binded green-sheaf are shown. The average torques were calculated from the frequency distribution curves of the fluctuating torque oscillograms.

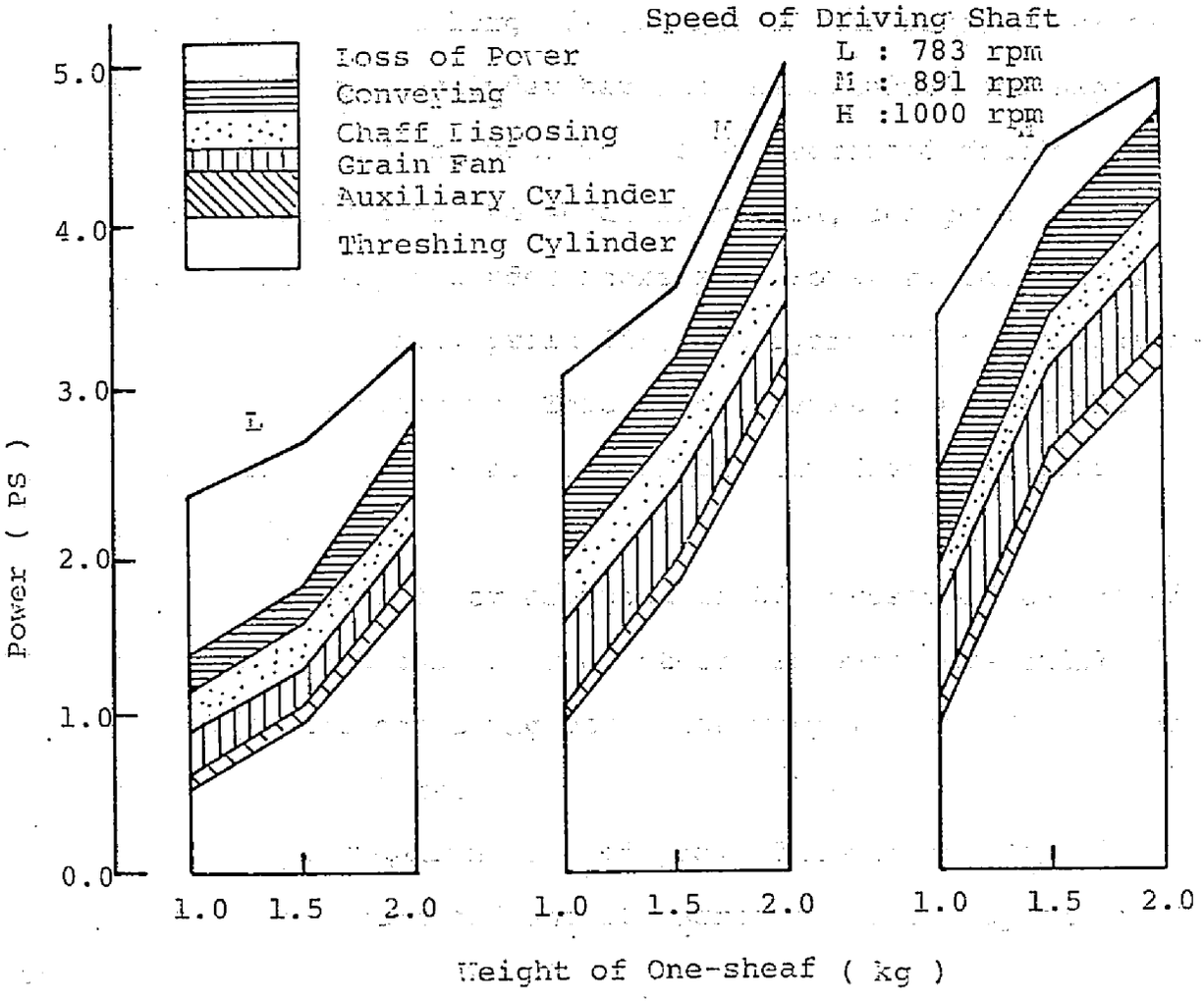

Fig. 2-6 Power Requirements of the Head-feeding Thresher for Feeding One-sheaf just after Reaping

These figures show the relations between the power requirements and the weights of one-sheaf for three different speeds of the driving counter shaft. The power of the conveyer was given with the sum of the powers of the chain conveyer and augers, because these powers were small.

i) Threshing of the binded green sheaf

The total power requirements depended mainly upon the power requirements of the threshing cylinder and the lost power was relatively large. The results are concluded as follows.

There was not a large difference of the power requirements of the threshing cylinder between the standard and high speeds. But for the lower speed the power decreased fairly.

As the weight of the sheaf increased, the power requirements of the threshing cylinder increased. However, the powers of the auxiliary cylinder, grain fan, conveyers and chaff disposing fan were almost constant. This might result from that the grain did not flow so much because of the low feed rate like binded one-sheaf.

The threshing power amonnted to 60 percent of the total power requirement but the power of other elements were fairly low. Especially, the conveying power was very low because of the low speed and low feed rate.

The power requirements of grain fan did not depend upon the weight of the sheaf and it increased as the speed increased.

The power loss showed the high percentage. Especially, it showed the very large value and amounted to 1 PS (40 percent of the total power requirement). This might result

from the complicated power transmission system with many V-belts. Furthermore this might occur because the diameter of the pulley of the prime mover was so small that the slip occured between the V-belt and pulley. But, as the weight of the binded sheaf was increased, the power loss decreased. This phenomena might result from the increase of the wedge action due to the high tension of the V-belt which occured with the increase of the load. These high values of the lost powers could no be disregarded from the point of view of effective utilization of the engine power. For the combine, espesially, the power transmission may be more complicated, so the power loss may increase. Therefore, the effective power transmission system must be studied.

ii) Threshing of the binded dried sheaf

The power requirements of each element of the thresher for the similar feeding mode of the binded dried sheaf as green sheaf are shown in Fig.2-7.

From these figures the following results were obtained.

For the dried sheaf, the total power requirements were lower than for the green, and the maximum difference of the power between the green and dried was 1.8 PS. This shows that it was easier to thresh the dried than the green.

The power requirements of the threshing cylinder were half of those for the green sheaf and the maximum value of them was about 1.6 PS.

The powers of the grain fan, conveyers and chaff-disposing fan showed the higher ratio for the threshing power than for the green rice. This might result from that the flow

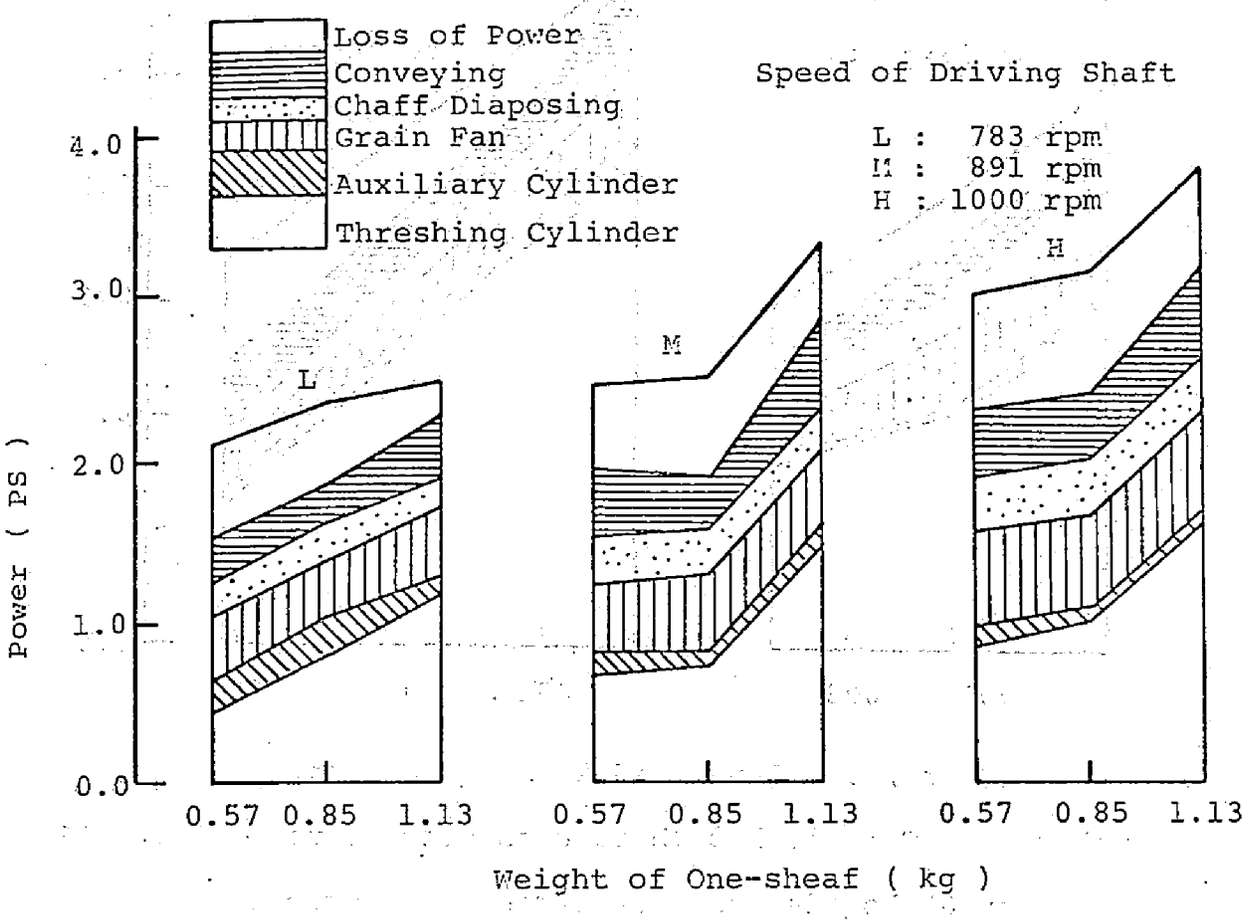

Fig. 2-7 Power Requirements of the Head-feeding Thresher for Feeding One-sheaf Dried for one week

rate to the conveyer increased because of easy thresh of the dried rice and speeds of fan did not so decrease as for the green rice.

iii) Threshing of the two sheaves at interval of 40 cm and Continuously

Fig. 2-8 shows the relationships between the power requirements of the elements and the speeds for threshing two sheaves at interval of 40 cm and for threshing continuously with feed rate of 1.5 kg/40 cm. For these

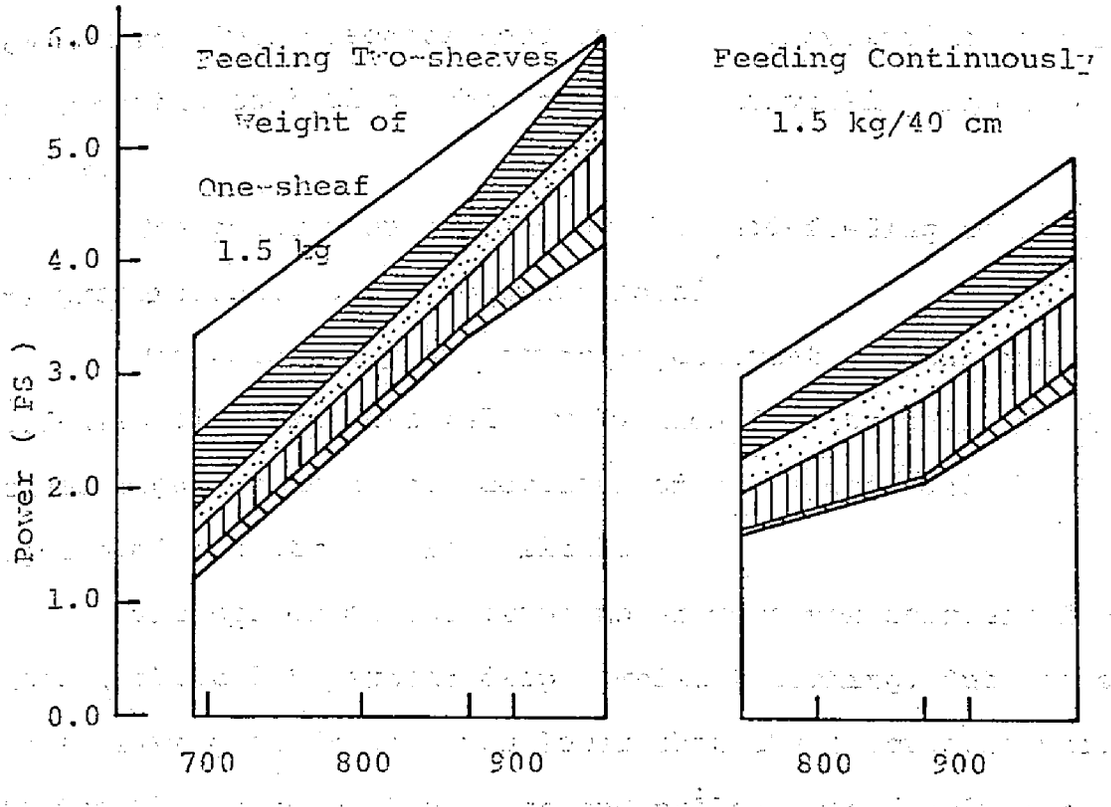

Fig. 2-8 Power Requirements of Head-feeding Thresher for Feeding Two-sheaves at Intervals of 40 cm and Feeding Continuously

two cases, the feed rate of rice plant were equal and 40 kg/min, therefore these experiments might be appropriate for the experiment which was produced to simulate the response of the combine with the head-feeding thresher.

Although the feed rate of rice for these two different feeding mode were equal, the power requirement for continuous feeding was fairly lower than for threshung two-sheaves. The power requirement of the threshing cylinder for continuous threshing was less than for threshing binded sheaves by 1.2 PS at maximum(equivalent to 30 percent). This shows that the power requirement of the combine may increase if the discontinuous

feed occurs. Such discontinuous feed may be avoided by means of the automatic control of the feeding or travelling speed of the combine.

The power requirements of the head-feeding thresher were proportional to the rotating speed.

The reason why the power requirements of the grain and chaff-disposing fan were relatively high for threshing binded sheaves might be that the decreases of the speeds and the clogging of the straw were a little.

The speeds of the prime mover were not scarcely decreased (about 0.8 percent drop) while threshing. But the speed of the driving shaft was much lower than the calculated value, thus the slip between the belts and pulleys was fairly large. For threshing binded two-sheaves, when the diameter of the pulley was small, the power loss reached to 0.8 PS (this was equivalent to 26 percent of the total power requirement). The power loss might occur also because the ineffective work such as acceleration of the elements of the thresher, which resulted from the great changes of the speeds of the threshing cylinder due to the discontinuous feeding by the binded sheaves and the transportation time lag of the load torque, were done and the transmission losses with acceleration and deceleration were great. On the other hand, for feeding continuously, the changes of the speeds of the elements were small, then the power loss was lower.

c) Changes in the Power Requirements due to the Feed Rate and Moisture Content

i) The relations between the power requirements and the feed rate

For feeding continuously, the feed rate of rice was

varied with changing the speed of the chain conveyer. The changes in the power requirement of the threshing cylinder due to the change in the feed rate in this case are shown in Fig.2-9, with

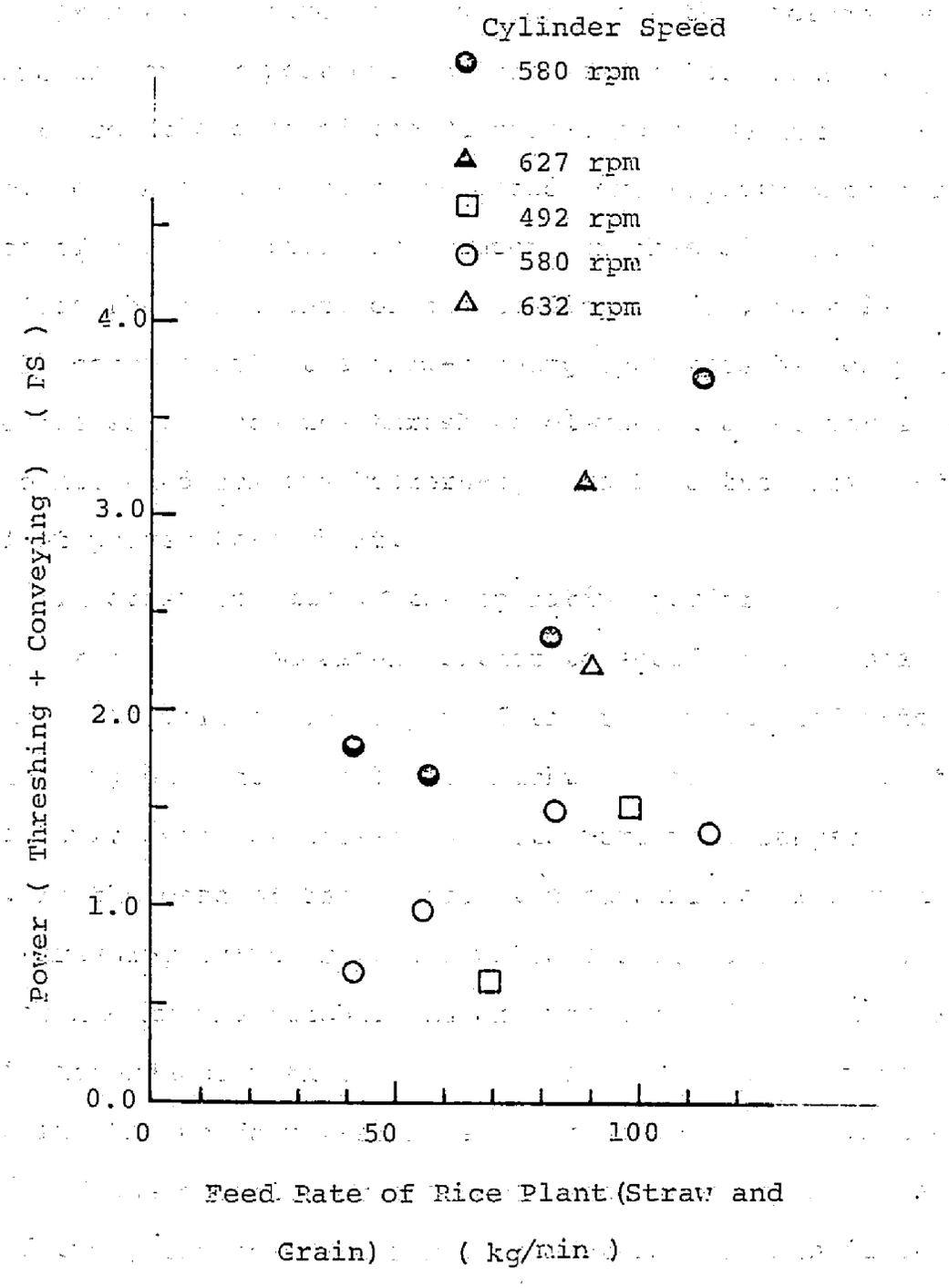

Fig. 2-9 Power Requirements of Threshing Cylinder and Chain Convever

the moisture contents and the speeds as the parameters. In this figure, however, the feed rate for the dried rice was converted into that for the green rice.

From this figure, it was found that the average power requirements were proportional to the feed rates. This was different from the case of the Western-type small rice combine, for which the power increased more rapidly with the increase of the feed rate. The reason for this difference might result from the difference of the feeding method, that is, for the small combine with the head-feeding type thresher only the panicle passed through the threshing element and was threshed, on the other hand for the Western-type combine the entire of rice plant passed through it.

In order to increase the operating performances of the combine, it might be necessary either to speed up the chain conveyer or to thicken the layer of the rice plant fed into the threshing element. The latter might be possible within the certain limit when the threshing teeth were made longer or higher. In the case of the former, the circumferential speed of the threshing cylinder was limited and it would be necessary to research the pitches and arrangements of the threshing teeth in accordance with the speed-up of the chain conveyer. Controlling the uniform feed rate might be possible with the speed-up of the cylinder or chain conveyer, but in the case of the former, the power requirement increased as mentioned above.

ii) The relations of the power requirements to the moisture content, weight of the sheaf and the rotating speed

For threshing binded one-sheaf, the dependence of the power requirements upon the rotating speed of the threshing cylinder and the weight of binded one-sheaf in the case where as parameters the weight of the sheaf and the cylinder speed were taken are shown in Fig. 2-10 (a) and (b), respectively.

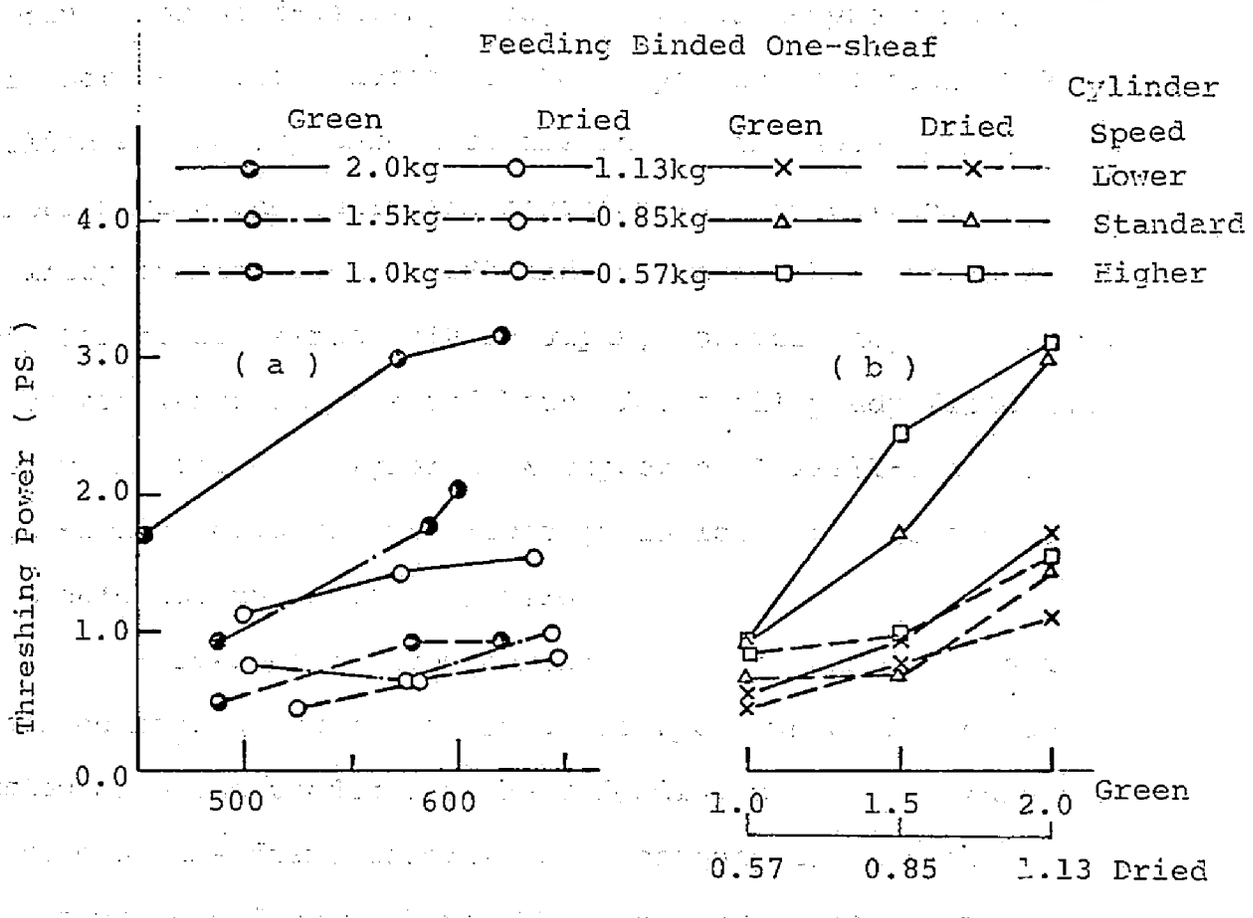

Fig. 2-10 Variations of Threshing Power with (a) cylinder Speed and (b) Moisture Content of Rice

The ratio of the change in the average power requirement for threshing green rice to the cylinder speed was greater than that for the dried rice (Fig. 2-10 (a)) .

The influence of the weight of the sheaf for the green rice to the power requirement was greater than that for the dried.

2-3 Power Distribution of the Head-feeding Type Small Rice Combine***

Rice has been harvested in Japan mainly with hand sickle and threshed with stationary thresher, so called head-feeding or self-feeding type, and Western-type combine thresher was seldom accepted. Nowadays, approximately 3.2 million stationary threshers are in use in Japan. For the labour saving and full mechanization in rice cultivation, ordinary combine used in USA and Europe has been introduced only for trials since 1960 in Japan, however they were found to be too large in size and heavy for small paddy field and its grain loss was higher than expected. A small-sized and light-weight combine with lower grain loss is, therefore, desirable for the Japanese field conditions.

Head-feeding type combine (Jidatsu combine) is a small combine thresher of Japanese type, which is constructed with the traditional head-feeding type power thresher mounted on the frame together with components of transporting, cutting and travelling. There are two types, namely walking type and riding type. Main construction of these combines are as follows (Fig.2-11): the cutting device is ordinary reciprocating cutter bar of 50 cm width for two rows. The pick-up tine instead of the reel is used to pick up lodged crops. To convey the crop to the thresher, lifting and transporting chain conveyer are used, which convey not only straw without disturbing the head and straw, but also change the position of straw to horizontal movement

ready for feeding into the cylinder.

Head-feeding type thresher is an axial flow type thresher, of which feeding chain conveyer parallel to the cylinder axis constrains the lower part of straw and conveys straw in such a way that the head part is fed into the threshing chamber between the cylinder and the concave of crimp screen. The threshing tooth is ordinary inverted V-shaped steel wire. The cleaning device is the oscillating sieve with suction fan or a winnower.

These combines have following advantages; power consumption is low and the size of cleaning device is smaller and its working mechanism is simpler, because the main part of straw does not pass through the threshing part. Ordinary grain loss of these combines is less than 3.5 %, damaged grain 2.1 % and straw mixed in grain 1.5 % respectively. Ordinary combine with 1.5 m cutting width has in rice harvesting 5.2 % grain loss, 3.5 % damaged grain and 3.0 % straw mixed in grain, respectively. On the contrary, if the size of combine becomes large, thickness of straw becomes excessively thick to thresh the head and to convey the straw. The capacity of combine is, therefore, limited under 1 to 1.5 m cutting width.

Rice combine has ordinary track-shoes covered with thick rubber under 0.2 kg/cm^2 ground contact pressure to make it enable to travel over soft paddy field. And also the endless track should be used. The head-feeding type combine may be assumed to have a different power consumption characte-

ristics from ordinary combine. Therefore, it is necessary to obtain the informations on the operating performances, power requirements and the power distribution pattern of the individual component of the small rice combine for the design and further improvement of the machine.

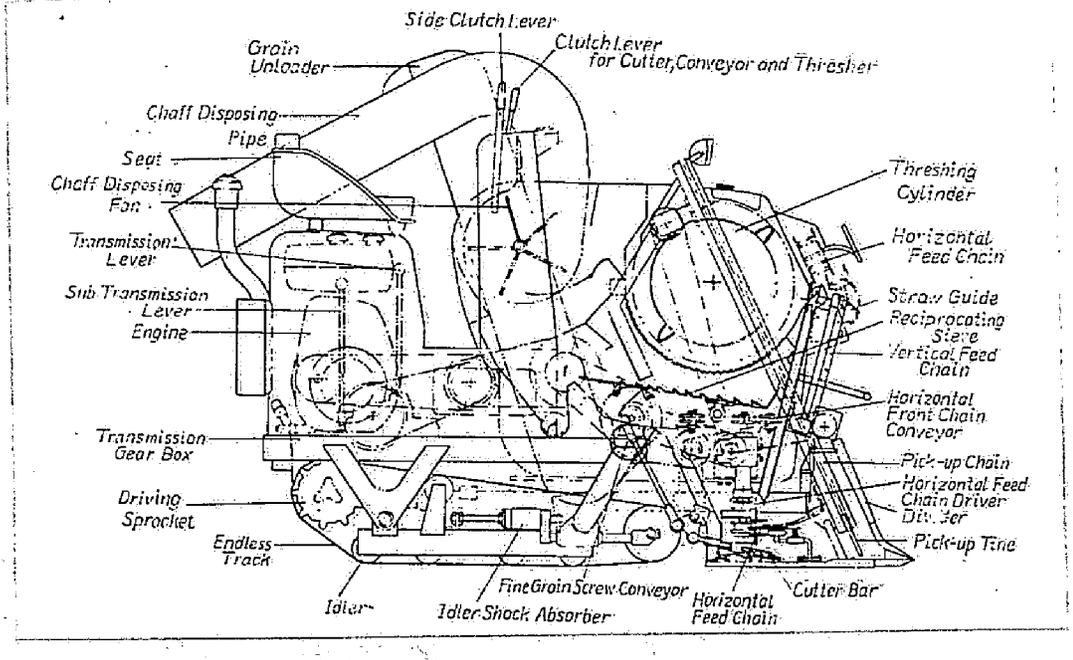

Fig. 2-11 Sectional View of the Head Feeding Combine

2-3-1 Principal Description of the Experiments

Two of small sized rice combine of head feeding type were supplied by different manufacturers for the experiments and here in this paper called the combine A and the combine B.

These combines were mounted with endless track as its travelling device in order to decrease the ground contact preassure. The combine A was a walking type, while the combine B was a riding type. The principal specifications of the combines used for the experiments are shown in Table 2-6. The power transmission systems of these combines are shown in Fig.2-12. For both combines, the power was trans-

Table 2-6 Specifications of the Experimented Combine

Appellation	Combine A	Combine B
Weight	580 kg	700 kg
Operator	Walking	Riding
Turning mode	Left-handed	Right-handed
Engine	Air cooled	Air cooled
	One cylinder	One cylinder
	4 cycle	4 cycle
Rated power	7.0 hp/1600 rpm	6.5 hp/1600 rpm
Max. power	9.0 hp/1800 rpm	9.0 hp/1700 rpm
Cutting width	500 mm (Two rows)	500 mm (Two rows)
Cutting device	Reciprocating cutter	Reciprocating cutter
Threshing cylinder		
Diameter	460 mm	364 mm
Length	500 mm	482 mm
Speed	430 rpm	550 rpm
Travelling device	Endless track	Endless track
Travelling speed		
Forward	0.44-1.30 m/sec	0.08-0.79 m/sec
Backward	0.40 m/sec	0.13-0.84 m/sec
Cleaning device	Grain fan	Reciprocating sieve

mitted to each component mainly by the V-belts and the combine B is equipped with stepless speed reducer system for travelling.

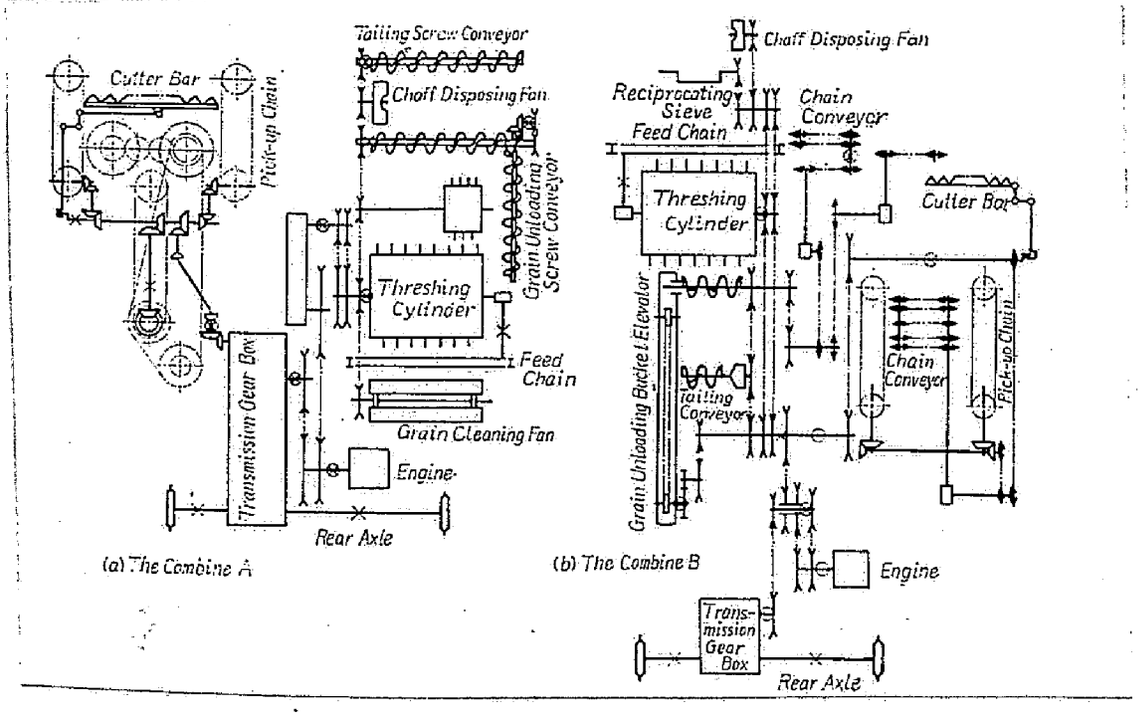

Fig. 2-12 Schematic Diagram of the Power Transmission Systems of the Experimented Combines

For the combine A, in order to determine the power distribution to individual component and to eatimate the power loss, the torques and speeds of the shafts of the functional components, such as the threshing cylinder, conveying chains and screws, cutter-bar and travelling shafts, were measured. For the combine B, the torques and speeds of the shafts of the components which responded relatively cleary to the fluctuating feed rate were measured. The measured points of above-mentioned torques and speeds are shown in Fig. 2-12 (a) and (b) by the symbols x and O, respectively.

The experiments for the combines A and B were conducted from November 8 to 21, 1967 and from October 1 to 15, 1968. The rice field conditions are shown in Table 2-7.

Table 2-7 Conditions of Rice Plant

	For the combine A	For the combine B
Variety of rice	NAKATE-SHINSENBON	MANRYO
Planting condition	Transplanting	Transplanting
Grain-straw ratio	Grain 33 %, Straw 67 %	Grain 31 %, Straw 70 %
Moisture content	Grain 18.9 %, Straw 68.3 %	Grain 24.9 %, Straw 73.0 %
Planting density	0.65 kg/m/row	0.61 kg/m/row

The experiments for the combine A were conducted in order to discuss the stationary characteristics of the combine under the ordinary operating conditions. The travelling and cutting conditions of the individual experiment are shown in Table 2-8.

The experiments for the threshing device, which is the most important device of the combine, were conducted in order

Table 2-8 Operating Conditions for the Combine A

Experiment No.	Travelling speed	Cutting width	Feed rate
1	0.405 m sec	2 rows	31.4 kg min
2	0.612 m sec	2 rows	47.3 kg min
3	0.398 m sec	1 row	15.5 kg min
4	0.598 m sec	1 row	23.2 kg min
5	0.526 m sec	2 rows	40.8 kg min
6	0.436 m sec	1 row	16.9 kg min
7	0.622 m sec	1 row	24.1 kg min
8	0.433 m sec	2 rows	34.2 kg min
9	0.620 m sec	2 rows	48.0 kg min

to discuss the dynamic characteristics of the threshing cylinder. The conditions for these experiments are shown in Table 2-9.

Table 2-9 Conditions of the Threshing Experiments for the Combine B

Test appellation	Feed rate	Speed of cylinder
A	134.0 kg/min	402 rpm
B	100.0 kg/min*	376 rpm
C	——	393 rpm

* Rice plant was fed more deeply by approximately 10 cm than test A.

In order to discuss the response of the combine not only to the ordinary operation but also to the extraordinary fluctuation of the feed rate, the experiments for the combine B were conducted. The conditions for these experiments are shown in Table 2-10. Table 2-10 Operating Conditions for the Combine B

Experiment No.	Travelling speed	Cutting width	Planting mode	Feed rate
1	0.4 m/sec	1 row	Uniform	14.6 kg/min
2	〃	2 rows	〃	29.3 kg/min
3	0.65 m/sec	〃	〃	47.5 kg/min
4	0.40 m/sec	〃	Step (Double)	29.3 kg/min (First half) 58.6 kg/min (Latter half)
5	〃	〃	Step (Triple)	29.3 kg/min (First half) 87.9 kg/min (Latter half)
6	〃	〃	Rectangle (Wave length 1.2 m)*	
7	〃	〃	Rectangle (Wave length 1.6 m)*	
8	〃	〃	Rectangle (Wave length 3.2 m)*	

* Average planting density was 2.4 kg/m and amplitude of planting density was 2.4 kg/m.

2-3-2 Experimental Results and Their Discussions

The operating performances of the combine A for three different speeds of the threshing cylinder are shown in Table 2-11. As the speed of the cylinder increased, the unthreshed grain decreased, however, the husked rice which would be considered as grain loss in the drying process increased.

Table 2-11 Operating Performances Of the Threshing Device of the Combine A

Speed of cylinder	Ratio of husked rice	Ratio of unthreshed head
360 rpm	0.2 %	5.0-6.0 %
404 rpm	0.2 %	5.0-6.0 %
434 rpm	1.7-2.2 %	3.0-4.0 %

The power distributions to individual component of the combine A and B are shown in Fig. 2-13 (a) and (b), respectively. For the combine B, the power of the engine could not be measured due to its construction, therefore, the power loss was estimated. The characteristics of the power distribution to main components of the combine A and B will be discussed in comparison with the Western-type rice combine.

The power for travelling occupied 30-35 percent of the engine power for the combine A, and 30 percent for the combine B. For the Western-type rice combine with the half-track, however, the power for travelling occupied 20 percent of the engine power*. It depends on the soil condition, small engine power compared to total body weight as well as its construction. Therefore, it is necessary to improve the travelling device with the endless track for smaller combine. The details about the travelling power will be discussed in Chapter 4.

For the combine A, the power for threshing occupied

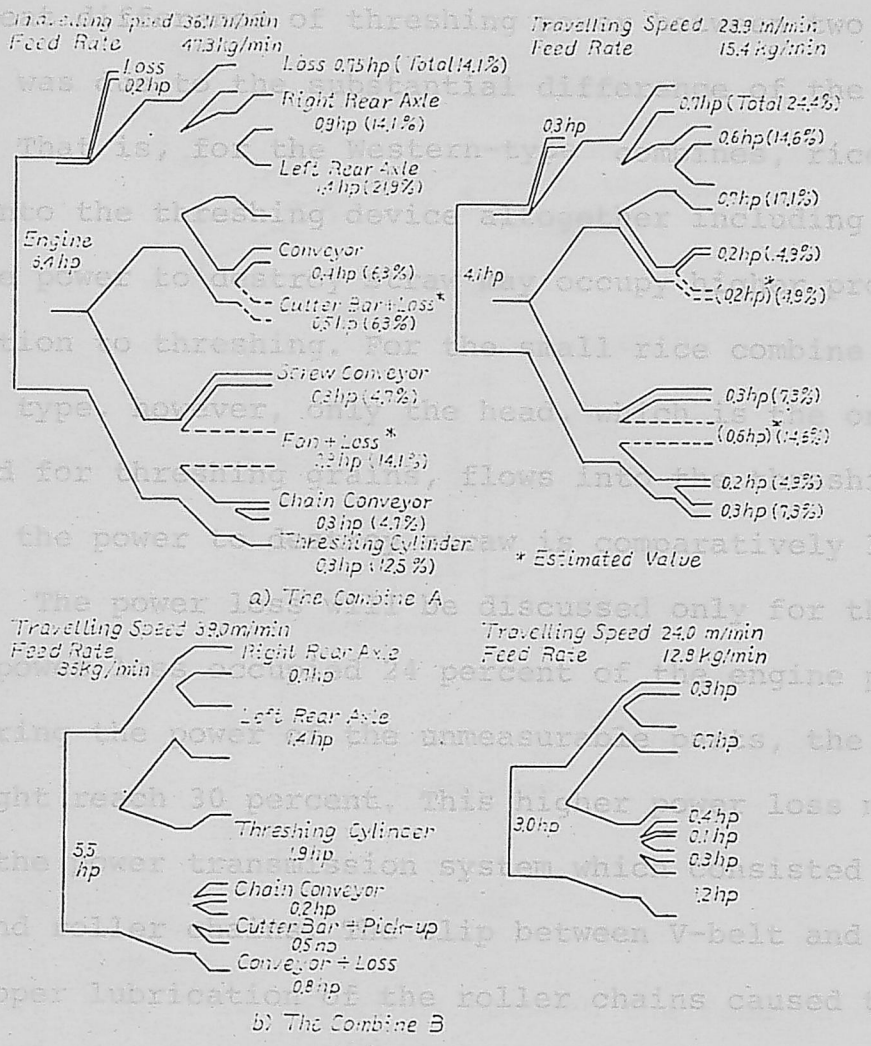

Fig. 2-13 Power Distribution to Individual Component of th Combins A and B

10 percent of the engine power, while for the combine B, it increased rapidly as the feed rate increased, and occupied 30 percent of the engine power. The reason for this phenomenon might be due to the differences of the major specifications, size and construction of the threshing components between two combines. In both combines, the fact that the threshing power occupied lower ratio is one of the merits of the small rice combine of head-feeding type in comparison with the Western-type combines, in which the threshing power occupied 50 percent of the engine power.

This great difference of threshing power between two types of combine was due to the substantial difference of the threshing method. That is, for the Western-type combines, rice plant flows into the threshing device altogether including straw, so that the power to destroy straw may occupy higher proportion in addition to threshing. For the small rice combine of head feeding type, however, only the head, which is the only part required for threshing grains, flows into the threshing device so that the power to destroy straw is comparatively lower.

The power loss will be discussed only for the Combine A. The power loss occupied 24 percent of the engine power. Considering the power of the unmeasurable parts, the power loss might reach 30 percent. This higher power loss might be due to the power transmission system which consisted of the V-belts and roller chains. The slip between V-belt and pulley or improper lubrication of the roller chains caused the decrease of the power transmission efficiency. As mentioned later, considering the lower efficiency of the endless track and the sprocket, the total efficiency of the power transmission of the small combine might be of low value, likely less than 50 percent. Therefore, it is necessary to study the power transmission system from a point of view of the effective utilization of the engine power.

For both small rice combines of head feeding type, the rice plant was fed between the chains and the guide rails, so the feed rate was limited at about 50 kg/min. The relations between the feed rate and the mean power requirement for the combine A and B are shown in Fig.2-14 (a) and (b), respectively.

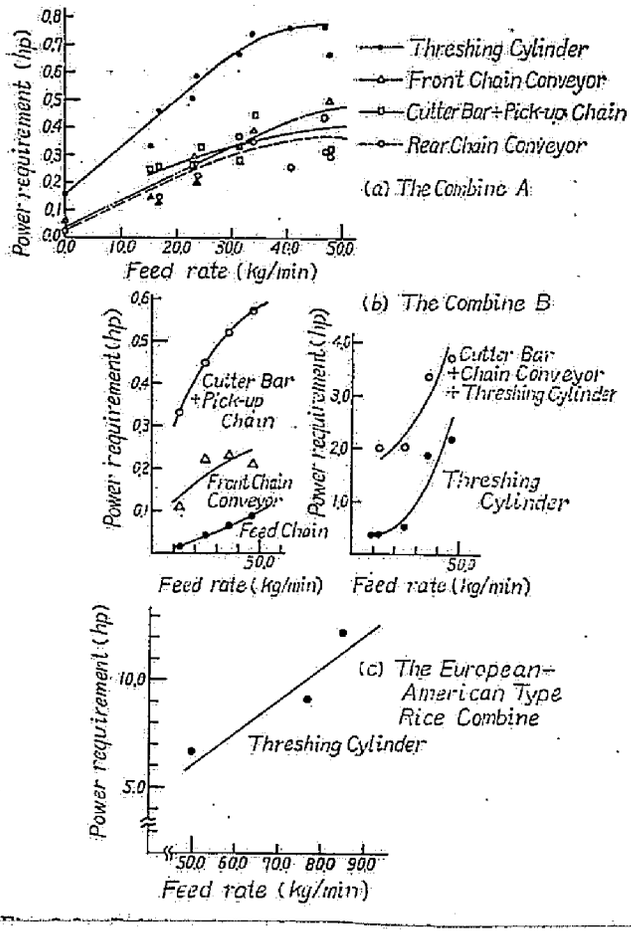

Fig. 2-14 Relations between the Feed Rate and the Mean Power Requirement

Threshing power of the combine A showed the maximum value of 0.8 PS, and of the combine B of 0.5 PS. This difference of the threshing power might be due to the fact that the moisture contents of grain and straw for the combine A were higher by 6 and 5 percent respectively, as shown in Table 2-17, than for the combine A, and the speed of cylinder of the combine B was 1.3 times faster than A. In Fig. 2-14 (c), the threshing power of the Western type rice combine is shown as a comparison. From this figure, the threshing power of the small combine may be considered to be fairly low. Powers required for cutting and picking up of the combine A were higher than those of the combine

B. This difference might be caused by the difference between the transmission efficiencies of the combines. That is, the universal joint was used in the combine A which was not used in the combine B and the power transmission systems which consisted of seven pairs of the bevel gear were used in the combine A, so that the power transmission efficiency of the cutting and picking up devices of the combine A might be decreased. The power requirements of the other components were of low value of approximately 0.5 PS.

2-4 Conclusions of This Chapter

Combines posses the complicated mechanisms and characteristics of the power requirements. Grain losses, torques and rotating speeds at each element of the small rice combines and the thresher of head-feeding type were measured and the comparison of the differences in functions between these machinery were investigated. Especially, in this chapter the power requirements and the power distributions to each functional element were discussed for the individual machine.

As a result of these experiments and discussions, the followings were obtained. For the Western-type small rice combine,

1) The grain loss was 4.5 percent when the operating condition was good, but in case of harvesting the lodged rice plant the grain loss amounted to 20.0 percent. The greater part of this grain loss was the cylinder and straw rack loss, especially the most part of the cylinder loss was caused by the unripened grains.

2) The power requirements of this combine were closely related with the feed rate of the rice plant to be threshed, that is, power requirement was 26.5 PS when the feed rate was 85.1 kg/min and 13.5 PS when 49 kg/min.

3) The characteristics of the load at each element were different. That is,

a) The power at the threshing cylinder was most closely related with the feed rate. It was 11.6 PS on the average when the feed rate was 85.1 kg/min and 4.7 PS when 49 kg/min.

b) The cutter-bar power did not vary widely depending on the

operating conditions and its value through the experiments was small, about 1.0 PS.

c) Because of the low travelling velocities through the experiments, the maximum travelling velocity was 0.32 m/sec, the travelling power were small, that is from 4.0 PS to 8.0 PS.

4) The forces acting on the concave through the rice plant by the threshing cylinder increased at intervals of the uneven flow of rice plant fed into the threshing room. Hence, the torque at the threshing cylinder shaft also showed the wide fluctuation.

The small combine with the head-feeding thresher, which has the chain conveyor to feed the straw along the threshing cylinder axis and of which cylinder teeth beat only the ear part of the straw, has many feature. In order to make clear the threshing function of the small combine of this type, the power requirements of the head-feeding thresher, which constitutes the conveying, threshing, cleaning and unloading elements of the combine, were measured and the following power requirements characteristics of the thresher were obtained.

1) Observing the cylinder torque fluctuation when binded one-sheaf was fed, it was found that the threshing function was carried out for the first half of the cylinder length.

2) The threshing power requirement for the continuous feeding was about 70 percent of the power for the sheaf feeding. It was favourable to feed continuously and uniformly for the combine of head-feeding type.

3) When binded one-sheaf of green rice was fed, the threshing cylinder power requirement was relatively high. It rated to 60 percent of the total power input.

4) The power loss was considerably high, because of the slippage between the V-belts and pulleys of the power transmission system.
5) The power requirement of the threshing cylinder for the dried rice was about 50 percent of that for the green rice.
6) The relationships between the feed rate and the power requirements were quasi-linear for both dried and green rice.
7) For threshing of the binded one-sheaf of green rice, the threshing power increased more largely with the increase of the sheaf weight than of the dried rice.

The characteristics of the power requirements of the combine of head-feeding type are concluded as follows.
1) The operating performance was fairly good, that is, grain loss was below 6 percent, but for the Western-type small rice combine it was 10 percent or more.
2) The power for threshing occupied from 10 to 30 percent of the engine power, but the threshing power of the Western-type small rice combine occupied 50 percent of the engine power. This difference of threshing power was due to the difference of the threshing method and the lower threshing power is one of the merits of the head-feeding type combine.
3) Power loss showed considerablly high value.
4) The power requirement for travelling occupied the higher proportion, that is, from 30 to 35 percent of the engine power, however, for the Western-type rice combine with a half-track, the power for travelling occupied 20 percent of the engine power.

CHAPTER 3

Dynamic Characteristics of the Combine Loads

In the preceding chapter, the power distribution patterns to each functional element of the combines and the thresher, and the relationships between the average power requirements and the feed rate of rice plant fed to the combine and thresher were discussed. However, the characteristics such as the amplitude and the relative frequency distributin of the fluctuating torques caused by the mechanical vibration of the combine elements and the uneven flow of rice plant fed into the combine could not be clarified.

In this chapter, the dynamic characteristics such as the amplitude of the fluctuating torque by means of the above-mentioned relative frequency distribution curves, the frequency domain characteristics of the fluctuation of the torque by means of power spectral density and the time domain characteristics of the trend by means of the moving average method from the view point of developement of a combine such as an automatic control of harvesting.

3-1 Dynamic Characteristics of the Loads of the Western-type Small Rice Combine * , **

In order to find the smoothed fluctuation of the torque recorded under a certain operating condition, the method of moving average was taken, that is,the very minute fluctuation were filtered out. Thus the trend of fluctuating torque could be shown.

Besides, for the purpose of discussing the characteristics of fluctuation including the very minute fluctuations of the torques, the relative frequency distribution curves for the whole records of the torques were obtained and the amplitudes and other statistic characteristics were revealed. This method of the relative frequency distribution curves can sufficiently represent the characteristics with the mean, median, mode and range. Hence, in order to discuss more sufficiently the fluctuation of the torques, the relative frequency distribution curves of the original records of the fluctuating torques corresponding to the neighbours of the maximum and minimum values of the smoothed curves of the torques were obtained and the differences between these distribution curves, that is, the nonstationary dynamic characteristics of the fluctuating torques were discussed.

In case of discussing the periods of the fluctuations, the autocorrelation functions or correlograms and power spectral densities are usually used[1),2),3),4)], but in this section these techniques were not adopted since the longer periods of the fluctuation of the torque could be found by the moving average method.

There are many methods for counting frequencies in a distribution curve[5)], the following two methods were adopted in this section.

i) When a fluctuating torque passes through the class limit torques at the level T_1, T_2, ..., T_n, which were set up in advance, f_1, f_2, ..., f_n times respectively, the frequency H_k of the torque T_k is given by the following equation.

$$H_k = \left(f_k / \sum_{j=1}^{n} f_k \right) \times 100 \quad \text{(percent)}$$

for k = 1, 2, ···, n

For example, the calculating results of such the fluctuating torque as shown in Fig.3-1 is given in the right column in this figure. In this section the number of the classes of torques n are from 7 to 30. And hereafter this method will be called the A-method (Amplitude method).

ii) The ten levels of the torques are set up at the value of T_0, T_1, ..., T_9 through dividing equally the range of the fluctuation of the torque with the aid of the helical potentiometers of the analog data processing system. And using the oscillogram tracer, A-D convertor, comparater, logic circuit and magnetic counter of this data processing system the values of the torque are sampled at the constant time interval Δt out of the original oscillogram records, to which class do these sampled values belong is determined and the frequencies of the torques belonging to each class are counted with the magnetic counter (see Fig.3-1). In this section the sampling interval Δt is 1/5000 sec. Because the period required for a complete rotation of the threshing cylinder was about 1/15 sec and the minimum period of the fluctuation of the engine torque was about 1.5/500 sec, therefore the time interval for sampling was short enough. The characteristic value of the class was $\frac{1}{2}(T_n + T_{n+1})$ for n = 0, 1, ..., 8. And hereafter this method for counting frequencies will be called the S-method (Step method).

The experimental conditions were given in 2-1-1.

3-1-1 Amplitude of Fluctuating Torque of Each Functional Element

For Test 3, when the feed rate was maximum of all

experiments, in order to find the range of the fluctuation of the torques including the minute fluctuation such as the tortional vibration of the shaft, the relative frequency distribution curves of the torques of the engine, threshing cylinder and travelling counter shaft for 6.6 seconds were obtained with the A-method, as shown in Fig. 3-2. It was revealed that the torques of the threshing cylinder shaft fluctuated widely, but at the engine and travelling counter shaft did not so widely and their distributions were approximately normal. Namely, the maximum value of the threshing cylinder torque was five times as much as its mode and the maximums of the engine and travelling torque was about two or three times as much as their modes. Thus, it was a very peculiar and unique phenomenon that only the threshing cylinder torque fluctuated over a wide range.

Similarly to Test 3, in order to discuss the details of the fluctuation of the torques and to find out the nonstationary characteristics of the fluctuating torques, the relative frequency distribution curves were obtained with A-method for the part at which the threshing cylinder torque gave a lower value (A), the part at which the cylinder torque increased (B) and decreased and gave a low value once more (C).

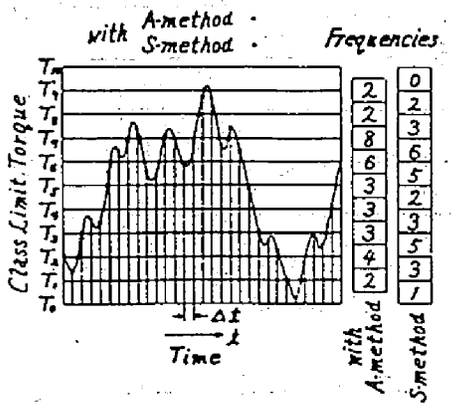

Fig. 3-1 Method for Counting Frequencies

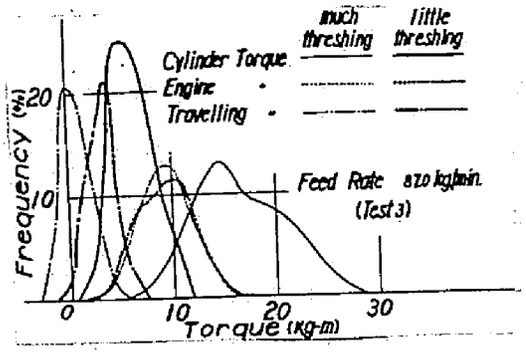

Fig. 3-2 Vriatin of Torque Distribution

The results of calculation are given in Fig.3-3

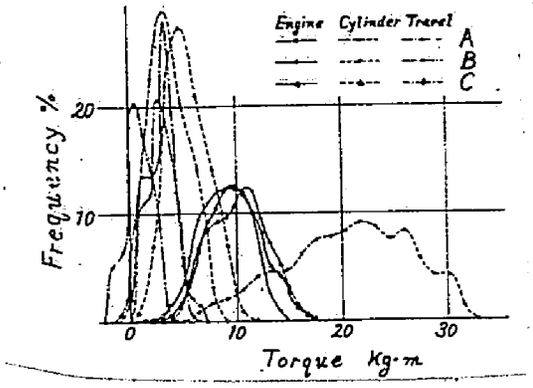

Fig. 3-3 Shifting of Distribution Curves of Torques because of Uneven Flow of Rice Plant

For the same part of the oscillograms of the torques as the above, the relative frequency distribution curves were obtained with the A-method. The results are shown in Fig. 3-4.

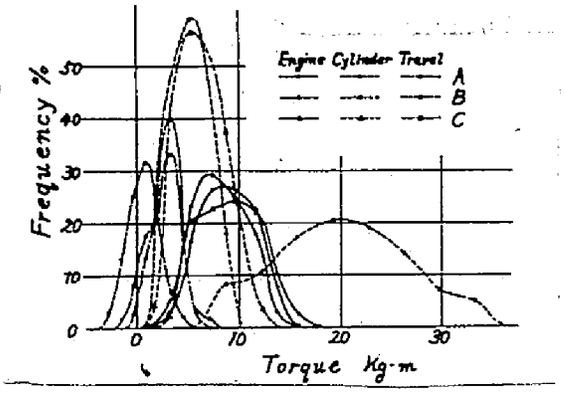

Fig.3-4 Shifting of Distribution Curves of Torque because of Uneven Flow of Rice Plant

Compared these two groupes of the curves, it was noticed that there was a fairly large difference of the shapes between distribution curves. This was due to the fact that with the A-method the time required for the fluctuating torque to pass the adjacent level value after passing a certain level value was not considered but only the amplitudes of fluctuation were considered for calculating frequencies, however with the S-method the frequencies of the sampled torques belonging to a certain range increased in proportion to the time required for passing this range. In both figures obtained with the different two methods, however, the tendencies of shifting, which was caused by the nonstationary characteristics of the fluctuations of the torque, of the relative frequency distribution curves corresponding to each part of the oscillogram were similar. Namely,

i) When the feed rate of rice plant increased instantaneously because of the uneven flow of rice plant, the mean value of the threshing cylinder torque increased and thus its frequency distribution curve moved to the right. At that time, however, the engine torque did not change so largely as the threshing cylinder and the mean value of the travelling counter shaft torque decreased as contrasted with the above two elements and its frequency distribution curve moved to the left. When the feed rate decreased soon after, the mean value of the threshing cylinder torque decreased and its distribution curve moved to the left and returned to the previous position and the distribution curve of the travelling counter shaft torque returned to the right but the fluctuation of the engine torque was small..

ii) When the average torque of the threshing cylinder increased, the range of fluctuation of this torque at this time became wide. This phenomenon indicated that the load for threshing grains and cutting straws became heavier when the flow of rice plant increased.

3-1-2 Smoothed Fluctuation of Torque of Each Functional Element

In order to find the trends of the fluctuation of the torques and angular velocities, the moving average method was used and filtered out the minute fluctuations. The moving average methods of various type are given in the references 6) and 7). But the moving average process used in this section was as follows. The average values of the torques of each functional element at an interval of one revolution of the threshing cylinder and the average values of the angular velocities of each element at an interval of one revolution of each corresponding element were calculated. The results are shown in Fig. 3-5.

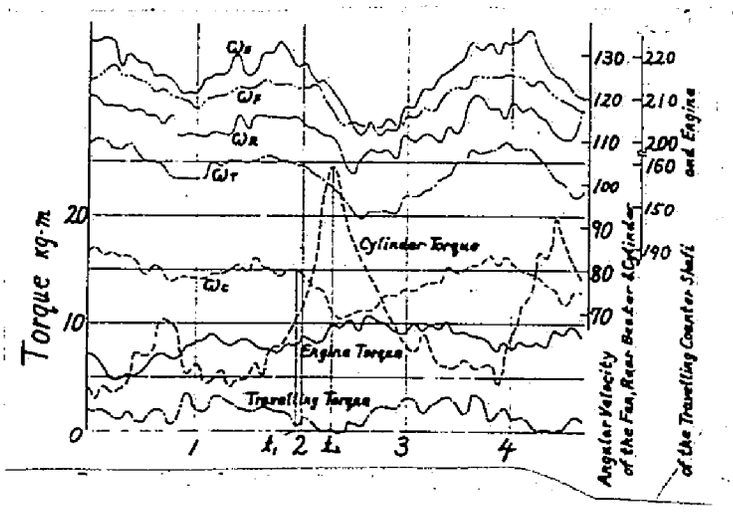

Fig. 3-5 Smoothed Fluctuations of Torques and Angular Velocities

i) It was revealed from this figure that the threshing cylinder torque increased at an interval of 1.6 sec and 2.1 sec. Such

phenomenon as this was observed during every experiments and the intervals of these increases of the threshing cylinder torque were from 1.2 sec to 2.5 sec. This fact seemed to show that the flow of rice plant fed into the threshing roon was not uniform [8), 9)].

ii) Although the threshing cylinder torque increased instantaneously, the engine torque did not so increased and the travelling torque decreased at this time on the contrary. This seemed to show that because of the great mass moments of inertia of the main rotating parts, especially of the threshing cylinder of the experimented combine, the kinetic energies of these parts compensated the instantaneous increase of the loads at the threshing cylinder.

That is, when the loads of the threshing cylinder was low (for example, at $t = t_1$ in Fig. 3-5), let the angular velocity of the cylinder shaft be ω_1 and the travelling velocity of the combine be v_1. And when the flow rate of rice increased and therefore the threshing cylinder torque increased ($t = t_2$ in Fig.3-5), the angular velocity of the cylinder decreased to ω_2 after dt ($= t_2 - t_1$)sec. Let the total equivalent moment of inertia about the cylinder shaft of the main rotating elements of the combine be I_{ceq}, the total weight of the combine be W (kg) and the change of a kinetic energy for dt sec be dE, the work done for a unit time, that is, power H is given by the following equation.

$$H = \frac{dE}{dt} \times \frac{1}{75} = \frac{1}{dt}\{ I_{ceq}(\omega_1^2 - \omega_2^2)/2 + \frac{W}{g}(v_1^2 - v_2^2)/2\}/75 \quad \text{in PS} \qquad (3\text{-}1)$$

Because of the low travelling velocity the second term in the parenthesis of the right hand side of Eq. 3-1 can

be neglected. Finally, the following equation representing the compensating power of the rotating elements of the combine is obtained.

$$H = I_{ceq}\omega\frac{d\omega}{dt}\frac{1}{75} \quad (PS) \qquad (3\text{-}2)$$

where $\omega = \frac{1}{2}(\omega_1 + \omega_2)$, $d\omega = \omega_1 - \omega_2$.

The main rotating parts were connected with V-belts as shown in Fig. 2-1. The mass moments of inertia of each rotating element could be reduced to the equivalent mass moment of inertia about the threshing cylinder shaft I_{ceq}, which was given by the following equation.

$$I_{ceq} = I_C + I_R\left(\omega_R/\omega_C\right)^2 + I_T\left(\omega_T/\omega_R\right)^2\left(\omega_R/\omega_C\right)^2 + I_E\left(\omega_E/\omega_R\right)^2\left(\omega_R/\omega_C\right)^2 \qquad (3\text{-}3)$$

where I_C, I_R, I_T and I_E were the mass moments of inertia about the threshing cylinder, cylinder beater, travelling counter shaft and engine, respectively. And ω_C, ω_R, ω_T and ω_E were the angular velocities of the above, respectively. These values of the experimented combine were as follows.

$I_C = 51.0$ kg-cm-sec^2, $I_R = 7.97$ kg-cm-sec^2
$I_E = 2.6$ kg-cm-sec^2, $I_T = 2.3$ kg-cm-sec^2

$\omega_R/\omega_C = 1.49$, $\omega_T/\omega_R = 1.39$, $\omega_E/\omega_R = 1.91$

For example, the change of the energy from $t = t_1$ to $t = t_2$ in Fig. 3-5 could be calculated as follows. In this case,

$\omega_1 = 80\ sec^{-1}$, $\omega_2 = 70\ sec^{-1}$, $d\omega = 10\ sec^{-1}$, $dt = 0.34$ sec and $\omega = 75\ sec^{-1}$. The compensating power was calculated from Eqs. (3-2) and (3-3) and it amounted 27.6 PS. Therefore it could be said that the flywheel effect or compensating effect of the rotating elements of the combine was large.

In such a manner, there was compensating function of the power requirement between each functional element of the combine and therefore the instataneous increase of the load at the threshing cylinder could be compensated by the kinetic energy of the rotating parts of a combine without increasing the engine power.

In order to design a combine effectively with regard to the characteristics of the load at each element and to good utilization of power compensating function between the functional elements, not only the independent and peculiar function of each element, but also the mutual action between the combined elements will have to be analized. For this purpose, the further studies of a combine must be made from a point of view that the power transmission system of a combine is a dynamic system including an engine.

3-1-3 Characteristics of Fluctuation of Torque of Threshing Cylinder

The most important functional element of the combine is the threshing cylinder. In the previous section the characteristics of fluctuation of the main functional element were discussed. It is necessary for designing and developing the threshing element that the dynamic characteristics of the threshing torque are clarified and in this section the change

in the amplitude of the fluctuation of the threshing cylinder torque with the change in the feed rate of rice plant by means of the relative frequency distribution curves will be investigated and the threshing process of the threshing device with spike-tooth cylinder and concave will be presumed by the oscillogram traces of the wave forms of the threshing cylinder torque and concave reaction torque.

The threshing cylinder torque fluctuated with the longer period by the change in the flow of rice plant and this phenomenon was clarified by the moving average method in 3-1-2. The actual fluctuation consisted of the longer fluctuation mentioned above and the shorter fluctuation caused by the threshing action of the teeth of the cylinder and concave as well as the torsional vibration of the cylinder shaft.

In 3-1-1, for the purpose of verifying the compensating function the two kinds of distribution curves corresponding to the instances at which the flow of rice plant increased and decreased. In this section the frequency distribution curves obtained from the longer time records were discussed in disregard of change of the rice flow during an experiment are examined and the change of the distribution curves caused by the change of the experimental condition are investigated.

The relative frequency distribution curves of the threshing cylinder torque for the various experimental conditions, which were obtained from the original long oscillogram charts for 5 to 7 seconds with the A-method explained in 3-1, are shown in Fig. 3-6.

The distribution curves corresponding to the low

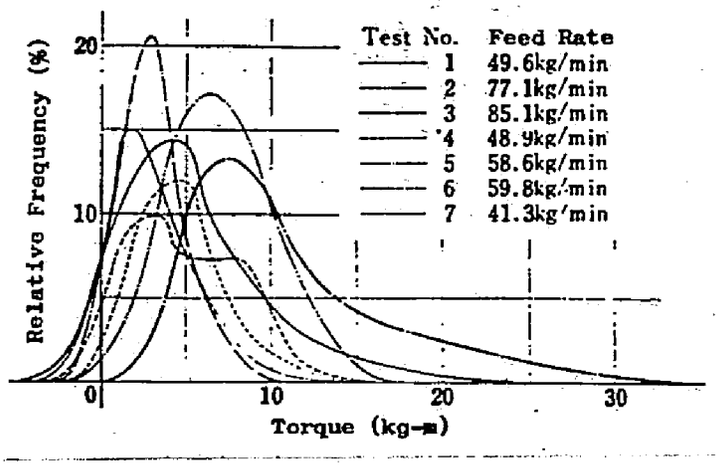

Fig. 3-6 Frequency Distribution Curves of Threshing Cylinder Torque

average feed rates of rice plant might be considered approximately normal, but to the high feed rates they were skewed. The ranges of the amplitudes of fluctuations were fairly wide and the maximum torques were 5 to 6 times as large as the modes (3.5 times as large as the mean), and this must be taken into consideration on designing the strength of the threshing cylinder shaft of the combine.

The reaction of the threshing force of the cylinder was transferred as the torque to the worm wheel shaft of the worm gear box for adjusting concave clearance. This torque was transmitted through the threshed rice grains and pressed and crashed straws from the threshing cylinder and might display the force acting upon the concave approximately. Fig. 3-7 indicates the oscillogram traces of the torques of the cylinder and the worm wheel shaft for the feed rate of 85.1 kg/min. In this figure, (a) was recorded when the flow of rice decreased and (b) was recorded

when increased instantaneously.

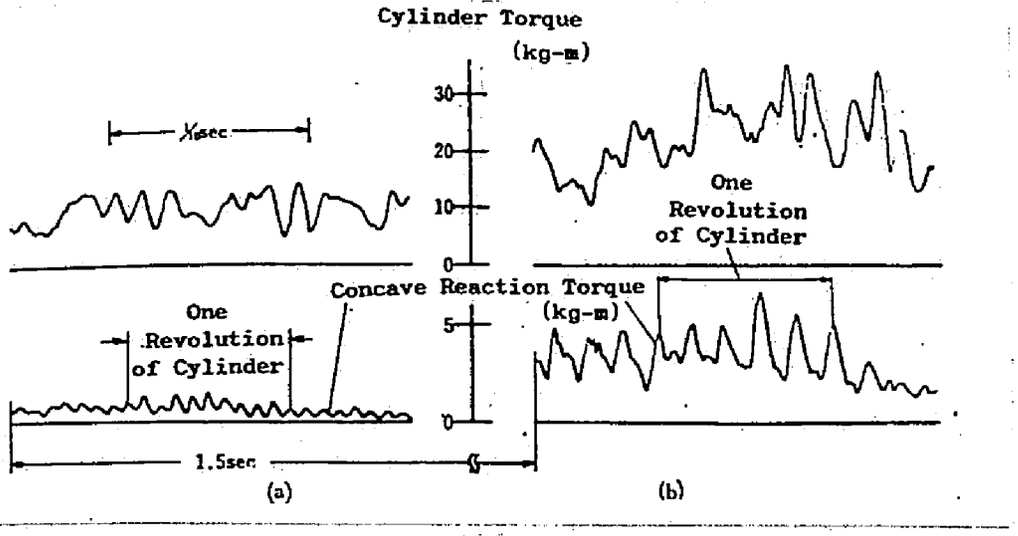

Fig. 3-7 Oscillogram Traces of Torque at Cylinder and Concave for Test No.3

The period of the fluctuation of the concave torque was different from that of the cylinder. The fluctuation with longer period (more than 1.0 second) of the force acting upon the concave was caused by the uneven flow of rice mentioned previously. The fluctuation with the shorter period might be caused by the fact that when the teeth of cylinder passed through the teeth of the concave, there were actions of threshing grains, cutting and pressing straws among these teeth. This phenomenon is revealed in Fig. 3-7 (a). That is, the force of the concave fluctuated ten times for one revolutions of the cylinder, this might be caused by the fact that the teeth were placed on the cylinder in the direction of the circumference in ten columns at regular intervals. For convenience, the teeth placed in order in direction of the shaft of the cylinder will be called the column of the teeth hereafter.

When the columns of the teeth of the threshing cylinder passed through the first column of the teeth of the concave (this column was placed near the entrance of the concave), the forces were little acted. The forces acting upon the concave seemed to fluctuate exactly corresponding to the threshing forces. On the other hand, the cylinder torque did not always fluctuate with the threshing forces. When the cylinder shaft was considered as the torsion spring and the cylinder and pulley was considered as the inertia masses, the natural frequency of this vibration system was about 77 Hz. When the rice flow decreased, the cylinder torque fluctuated at 77 Hz as indicated in Fig. 3-7 (a). This indicates that the fluctuation of the torque with the short period was caused by the torsional vibration. However, when the flow of rice plant increased and the load at the cylinder increased, it did not always fluctuate at 77 Hz. The fluctuation of the cylinder torque with a short period might be caused partly by the free vibration of the cylinder shaft, but fluctuation of the cylinder torque was much complicated by the V-belt as a nonlinear spring and nonlinear factor such as slip between the belt and pulley and the frictional resistance of rice. When the flow of rice plant increased, the aspect of the fluctuation of the concave force was altered as shown in Fig. 3-7 (b). By this time, the period became twice as long as (a). The cause of this phenomenon was not clarified, but it seemed that when the flow of rice plant increased, the rice plant was drawn in the teeth of the concave by the teeth of the cylinder in large quantities, the rice flow was intercepted and the resistances

of the rice flow against the next column of the teeth of the cylinder became lighter, or considering the fact that in Test No.3 the grain loss over strawrack was fairly more (that is, 7.0 percent) than in other tests, straw was strongly pressed and so period of fluctuation of the concave force became longer. These phenomena must be analized more minutely in order to clarify the threshing mechanism of the threshing device with the spike tooth cylinder and concave.

Moreover, in Fig. 3-7, the peaks of the threshing cylinder torques lagged behind that of the concave force. This might be caused by the large inertia of the cylinder, that is, the compensating function of the cylinder.

3-2 Dynamic Characteristics of the Load of the Head-feeding Type Thresher***

In 2-2, the mean power requirements of the functional elements and power distributions to them of the head-feeding type thresher were discussed. However, it was insufficient that the load characteristics were indicated only by means of the average torques of the functional elements; and was found to be necessary that they had to be represented by means of the relative frequency distribution curves showing the characteristics in disregard of time axis and the correlograms and power spectral dencities showing the characteristics considering time axis or frequency domain.

In this section the dynamic characteristics by means of the above-mentioned methods will be discussed and the smoothing technique of the moving average will be used as in the previous section. As the results of these discussions the fundamental informations for the automatic control of the small combine with head-feeding type thresher will be obtained.

The principal descriptions of the experiments were given in 2-2-1.

3-2-1 Stationary Dynamic Characteristcs of the Torque of Each Functional Element

The torque wave form of each functional element which was recorded for no-load operation presented the complicated fluctuation by reason of the torsional vibration. When rice plant was threshed, the fluctuations of the torques might become more complicated and the amplitudes of the fluctuations might also be varied according to the material condition..

Especially, as discussed in 2-2-1, the threshing cylinder torque was of the highest value and it might be influenced by the material conditions to a remarkable degree. Therefore, in order to reveal the amplitude of the fluctuating torque of the threshing cylinder, the relative frequency distribution curves of the fluctuating cylinder torques for no-load operation as well as threshing dried and green rices were obtained. The operating condition for threshing dried rice (moisture content of rough rice was 15.9 percent and that of straw was 34.5 percent) was feeding binded one-sheaf of 0.8 kg and that for threshing green rice (moisture content of rough rice was 24 percent and that of straw was 71.3 percent) was feeding binded one-sheaf of 1.5 kg. The method for counting frequencies was sampling method, and from the continuous wave record of the cylinder torque the values at interval of 1/2500 sec. were sampled and the level was decided to which each sampled value belonged and the number of the sampled values involved in each level was represented in percentage by the rate to the total number of the sampled values, as mentioned in 3-1 or reference 5). The obtained frequency distribution curves of the threshing cylinder torques for various operating condition are shown in Fig. 3-8.

i) The fluctuation of the torque of the threshing cylinder for no-load operation was heavy. The influence of the torsional vibration upon fluctuation of the torque seemed to be great considering the negative value of the torque and symmetry of the frequency distribution pattern.

ii) For threshing rice plant, the amplitude of fluctuation in

the threshing cylinder torque was fairly large but its frequency distribution curves were similar to the normal curves.

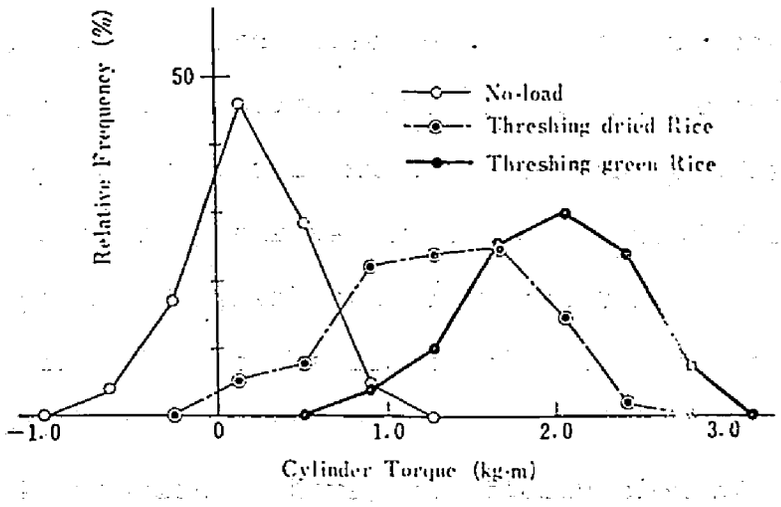

Fig. 3-8 Variation of Frequency Distribution Curves with Operating Conditions

This phenomenon was different from the case of the Western-type rice combine, that is, for the threshing torque of the Western-type combine the mean become greater than the mode as the feed rate of rice plant was increased. This might be caused by the difference of the threshing method. That is, for the head-feeding type thresher only the panicle (head) of rice plant was fed into the threshing device to the direction of the cylinder axis, on the other hand, for the threshing device of the Western-type combine the whole rice plant (panicle and straw) were fed into the threshing room to the tangential direction of the cylinder.

iii) As the load increased, the amplitude of the fluctuating torque increased and the maximum value reached 1.5 to 2.5 times of the mean (this value was nearly equal to the mode). However, for the Western-type combine the maximum

value reached 6.0 times of the mode and it was found that the fluctuation in the threshing torque for the head-feeding type was smaller than that for the Western-type. This was because of the fact that for the Western-type the fluctuation of the flow of rice plant appeared directly as the fluctuation of the threshing cylinder torque and the threshing process contained pressing and cutting straws, on the other hand for the head-feeding type the material stayed in the threshing room for rlatively long time so the fluctuation of the flow of rice was smoothed.

As mentioned above, the fluctuation of the torque contained the torsional vibration. In order to understand the characteristics of the fluctuating torque resulting from such inherent mechanical vibration of the experimented thresher, the correlogram for no-load operation will be discussed at first. The reason why it is easier to search the construction of the frequency component by means of the correlogram than the original wave form are as follows[7].

1) In the form of the correlogram the superior component of some frequency of the original wave form is emphasized (that is, it is appreciated by the squared amplitude).

2) Near $\tau = 0$, the components of the approximately same frequency are aggregated in the approximately same phase.

The calculation of the correlograms were produced for the torques of the driving counter shaft, threshing cylinder shaft, screw conveyer shaft, and chaff-disposing fan shaft. The number of data sampled at interval of 1/250 sec from the original continuous records was 300 and the number of shifting

was 60 (τ_{max} = 0.24 sec). The results of computation are shown in Fig. 3-9.

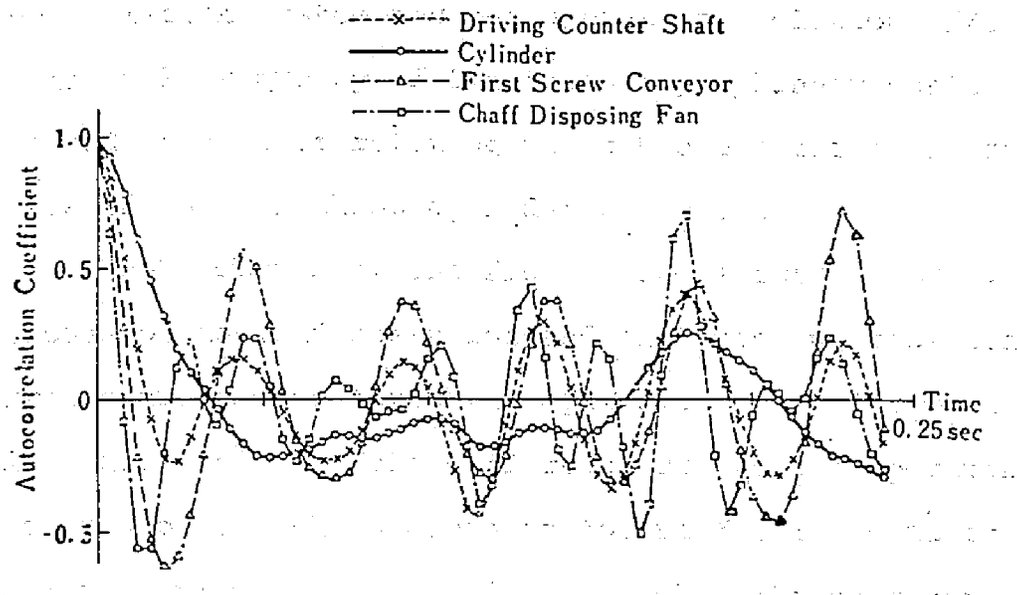

Fig. 3-9 Correlograms of Fluctuating Torques of Functional Elements of Head-feeding Type Thresher

i) The torque of the driving counter shaft and screw conveyer shaft fluctuated secondarily at 20 Hz and primarily at 5.5 Hz. The natural frequency of the torsional vibration of the driving counter shaft was about 130 Hz. The natural frequency of the screw conveyer shaft could not be calculated because of its complicated condition, but its frequency might be excessively about 20 Hz since the mass moment of inertia was very small. Finally, the higher frequency component of the fluctuating torque might be resulted from the natural frequency of the torsional vibration of the multi-degree of freedom system including the motor shaft. The fluctuation of 5.5 Hz will be discussed later on.

ii) The fluctuations of the short period of the shaft of the chaff disposing fan and threshing cylinder were different.

This might result from the reason that V-belts which transmitted power to the chaff disposing fan locating at the end of the power transmission system had the vibration isolation effect and the natural frequency of the threshing cylinder shaft was low compared with other rotating parts because the mass moment of inertia of the threshing cylinder was great.

The amplitudes of the fluctuating torques were different for the case of no-load operation and of threshing rice plant. The correlograms of the threshing cylinder torque for both cases in order to clarify the difference due to the operating condition and of the chain conveyer torque for the case of threshing rice plant are shown in Fig. 3-10. The operating condition was the continuous threshing of green rice of 1.5 kg /40 cm.

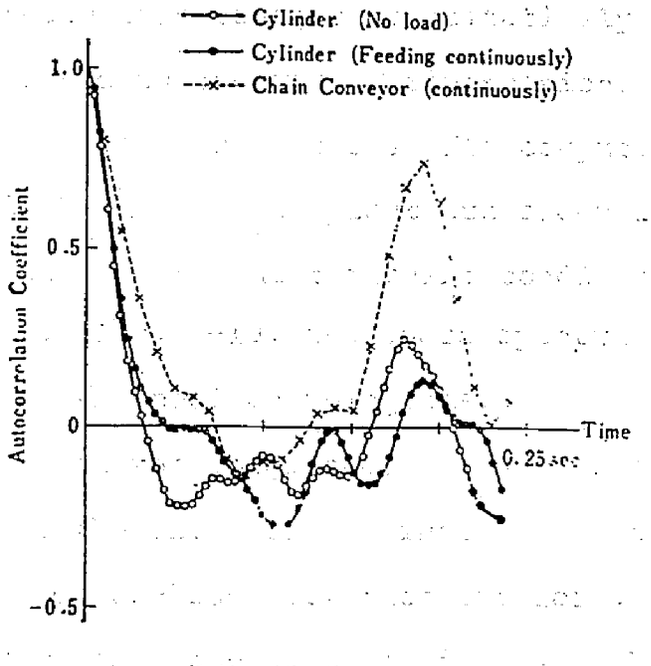

Fig. 3-10 Variationof Correlograms with Operating Condition

i) The fundamental shape of the correlogram of the threshing

torque was not changed when the load acted upon it. In other words, it was presumed that when the load acted upon the threshing cylinder the average torque was increased but the aspect of the fluctuation of the threshing torque did not changed.

ii) The torque of both the threshing cylinder and chain conveyer shaft displayed the fluctuation of 5.5 Hz. The fluctuation of the chain conveyer torque because of the intermittent engagement of the sprocket with the chain was slightly detected. The frequency of this fluctuation was 8.5 Hz, but when the load acted, the fluctuation of this frequency disappeared and the fluctuation of 5.5 Hz appeared. The reason of this phenomena was not able to be elucidated.

The power spectral density which is used to analyze the random fluctuation reveals quantitatively the superior component involved in the random fluctuation. The power spectral densities of the torques of the shafts computed for no-load operation and threshing rice plant are shown in Fig. 3-11 (1), (2), (3) and (4). The threshing conditions were identical with the case of Fig. 3-10, and these spectra were computed from the above-mentioned correlograms.

i) The spectra of the torques of the shafts of the functional elements except the threshing cylinder had the peak near 20 Hz in both cases for no-load operation and for threshing rice plant and power decreased abruptly in the higher range above 20 Hz.

ii) The threshing cylinder torque fluctuated differently. The spectra of this torque had not the peak near 20 Hz but the peak

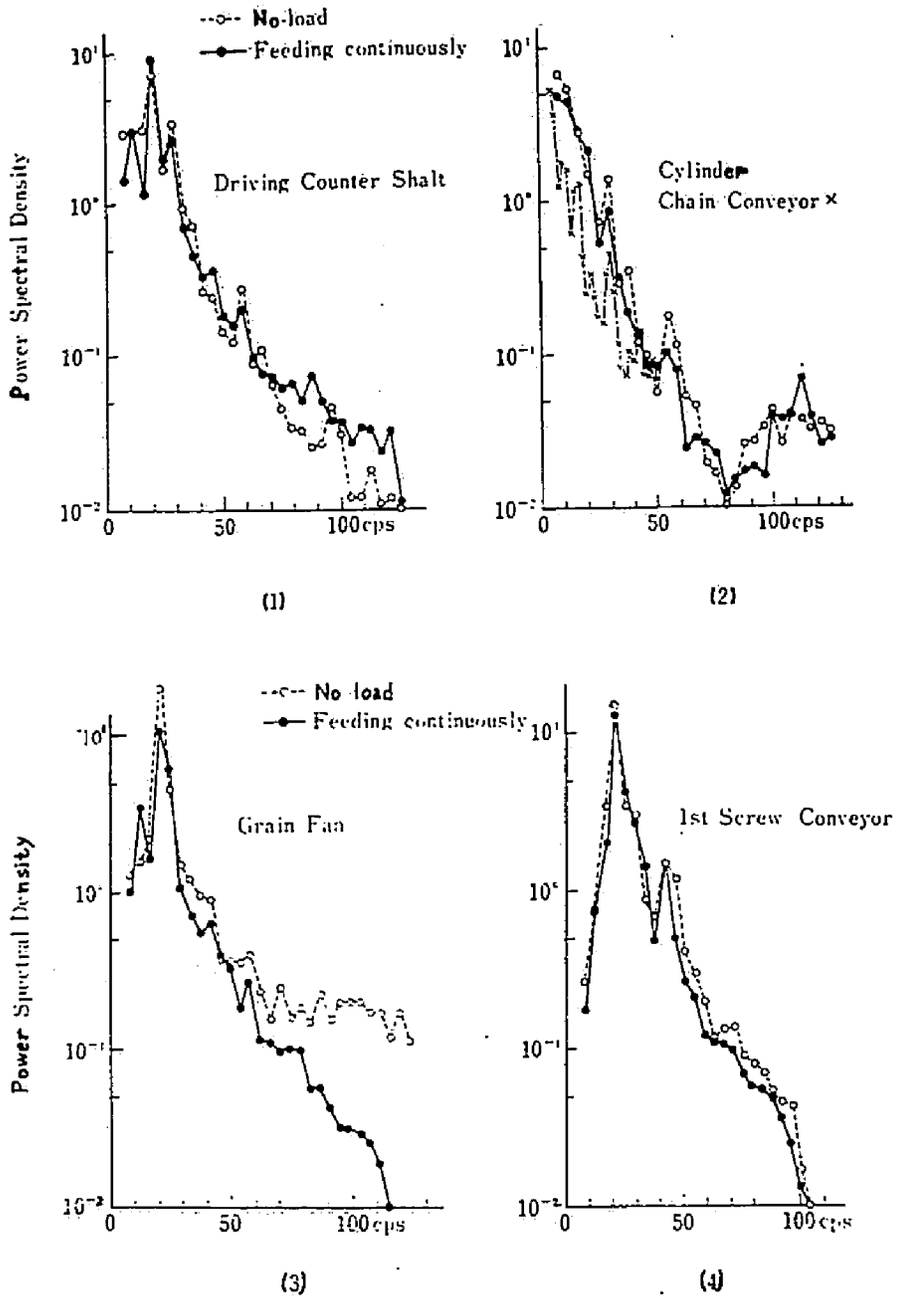

Fig. 3-11 Power Spectral Densities of the Fluctuating Torques of the Head-feeding Type Thresher (Each abscissa represents the frequency of fluctuation.)

of lower frequency. And in this figure the spectra of the

chain conveyer torque had the similar characteristic to that of the threshing cylinder torque. This meant that the vibration isolation effect did not exist in the power transmission from the threshing cylinder shaft to the chain conveyer shaft because this transmission system was constructed from the wheel worm gear and the threshing cylinder shaft and the chain conveyer shaft formed the independent vibration system which was isolated from other functional elements which formed the other vibrating system consisting of the shafts, V-belt and mass moments of inertia.

III) It could not be clarified that the power of the fluctuations of higher frequency than 40 Hz decreased and the fluctuations of frequencies above 40 Hz were smoothed when the load was acted.

From the above discussions it was revealed that the fluctuation characteristics of the torque of each element was hardly affected by the load and the distinguished reason of the fluctuation of the torque was the natural vibration peculiar to the experimented thresher in case of the stationary operation such as continuous feeding of rice plant.

3-2-2 Nonstationary Dynamic Characteristics of the Torque of Each Functional Element

In order to reveal the general characteristcs of the fluctuating torque which all the head-feeding type thresher had, the average values of each original wave at intervals of integral times of the inverse of the natural frequency were calculated and plotted considering the abscissa as time and the ordinate as torque. The fluctuation characteristics of the smoothed

threshing torque from the beginning to the end of threshing binded one-sheaf may be helpful to understand the mechanism of threshing process from a practical view point. The results of computations are shown in Fig. 3-12 (1) and (2). The oprating conditions of (1) and (2) are threshing dried one-sheaf of 0.85 kg and green one-sheaf of 1.5 kg, respectively. The

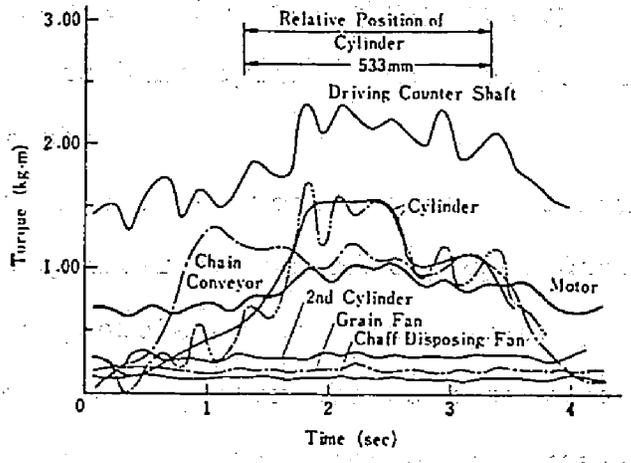

(1) Feeding one sheaf of dried rice

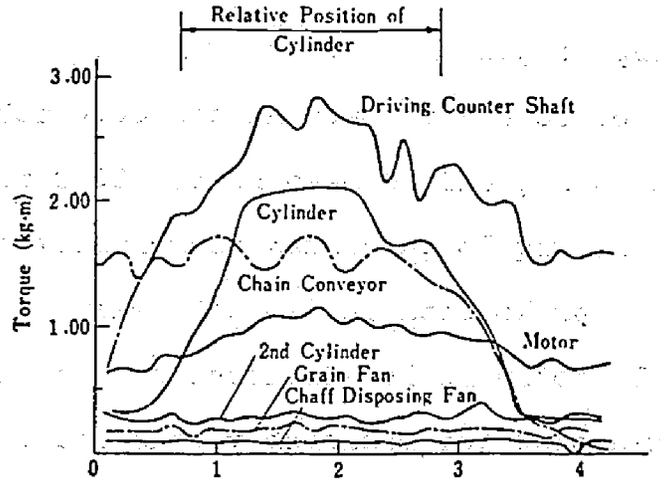

(2) Feeding one sheaf of green rice

Fig. 3-12 Transient Torques Obtained with Smoothing for Threshing Binded One-sheaf

relative position of the sheaf to the threshing cylinder

was detected by the displacement of the straw pressing plate under the chain conveyer.

i) For both cases of threshing dried rice and green rice the beginning of the increase in the torque of the chain conveyer was earlier by about 0.8 sec than that of the threshing torque. This might result from the structure of the thresher of this type, that is, when the chain conveyer began conveying the sheaf, the threshing cylinder did not yet thresh the panicle of that sheaf.

ii) The torque of the cylinder reached the maximum value at the position of quarter length of the cylinder. This indicated that part of the panicle of the binded rice plant was fed into the threshing room after the root of rice was conveyed by the chain,and was spreaded out by the resistances of the threshing teeth.

iii) The above mentioned maximum threshing torque was 1.5 kg-m and continued for 0.65 sec in case of the dried rice and 2.0 kg-m and for 0.95 sec in case of the green rice, respectively. This indicated that threshing of panicle was carried out at these intervals. The differences of the values of these maximum torques and the intervals of duration of these values represented that the energy demanded for threshing green rice was higher than that demanded for dried rice.

iv) After the threshing torque reached the maximum value, it decreased to 70 percent of the maximum in case of threshing dried rice and 75 percent in case of green rice, respectively. These threshing torques continued until the binded rice plant finished to pass through the threshing room. The phenomenon

that these torques continued after the end of threshing might be caused by the load to thresh the straw which was already threshed.

And the fact that its value was 1.0 kg-m in case of threshing dried rice and 1.5 kg-m in case of green rice, respectively, indicated that the resistance of the dried straw was smaller than that of green.

v) In Fig. 3-12 (1), the threshing torques are represented by the solid line and chain line. The averaging interval of the chain line was one half of that of the solid line and as shown by these two curves the curve with the shorter averaging interval represents the details of the fluctuation of the torque. That is, it showed the heavy load at the beginning of threshing.

vi) The torque of the threshing cylinder shaft increased more than those of the electric motor and driving counter shafts. This meant the existence of the compensation of power due to the mass moment of inertia of the electric motor, that is, the prime mover was not influenced by the load fluctuation.

vii) It was presumed that the fluctuation of the supplementary threshing cylinder (2nd cylinder) appeared behind that of the threshing cylinder, but the former showed the low value and imperceptible fluctuation, then it was revealed that the supplementary threshing cylinder was hardly acted upon by the load in case of threshing the binded one-sheaf of rice plant.

viii) The torque of the shafts of the grain fan, chaff disposing fan and the screw conveyer (this is not shown in

Fig. 3-12) showed the low value and imperceptible fluctuation.

Concluding Remarks

In order to obtain the fundamental knowledge of the threshing device which was the most important functional element of the combine with the head-feeding type thresher, the experiments of the stationary head-feeding type thresher were produced. It was revealed that power requirement of the threshing cylinder was fairly low under the ordinary operating condition and the threshing process had been almost finished until the binded rice plant reached the middle point of the threshing cylinder. If the mechanism of threshing process is analyzed in this manner from a practical viewpoint, the investigation into the shape and the optimal arrangement of the threshing teeth may become possible and the threshing cylinder will be improved. Considering the method for feeding rice plant to the threshing cylinder of the head-feeding type thresher, the relationship between rice plant fed into the threshing device and the threshing torque corresponds to that between the integrant and the integral, and it is expected that the fluctuation of the threshing cylinder torque will become smoother than that of the layer of rice plant fed into the cylinder by filtering effect. This effect was clarified by the characteristics of the smoothed fluctuation of the torque obtained for threshing binded rice plant. Therefore in controlling the threshing torque of the combine the characteristics of the input are different in both cases for detecting straw layer thickness and threshing torque. It is desired that the quant-

tative relationship between the fluctuations of straw layer thickness and threshing torque are analyzed.

The power requirements of the other functional elements were very low, but there were many problems which should be solved in future, for example, cleaning and conveying rough rice adhered water drops.

It was found that the small thresher used for experiment had also the mutual compensation of the power, and this will become the problem of the optimal power matching which will be the construction of the power transmission system utilizing the power of the engine effectively.

3-3 Dynamic Characteristics of the Loads of the Head-feeding Type Small Combine ****

In the preceeding section, namely 2-3, the operating performances, the relationships between feed rates of rice plant and the power requirements and the power distribution pattern of the individual functional component of the head-feeding type small rice combine were clarified. But these characteristics of the combine loads were discussed only by means of the averaged values of the torques of the functional elements therefore it is necessary for the further developement such as the automatic control of the combine that the dynamic characteristics of the loads is revealed.

In this section, by means of the relative frequency distribution curves, the power spectral density functions and the moving average methods, the dynamic characteristcs of the torques of the main functional elements will be discussed.

The principal descriptions of the experiments were given in 2-3-1.

For the combine B, the torques and speeds of the shafts of the components which responded clearly to the fluctuation of feed rate were measured.

In order to investigate the fluctuating feed rate due to the natural fluctuation of planting density of rice plant in the field, the change in the straw layer thickness of the rice plant fed into the combine was measured by the phosphor-bronze thin cantilever
on which the strain gages were bonded to detect its deflections. This cantilever was set up parallel to the chain convey-

er immediately after the cutting device of the combine A and the deflection of this cantilever was considered zero when the straw was not conveyed by the chain conveyer.

3-3-1 Dynamic Characteristics of the Torques of Each Functional Element

The amplitude of the fluctuating torque at individual component is of significance from a view point of the fatigue strength and the vibration, so that for the combine A the torque distribution curves of the shafts of the components which transmitted relatively higher loads were obtained and the results are shown in Fig. 3-13 (a) and (b).

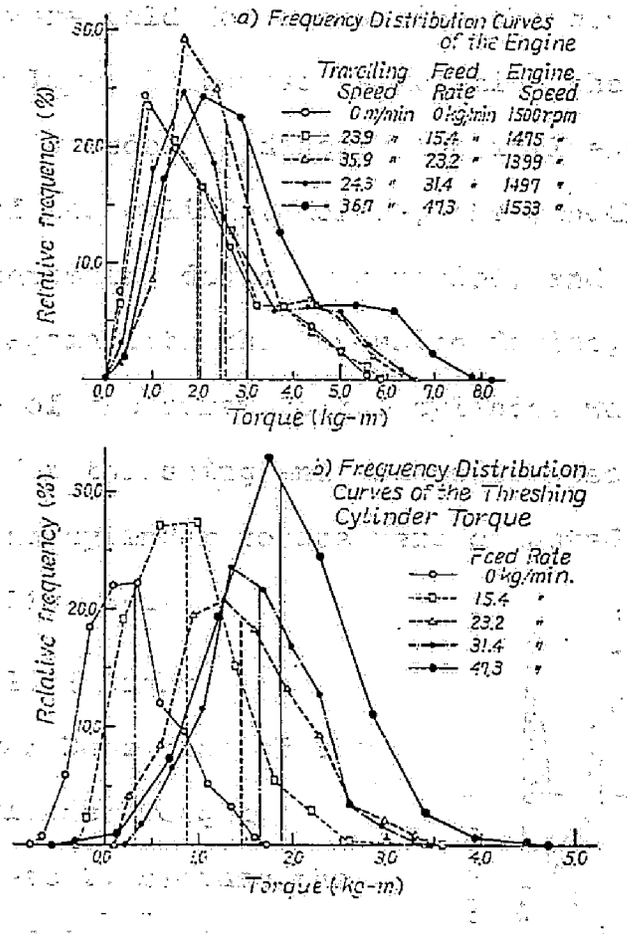

Fig. 3-13 Frequency Distribution Curves and the Mean Values of the Torques of the Engine and the Threshing Cylinder of Combine A

In this figure the verticalline under each curve represents its mean value. The torque frequency distribution curves except the engine and travelling shafts were approximately normal, but the frequency distribution curve of the travelling shaft will be discussed later. The curves of the engine were skew. This might be due to the maximum torque which occured at the ignition time of the engine.

In order to discuss the dynamic characteristics of the threshing device of the combine A, experiments of especially high feed rate were conducted. Rice plants were fed with two steel bars between which the parts near the roots of rice plant were held for containing the continuous and constant straw layer thickness, simulating the combine operation. Further, in order to discuss the influence of the threshing function of the cylinder torque, the length of the rice straw in the threshing device was varied, and the threshed straw was fed again into the threshing device, so that the net resistance of the straw to the cylinder was measured. The average power for threshing and the power spectral densities of the threshing cylinder torque were computed and the results are shown in Fig. 3-14.

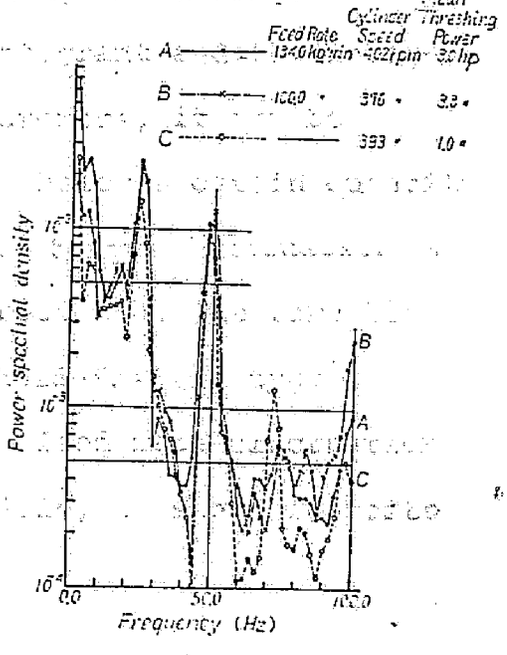

Fig. 3-14 (Right)
Power Spectral Densities of the Threshing Cylinder Torque

In test B, because the rice plant was fed more deeply by 10 cm than in test A, the power requirement for test B was higher

by 30 percent than in test A though in test B the feed rate was below of 25 percent.

In test C, the power decreased to one third of test A. These showed that the resistance of the straw to the threshing cylinder was fairly large.

In the power spectra, the peaks at 6,16,24,48,72 and 100 Hz were found independent on the experiment condition. Particularly, a remarkable peak at 24 Hz might be due to the forced vibration by the reciprocating motion of the unbalanced part of the engine, because the engine speed was approximately 1450 rpm (or 24.2 rps), therefore the main components of the fluctuating cylinder torque consisted of the torsional vibration of the engine crank shaft, its harmonics and subharmnics were not likely influenced by the threshing function.

3-3-2 Smoothing Effect of Threshing Device

In case of small rice combine of head-feeding type, only the panicle (head) of rice plant are fed into the threshing device in the longitudinal direction to the threshing cylinder successively, so that the relation between the rice plant fed to the cylinder and the cylinder torque is similar to the relation between the integrant and the integrated value as discussed in 3-2-2. Therefore, it may be thought that the feed rate fluctuation below a cetain quantity of the wave length does not affect the torque fluctuation of the cylinder. That is, it may be supposed that the threshing device of the small rice combine of head-feeding type may act as the low pass filter. So the feed rate fluctuation which could not exist in the actual field, as shown in tests

4 to 8 in Table 2-10, were produced and this filtering phenomenon was discussed. For example, the periodic square planting density with the wave length of approximately 1.2 m, the average planting density of 2.4 kg/m in two rows and the planting density amplitude of 2.4 kg/m was produced artificially, the combine B was operated under this condition and the cylinder torque was measured. The smoothed wave form through the digital low pass filter with the cut-off frequency of 2.0 Hz is shown Fig.3-15 (b). Because Fig. 3-15 (a) and (b) represent one cycle of the fluctuating planting density and the cylinder torque, it is immposible to find out the filtered components. Therefore, in order to investigate the frequency response charscteristics of the threshing device, the time series corresponding to 40 cycles of the above-mentioned wave were spectrally analized. The results are shown in Fig. 3-16. From this figure, it was found that only the component of 0.2 Hz of the fluctuating planting density affected the fluctuation of the cylinder torque. Therefore, the existence of the filtering effect of the threshing cylinder was verified.

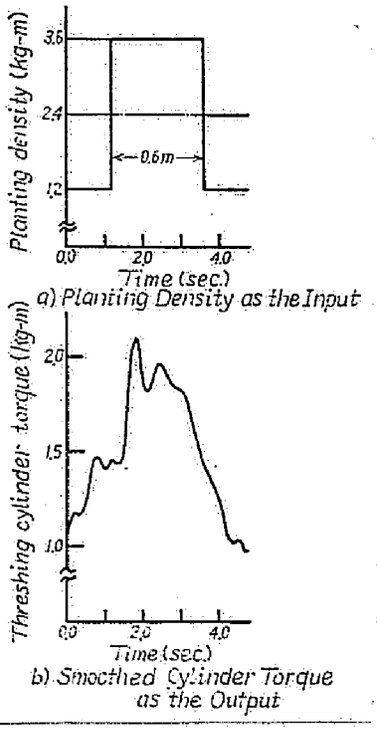

Fig 3-15 Filtering Effect of the Threshing Cylinder

The operating performance of the combine depended upon not only the changes in the smoothed feed rate but also the fluctuating feed rate. Therefore, in order to determine

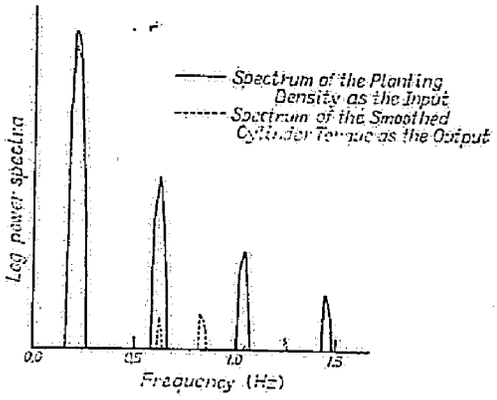

Fig.3-16 Power Spectra of the Planting Density and the Cylinder Torque

the degree of the fluctuation of the feed rate which was the disturbance when the combine was controlled automatically, the natural fluctuation of the feed rate of rice plant in the actual field which was fed into the combine A travelling distance of 6.0 m were measured.

The state of the fluctuation of the straw layer is shown in Fig.3-17 (a). From this figure, it might be obtained that the thickness of the straw layer had the average value of approximately 20 mm and the range of the fluctuation of 10 mm.

Fig. 3-17 (Right)
Fluctuation of the Straw Layer Thickness Fed to the Combine A

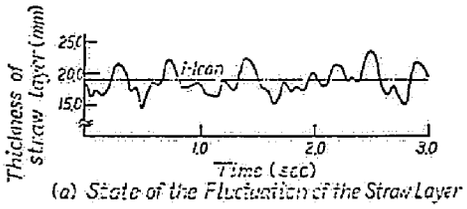

(a) State of the Fluctuation of the Straw Layer

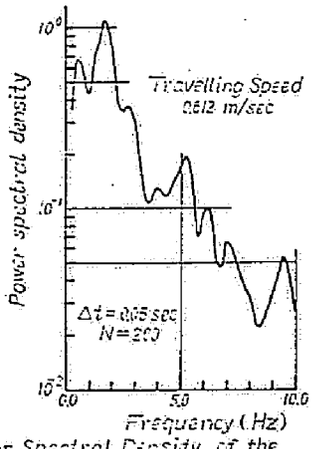

(b) Power Spectral Density of the Fluctuating Straw Layer

The power spectral density of the time series shown in Fig. 3-17 (a) is indicated

in Fig. 3-17 (b). The peak at 1.8 Hz might result from the rupture of the straw layer due to the projection of the link plate of the conveying chain. That is, using the speed and pitch of the conveying chain of the experimented combine, the calculated frequency of this rupture of the straw layer was 1.6 Hz.

Although the frequency of the fluctuation of the straw layer due to the planting interval of the rice plant in the actual field with 0.612 m/sec travelling velocity was to be 3.2 Hz, the peak at this frequency did not appear. This might be due to the fact that because of cutting two rows the flow of rice plant fed into the combine was smoothed in the conveying chain and the ruptures due to the planting interval of the crop were hidden. In the results, the remarkable fluctuation of the feed rate was not observed in the interval of 6.0 m, and the fluctuation of 1.6 Hz could be filtered out and hidden by the above-mentioned filtering effect.

3-4 Conclusions of This Chapter

Combine has the complicated dynamic characteristics of the load at each functional element, especially at the threshing cylinder. In this chapter, for the purpose of obtaining the fundamental knowledge required for the further developement of the combines such as improving the fatigue strength of the functional elements and the functions themselves of the elements of the combine and controlling automatically the combine, a series of experiments of the Western-type small rice combine, the thresher of head-feeding type and the small combine of head-feeding type were conducted and the relative frequency distribution curves which indicated the amplitudes of the fluctuation of the torques of the functional elements, the smoothed fluctuating torques which represented the trends of the fluctuation due to the uneven flow of rice plant fed into the combine and showed the existence of the compensating function among the elements, the correlograms and the power spectral densities which revealed the frequencies of the fluctuations of the torques were computed and discussed for the individual machine. As a result of these experiments and discussions, the following were obtained. For the Western-type small rice combine,

1) According to the relative frequency distribution curves, it was revealed that the torque of the threshing cylinder fluctuated over a wide range but the distribution curves of the engine and travelling counter shaft were not so wide and approximately normal.

2) The smoothed waves of the fluctuating torques showed that the threshing cylinder torques increased at the intervals of 1.2 sec to 2.5 sec, however the engine torque did not so

increased and the travelling torque decreased at these times on the contrary. This seemed to show that because of the great mass moments of inertia of the main rotating parts, especially of the threshing cylinder of the experimented combine, the kinetic energies of these parts compensated the instantaneous increases of the loads at the threshing cylinder.

3) The ranges of the fluctuations of the threshing cylinder torque were wide and their frequency distribution curves were approximately normal at the low feed rates but skewed at the high feed rates. It is noteworthy in case of designing the cylinder shaft that the maximum torque amounted to 6 times as much as the mode at the high feed rate.

4) The fluctuation of the cylinder torque might be caused by the free vibration of the cylinder shaft, the complicated system for power transmission in the combine and the intricate external forces through threshing.

5) Although for the lightload the force acting upon the concave was fluctuated by the teeth of the cylinder and concave, at the heavy load the frequency of the fluctuation reduced to a half for the light load. This phenemenon seemed to show that threshing grains as well as cutting and pressing straws were carried out at the first column of the concave teeth in case of the light load, but for the heavy load the flow of rice fed into the threshing device was changed.

For the head-feeding thresher, the dynamic characteristics of the torques of the main functional elements were discussed by means of the relative frequency distribution curves, autocorrelation functions and power spectra

and the moving average method. The following results were obtained.

1) The maximum value of the threshing cylinder torque of the head-feeding thresher was from 1.5 to 2.0 times of its mode, and the cylinder torque of the head-feeding thresher did not fluctuate so heavily as the cylinder torque of the Western-type small rice combine.

2) As the result of the power spectral analysis, the distinguished frequency of the fluctuating torque of the threshing cylinder was about 5.5 Hz and those of others about 20 Hz, independently of load, respectively. These fluctuations of the torques seemed to be peculiar ones of the experimented thresher.

3) By filtering the above-mentioned fluctuations by means of the moving average method from the original oscillograms which was recorded for feeding binded one-sheaf, the transient fluctuations of the torque at the beginning of threshing was discussed and the following results were obtained.

a) The threshing torque reached the maximum value when the binded sheaf was conveyed with the feed chain from the portion of 1/4 of the cylinder length. This showed that the threshing operation was almost finished between these portions and the panicle (head) was spread and threshed gradually.

b) The maximum values of the threshing cylinder torques for dried rice plant were about 1.5 kg-m and continued for 0.65 sec, and those for green rice plant were about 2.0 kg-m and 0.95 sec. This showed that it was more difficult to thresh green rice than dried.

c) After these maximum values, the torque of the cylinder

decreased to 1.0 kg-m for dried rice and 1.5 kg-m for green rice, and these values continued until the binded sheaf was transported to the end of the cylinder.

d) The torque of the supplementary threshing cylinder, fans and screw conveyer shafts did not almost fluctuate.

For the head-feeding type small combine, the following results were obtained.

1) The relative frequency distribution curves of the threshing cylinder torque were approximately normal but the distribution curves of the engine and travelling shafts were skew.

2) The resistance of the straw of the rice plant to the threshing cylinder was fairly large.

3) The main components of the fluctuating cylinder torque consisted of the torsional vibration of the engine crank shaft, its harmonics and subharmonics and were not likely influenced by the threshing conditions.

4) The filtering effect of the threshing device to the fluctuating planting density was clarified. Namely, only the component of 0.2 Hz of the fluctuating planting density affected the fluctuation of the cylinder torque.

5) Remarkable fluctuation of thickness of the straw layer flowing into the combine was not observed for travelling distance of 6.0 m and the fluctuation of 1.8 Hz might result from the ruptures of the straw layer due to the projection of the link plate of the conveying chain.

CHAPTER 4

Fundamental Studies of Travelling and Vibration Characteristics of the Combine

4-1 Travelling Characteristics of the Full-tracked Western-type Small Rice Combine*

In Japan, it is necessary to decrease the ground contact pressure under the combine because it must be operated on the soft field for harvesting rice. Usually, ground contact pressure which is the value obtained by dividing the weight of the combine by the ground contact area under its tracks has been used. However, the actual contact pressure is different from the above-mentioned value. That is, the contact pressure under the tracks is varied by the weight distribution of the combine, the dynamic behavicrs such as pitching and rolling of the combine body , and the soil codition on which the combine travels.[1)-4)]

As mentioned above, it is necessary to decrease the ground contact pressure, so the travelling device must be the track layer system. This track layer system and the reciprocating elements such as the straw racks seem to make the combine travelling not smooth. The characteristics of the travelling torque and the acceleration of vibration of the combine were spectrally analyzed and the interrelation between them was revealed in this section.

4-1-1 Distribution Pattern of the Ground Contact Pressure under the Combine

The methods used in the past for measuring the ground contact pressure distribution were as follows; to measure the vertical force acting upon the track shoes with strain gages[1),2)]

and to measure soil pressure with the soil pressure cells laid under the ground[3] and on tyre and lags[5].

The soil contact pressure under the shoes of the combine were measured with the reconstructed track-shoe as shown in Fig. 4-1. The links welded on the flat shoe plate were detached

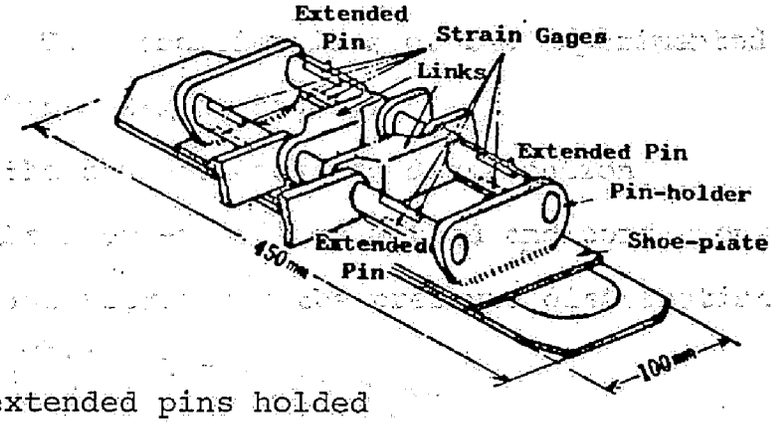

Fig. 4-1
Reconstructed Track Shoe for Measuring the Vertical Force

and suspended by the extended pins holded by the pin-holders at the ends of the shoe plate. When the track rollers rolled over these links, the extended pins were bended, so according to measuring the stresses caused by this bending, the vertical forces could be known. The contact surface of the shoe of the experimented combine with the ground was not flat, and therefore the contact pressure distribution under this track-shoe was not uniform, however it was assumed to be uniform. With the micro-switches the positions of the measuring shoe at which the shoe began to contact and finished to contact with ground surface were marked on the oscillograph and the fluctuation of the vertical force acting upon this shoe between these positions was considered as the contact pressure distribution pattern. At this time the torques at the travelling counter shaft and the acceleration of vibration at the rear of the combine were measured.

The field used for the experiments were the same as

Tests No. 6 and 7 (see Table 2-2 on page 11). Because the rice plant to be harvested were lodged perfectly, cutting height ranged from 7 cm to 35 cm and was 16 cm on the average. The soil in the experimented field was silty loam. The soil pressure distribution pattern were measured on the soft and hard ground conditions. The specifications of the experimented combine were given in Table 2-1 on page 7.

In Fig. 4-2, the contact pressure distribution patterns measured by the above-mentioned method and conditions are shown. The solid line represents the pressure distribution

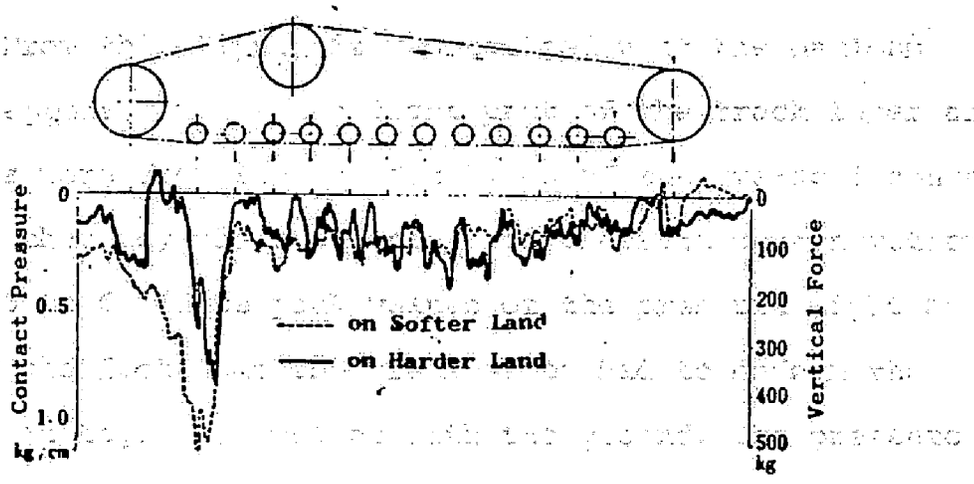

Fig. 4-2 Contact Pressure Distribution Patterns under Tracks of Combine

on the hard ground and the dotted line represents on the soft ground. These lines were drawn considering the change in the vertical forces acting upon the reconstructed track-shoe with time caused by travelling of the combine as the geometrical distribution of the contact pressure. Therefore the change in the vertical force under a track-shoe might be different from the actual pressure distribution which had to be measured at the same time with all the track-shoes reconstructed to

measure the forces as mentioned above. However, because the average contact pressure calculated from this figure was about 0.2 kg/cm^2 which was almost equal to the contact pressure calculated from the weight and the contact area of the experimented combine (namely 0.21 kg/cm^2), then the change in the vertical force under one of the track-shoes might be considered as the force distribution along the track-shoes. The pressure distribution pattern obtained by this method was similar to the influence line of the beams caused by the travelling load system.

From this figure it was noticed that the maximum pressure appeared under the front part of the track layer and its values were from five to six times of the averaged contact pressure, that is, the coefficient of pressure concentration was from 5 to 6. These peak values of the pressure might be caused by the fact that the track-shoes had to deform the soil when it began to contact with the ground. The pressure increased slightly under the center of the track layer. The aspect of the pressure distribution under the combine was very different from that under the tractor to which a drawbar load was applied[2),4),5) and 6)]. This phenomenon might be due to the fact that the drawbar load was not applied to the combine as mentioned above and the center of gravity of the experimented combine laid toward the front.

The pressure distribution on the soft ground was slightly smoother than that on the hard ground.[7)8)] This might be caused by the difference between sinking depthes of the track-shoes. It was very important to uniform the pressure distribu-

tion pattern for the good traficability on the soft ground.

There was not a clear relationship between the positions of the peaks of the pressure distribution and the track rollers. This might be caused by the fact that the pressure distribution pattern obtained by the method mentioned in this section was similar to the influence line of the travelling load system and the error was produced in measuring the positions of the track-shoes relative to the frame of the combine.

4-1-2 Characteristics of the Travelling Torque

The torque of the travelling counter shaft fluctuated at one third period of one revolution of the straw rack shaft on the oscillogram charts. Power spectral densities for the torque of the travelling counter shaft and the acceleration of vibration at the rear of the combine are shown in Fig.4-3.

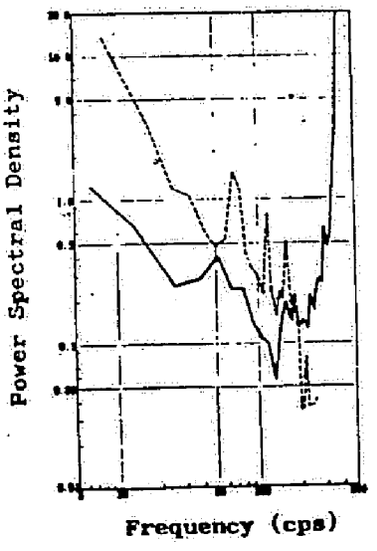

Fig.4-3 Power Spectral Densities of the Torque of the Travelling Counter Shaft (dotted line) and the Acceleration (solid line)

The experimented combine had three straw racks reciprocating at an interval of 120 deg, and it was revealed that the period of fluctuation of the torque of the travelling counter shaft was equal to one third period of reciprocating motion of the straw racks. Therefore, the experimented combine seemed to show pitching during operations because the great mass such as the straw racks reciprocated. That is, the fluctuation of the travelling

torque was assumed to be due to the pitching motion of the combine which was produced by the reciprocating motions of the straw racks. This was indicated in Fig. 4-3, namely the powers at the lower frequencies increased for both the travelling torque and vibration acceleration. Because vibration and pitching of the combine have the undesirable effects upon the operating performances, strength, durability, travelling performancs and stability of the combine, these problems on pitching and vibration must be studied in future.

4-2 Travelling Characteristics of the Head-feeding Type Small Combine**

On the travelling device of the small combine, there are number of limitations, such as the construction of the components, the soil conditions and the case of running over a ridge to move into the adjacent field. In this section, the travelling performances such as the pressure distribution under the small combine of the head-feeding type and the characteristics of the fluctuation of the travelling torque will be discussed for the purpose of developing the desired travelling device required for the small combine. The specifications of the experimented combines were given in Table 2-6. The track-shoes of the experimented combines were covered with the thick rubber in order to travel stably. For the necessity to run over the ridge, the driving sprocket-wheels were located at the upper and rear position of the travelling device and the take-off angle to the ground surface β was larger in comparison with that of the ordinary tracked vehicle (see Fig. 4-6). Since the driving sprockets were located at the upper and rear position and the numbers of the teeth in these sprockets were small, the power transmission from the sprockets to the crawlers was intermittent. Thus the fluctuation of the travelling torque and so the fluctuation of the travelling velocity may occur. The vibration of the small rice combine might be caused by these fluctuations of the torque and velocity.

Although the tracked vehicle has some problems as stated above, it is necessary to decrease the ground contact pressure under the combine for travelling on the soft paddy

field. The experimented combines had the above-mentioned characteristics and required the higher power for travelling as indicated in 2-3-2.

In this section, for the purpose of clarifying the travelling performances of the head-feeding type combine, the ground contact pressure under the track-shoe, fluctuations of the travelling velocity and torque, travelling efficiency and resistance will be discussed.

4-2-1 Distribution Pattern of Contact Pressure under the Combine

It is preferable to measure the vertical force acting upon the individual track-shoe simultaneously. However, this method was difficult because of the construction of the travelling device of the experimented combines, so the pressure cell was laid in the thick rubber coating of the center of the track-shoe lug.

The soil pressure cell must be produced in consideration of sensibility, measurable range, dynamic characteristics, direction property, linearity, mount of deflection and ease of construction[9),10),11),11')]. In Fig.4-4, the soil pressure cell used for the experiments is shown. Under pressure of 0.5 kg/cm^2, Ballstenius' condition $D/\delta > 1000$ was satisfied, where D was a diameter of the diaphragm and δ was deflection of the diaphragm at the center. Higher value of D/δ resulted in lower degree of deflection of the diaphragm. Therefore, the attention had to be given to the problem of temperature compensation of the strain gages under measuring. The force-strain curve of the pressure cell was obtained by laying the cell in the rubber coated track-sheo under the same situation as the experiment and applying the

forces upon the point over which the road wheel was to roll. In this calibration experiment, the track-shoe was placed on the standardized sand.

The experiments were carried out on sandy loam paddy field after harvesting with the combine A. In this field the combine depressed the soil surface approximately 2 cm and the clear track prints could be observed.

The distribution pattern of the ground contact pressure under the small combine is shown in Fig. 4-5. The peak values

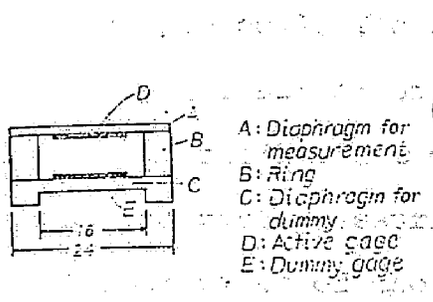

Fig.4-4 Soil Pressure Cell

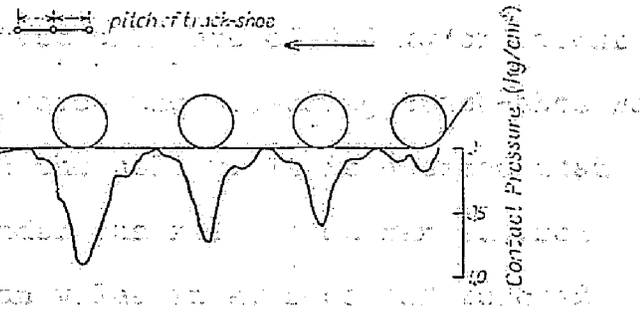

Fig. 4-5 Distribution Pattern of Ground Contact Pressure

of the contact pressure appeared under each road wheel (idler wheel) except the foremost wheel. Table 4-1 indicates the mean

Table 4-1 Characteristics Values of Contact Pressure (kg/cm^2)

		Mean	Under the 1st i. w.	Under the 2nd i. w.	Under the 3rd i. w.	Under the rear i. w.
Average	(R)	0.248	0.645	0.741	0.725	0.439
	(L)	0.285	1.11	0.826		0.537
Maximum	(R)	0.39	1.31	1.11	1.07	0.75
	(L)	0.55	1.77	1.29		1.16
Minimum	(R)	0.0	0.0	0.0	0.0	0.0
	(L)	0.14	0.57	0.22		0.16
Standard deviation	(R)	0.096	0.380	0.578	0.263	0.218
	(L)	0.11	0.375	0.574		0.370

i. w. : idler wheel.

values and the peak values under each road wheel of the ground

contact pressure. Numbers of data were 12 and 21 for right and left track shoe, respectively. Scattering of data was large, because the ground contact pressure acting upon the track-shoe was measured. However it was assumed to obtain the reliable value by increasing number of data.

Total value of the mean of the ground contact pressure was 0.27 kg/cm^2 and this value was higher than the indicated value in the specification. This difference might be due to the difference of the experimental conditions on the standardized sand and on the field of sandy loam as well as the position of the pressure cell. The contact pressure of 0.0 kg/cm^2 might be caused by the situation at which the measuring track-shoe was located unexpectedly just over the hollow. It is noticed that the ground contact pressure under the road wheel ranged from three to four times of the mean value in average and reached six times of that in maximum. That is, the maximum coefficient of pressure concentration amounted to 6.0.

4-2-2 Characteristics of Fluctuation of Travelling Velocity and Torque

With respect to the fluctuation of the travelling velocity of the tracked vehicle, Lwow obtained the velocity of a point A in Fig. 4-6 on the assumption that the crank OB and the slider A composed the slider crank mechanism[12]. Woelke had regarded the point A as an origin of a coordinate system and obtained the velocity of the point O as the function of the angle α. He obtained the following track-shoe velocity.

$$V_o = -R\omega\cos\alpha + (h - R)\cos\alpha \frac{R\omega\sin\alpha}{[l^2 - (h - R\cos\alpha)^2]^{1/2}} \quad (4\text{-}1)$$

where $\omega = d\alpha/dt$ and $l = AB$

Thus it may fairly be presumed theoretically that the travelling velocity of the tracked vehicle fluctuates. In order to verify this fluctuation of the velocity, the acceleration of vibration of the combine was measured with the unbonded strain gage type accelerometer (upper dynamic range of 10 g, natural frequency of 280 Hz and damping ratio of 0.7) and the wave form of the acceleration was recorded on the oscillograph chart by the galvanometer with natural frequency of 500 Hz. The acceleration wave was sampled at interval of 0.002 sec, the higher frequency components above 13 Hz contained in this wave were cut off with the digital low-pass filter and the smoothed acceleration data obtained were integrated with respect to time by the digital computer. These integrated values gave the fluctuation of the travelling velocity. The experiments were carried out, travelling combine B on the paved road under the constant and simple surface conditions. The result of computation is shown in Fig. 4-7. The frequency of the fluctuation was equal to one ninth of the angular velocity of the driving sprocket shaft. This

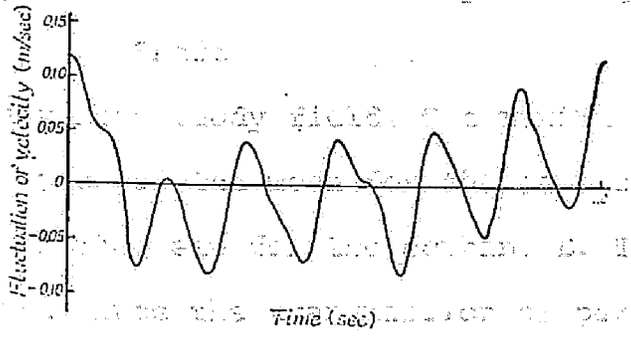

Fig. 4-7 Fluctuation of Travelling Velocity (Mean Velocity ; 0.42 m/sec)

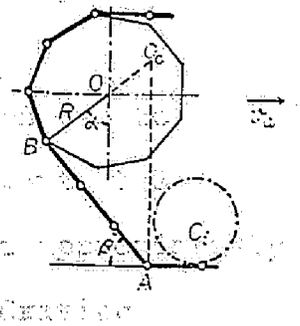

Fig. 4-6 Section of Track Assembly

fluctuation was caused by the intermittent transmission of power from the driving sprocket to the track-shoe since the number of

teeth in this sprocket was nine. It was revealed that the ratio of the maximum to the mean velocity was 1.135 for the experimented combine. The fluctuation of the travelling velocity has direct effects upon vibration of the combine as discussed in the latter chapter.

The torque of the driving sprocket shaft fluctuated at the same frequency as one ninth of the angular velocity of this shaft. The amplitudes of the fluctuating torques of the driving sprocket shaft can be indicated by the relative frequency distribution curves as shown in Fig. 4-8. The combine travelled

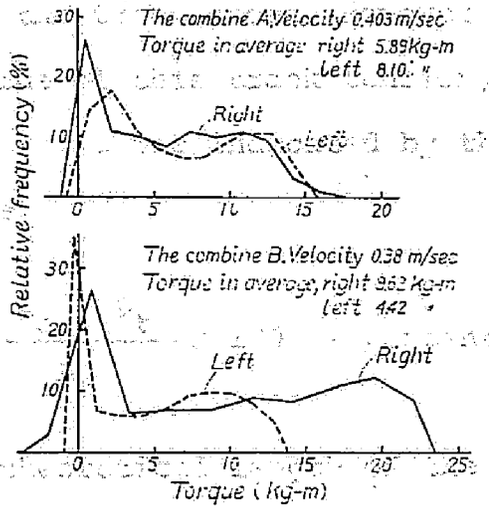

Fig. 4-8 Relative Frequency of Torque of Driving Sprocket Shaft

on sandy loam paddy field. The maximum torque was of two to three times of the mean for the combine A and of 2.4 to 3.2 times of the mean for the combine B. The modes were approximately 0.0 kg-m since the transmission of power from the driving sprocket to the track-shoes was intermittent and then the torque was not applied between each engagement of the teeth in the sprocket with the track-links of the crawler. The negative values

of the torque might be caused by the inertia effect of the combine body when the power transmission from the sprocket to the crawler was intermitted.

4-2-3 Travelling Resistance and Efficiency of Endless Track of Combine

The travelling performance is considerably affected by tightness of the endless track. The experiments were carried out for the combine A to clarify the effect of tightness of the endless track to the travelling efficiency. To indicate quantitatively the degree of tightness of the endless track, it is desired to use tension among the track-shoes. However, it was difficult to measure the value of this track tension, then in this section tightness of the tracks was indicated by the loose index (L.I.) defined as follows.

$$\text{L.I.} = \frac{L_o - L_t}{L_t} \times 100 \quad (\text{percent}) \qquad (4\text{-}2)$$

where L_t was the theoretical length of the tightened endless track and L_o was the length of the loosened endless track under operation. For the combine A, the recommended values of L.I. were 0.5 to 0.7 percent. The torques of the driving sprocket shaft was measured for both cases where the combine was lifted up, supported on the stand under the combine chassis and idled the tracks and where the combine travelled on the hard sandy loam. Let the average torque corresponding to the former case be T_i and to the latter case be T_r, then the net running torque is $T_r - T_i$ and the efficiency of the travelling device is given by the following equation.

$$e = \frac{T_r - T_i}{T_r} \times 100 \quad (\text{percent}) \qquad (4\text{-}3)$$

The relationships between the driving torque and the loose index are given in Fig. 4-9. It was revealed that the idling

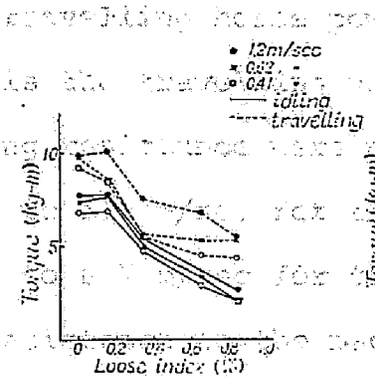

(a)

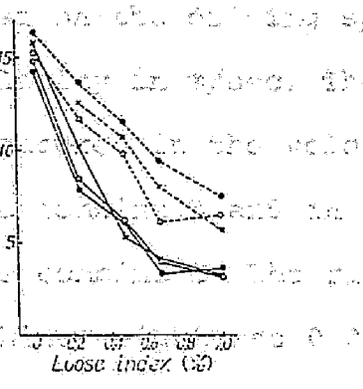

(b)

Fig. 4-9 Loose Index and Torque of the Right (a) ant Left (b) Driving Sprocket Shaft

torque was not affected by the circumferential velocity of the sprocket in the range of 0.4 m/sec to 1.2 m/sec but the travelling torque showed a tendency to increase as the increasing velocity. This was due to the increase of the travelling resistance as the increasing velocity. However, both the idling and travelling torques were considerably affected by the tension of the endless track. And it was revealed that the idling torque of the tracks was higher than the net travelling torque. The relationships between the efficiency of the travelling device and the tightness of the tracks are indicated in Fig. 4-10.

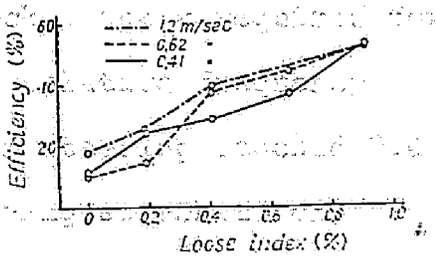

Fig. 4-10 Efficiency of Travelling Device

It was indicated that the tightness of tracks affected considerably the

efficiency of the travelling device. For the recommended tightness, the efficiency was 40 percent.

The travelling resistance r_t (kg) is given by

$$R_t = 75N_t/v \ , \qquad (4\text{-}4)$$

where N_t is travelling horse power on the driving sprocket shaft and v is the travelling velocity in m/sec. The values of the travelling resistance were measured in the velocity region of 0.4 m/sec to 1.2 m/sec for the combine A and in the region of 0.2 m/sec to 0.7 m/sec for the combine B. The ratio of the travelling resistance to the machine weight was 0.33 for the combine A and 0.2 for the combine B. It was reported that the travelling resistance of 25 track layer tractors on the harrowing field was approximately 0.1 of the tractor weight[14]. It was revealed that the travelling resistance of the experimented combines was considerably high. The net travelling resistance was 85 kg or 0.14 of the total weight by calculating from the values in Fig. 4-9 and in this section. This net resistance was assumed to be the net rolling resistance required for deflecting and flowing the soil under the tracks.

The maximum torque of both the right and left driving shafts required for starting the combine at rest were 91.4 kg-m for 1st velocity and 104 kg-m for 2nd velocity. These reached 6 and 5.2 times of the mean, respectively.

The torques of the driving sprocket shaft required for steering are shown in Fig. 4-11 with the relative frequency distribution curves. The mean torques for steering reached 2.4 to 2.7 times of the mean torques of the driving sprocket for

travelling. It was revealed that the torques of the driving

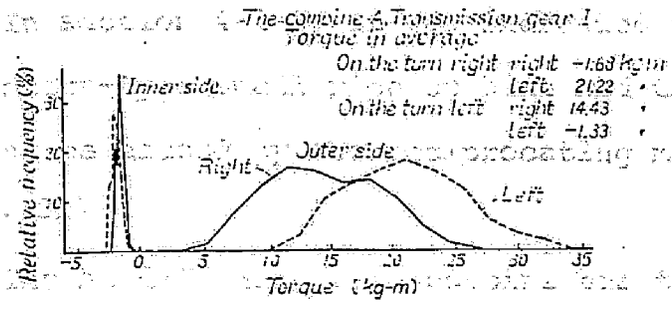

Fig. 4-11 Relative Frequency Distribution of Torque of the Driving Sprocket Shaft for Steering

sprockets were required to be fairly large for steering.

As the results of these experiments and discussions, although the track-type travelling device is necessary in order to decrease the ground contact pressure and to be enable to travel on the soft paddy field, it must be noticed that the travelling device of this type has direct effect upon vibration of combine, efficiency of power transmission and steering of combine.

4-2-4 Vibration Characterictics of the Head-feeding Type Small Combine

In section 4-1-2, it was indicated that the vibration of the Western-type small rice combine had the pitching motion which might be caused by the reciprocating motions of the straw racks.[20), 21)]

The head-feeding type combine has the travelling device of the endless track, and the complicated structure of many reciprocating or rotating parts such as a cutting, lifting, threshing and conveying devices. Therefore, higher degree of vibration may be induced to the combine. These vibrations produce various problems concerning maintenance of the machine and serious influences upon the operator of the combine.

In this section, for combine B the leading causes of vibrations will be investigated and the influences of vibration on the operator and the operating conditions will be discussed. The principal specifications of the experimented combine were given in Table 2-6. The supplementary descriptions of the experimented combine are as follows. The 3rd travelling velocity was 0.32 m/sec and 4th was 0.52 m/sec at the engine speed of 1600 rpm.

The vibrations were measured by the strain-gage-type accelerometers whose upper dynamic ranges were 2g,5g,10g, 20g or 50g. These accelerometers were placed on the cutting and lifting block, the chassis of the combine body, back rest of the seat and the operator's back. The accelerometers on the chassis were as apart as possible from the center of gravity of the combine in order to detect the pitching, rolling or yawing motion due to the intermittent power transmission from the driving sprocket

to the crawler. All the accelerometers could transduce the acceleration of vibration in three directions, namely the vertical, longitudinal and transverse directions. The rotating speeds and the torques of the driving sprocket shafts were also measured.

In order to measure the vibration under the ordinary operating condition, the combine was travelled on the flat field. But it was travelled on the paved road when it was necessary to discuss the situation when transporting the combine, to make the travelling condition simple and to avoid the absorption of vibration to soil. The experimental conditions are indicated in Table 4-2.

Table 4-2 Experimental Conditions

	Travelling	Measured objects
1. On the field	Stop Travelling at the 3rd speed Travelling at the 4th speed	Combine body Cutting and lifting block Back rest of the seat Combine operator
2. On the asphalted pavement	Travelling at the 4th speed With driving axles shifted a half pitch With non-shifted driving axles	Combine body

Since the frequency and phase characteristics of the combination of the accelerometers and the recording galvanometers were very important, before the travelling experiments on the field or road these characteristics had to be clarified by exciting the accelerometer with the sinusoidal input of the known amplitude and frequency and recording the output of the acclerometer and the galvanometer on the oscillogrph chart. The sinusoidal input had the magnitude of 0.2g and the frequency of 5 Hz to 400 Hz. The frequency and phase characteristics of

the instruments obtained by this method are indicated in Fig.4-12. The amplitude ratios were 1.0 within the frequency range of 40 Hz and the phase shifts were great even at 20 Hz. Therefore when the vibration characteristics of higher frequency than 50 Hz were to be discussed upon the wave forms on the oscillograph chart, these frequency characteristics had to be considered.

Results and Discussions

1 Analysis of Vibration in Combine Body

The acceleration data were spectrally analyzed in this section. The power spectral densities of the acceleration of vibration in three directions of the combine B, which travelled at the 3rd velocity on the field and of which all elements were rotated, are shown in Fig. 4-13.[22)]

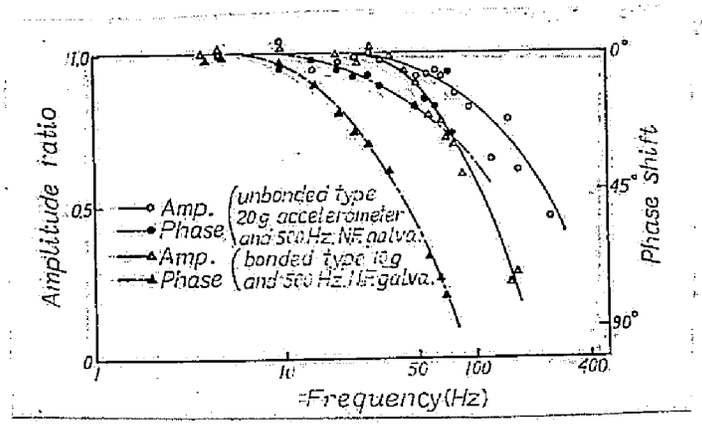

Fig. 4-12 Bode Diagrams of Accelerometer and Galvanometer System

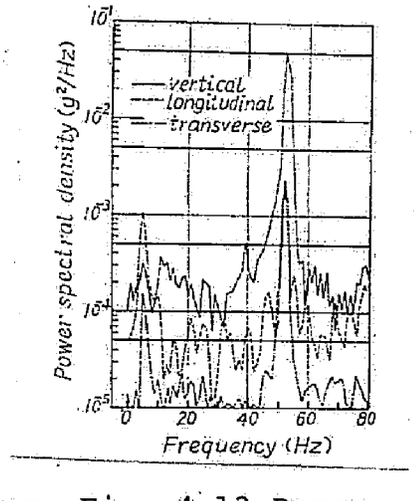

Fig. 4-13 Power Spectra of Vibration

The peaks of power of the acceleration were observed at the frequencies of 5 - 6 Hz, 52 Hz and at their multiplied.

At first, the low frequency, such as 5 - 6 Hz, components will be discussed. As mentioned in section 4-2-2, the travelling velocity of the tracked vehicle was not constant

according to geometrical analysis of kinematics of the endless track. Therefore, the period of the fluctuating velocity can be calculated from the values of the angular velocity of the driving sprocket and pitch of the endless track. When the combine travelled at 3rd velocity, this period was 6.06 Hz since the driving sprocket had nine teeth. Namely, the peaks at the frequency of 5 - 6 Hz in Fig. 4-13 was due to the fluctuation of the travelling velocity.

Although with the analysis of kinematics of the endless track the fluctuation of the travelling velocity was presumed to be in longitudinal direction, from Fig. 4-13 it became obvious that there also existed the lower frequency components of vibration in vertical and transverse directions. This lower vertical component of vibration might be caused by the fact that the under roller in the track assembly was raised a little with the upper sprocket and then pitch acclerations on the combine were observed.

The experimented combine had independent two driving sprocket shafts which were connected through the clutch-brake steering system. Since the clutches of this system was a jaw-type, the torque was not always transmitted in phase from the right and left drive sprocket to the right and left track-shoes according to the state of engagement of these clutches. The power spectra of vibration of the combine corresponding to the case where the phase difference of engagement of the sprocket and the track-shoe between the right and left travelling devices existed and where the phase difference did not exist are shown in Fig. 4-14. The phase difference was adjusted to be a half

pitch of the drive sprocket, namely 20 deg. When the above-mentioned phase difference existed between the right and left drive sprockets, it was presumed that the combine might yaw about the vertical axis. This is indicated in Fig. 4-14, that is, the peak of power spectrum of vibration in the transverse direction at the frequency of 12 Hz (= 6 Hz x 2) which was grown when the phase shift existed was more remarkable than that of 6 Hz which was grown when the phase difference did not exist, and than those of 12 Hz in the vertical and longitudinal directions.

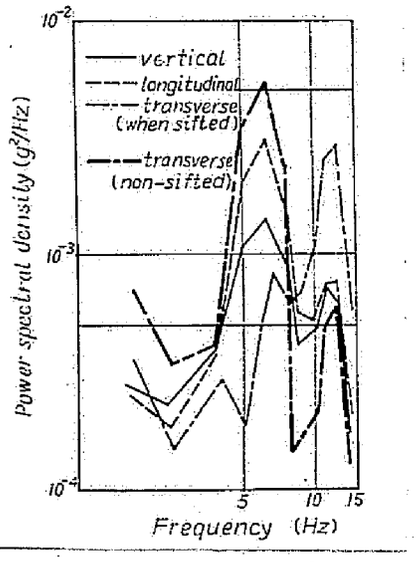

Fig. 4-14 Power Spectra of Vibration of Combine

These phenomena indicate that the low frequency vibration in the transverse direction is considerably influenced by the phase difference between the right and left driving sprockets and the combine may yaw about the vertical axis.

The engine of the experimented combine was of a four-stroke cycle and had the vertical one cylinder. Its speed was 1550 rpm under the experiments. Since the vibration of the engine was caused by inertia force of the reciprocating parts, the frequency of 52 Hz and its multiplied were assumed to be remakable. The peaks of 52 Hz in the power spectrum of vertical vibration in Fig. 4-13 resulted from the engine. The engine was directly mounted on the combine chassis, therefore the anti-vibration supporting should be considered.

The cutting and lifting block was jointed to the combine body with a pivot to adjust the cutting height of rice plant. It is indicated in Fig. 4-15 that the components of 5 - 6 Hz and 52 Hz were similarly remarkable as the vibration of the combine chassis except the peaks at 20 - 30 Hz were observed.

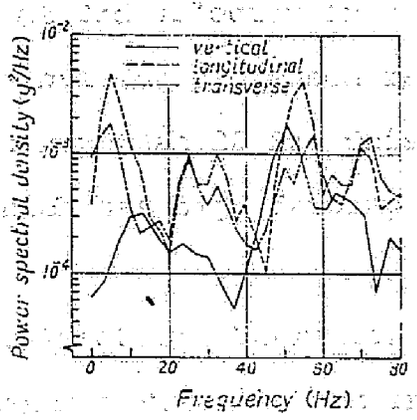

Fig. 4-15 Power Spectra of Vibration of Cutting and Lifting Block of the Combine Travelling at 3rd Velocity

This component of 20 - 30 Hz might be caused by the lifting and reciprocating motions of the conveying and cutting devices.

2 Effects of Vibration on Operator

It has been revealed in the preceding part of this section that there were various vibrations in the combine body excited by various sources. Therefore the operator is always exposed to mechanical vibration which will cause the fatigue of the operator. In the reference 15), the data on the driver disturbance on the concrete road, vertical acceleration at driver's waist level and truck driving over various test cources and average vertical acceleration and frequency distribution beneath the seat of a farm tractor on the

field were given.

In order to investigate the frequency characteristics, transmission ratio of acceleration and the magnitude of vibration, the acclerometers were mounted on the upper part of the operator's back and the vibration on him was observed. Fig. 4-16 indicates the power spectrum of vibration on the operator in case of travelling at 3rd velocity on the field. It was revealed that the power of vibration decreased remarkably in the region of the higher frequency than 20 Hz. This shows that the human body is a system which has high damping factor as a vibrating model.

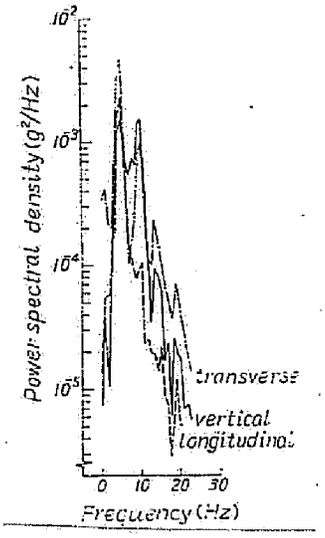

Fig. 4-16 Power Spectra of Vibration of Combine Operator's Back in case of Travelling at 3rd Velocity on the Field

Since it was interested and useful to investigate the detail of this absorbing characteristics of the human body, the transmission ratio of acceleration of the human body were calculated. Fig. 4-17 shows the power spectra of the acceleration at the back rest of the seat. Since the operator's seat of the experimented combine was just above the engine and was supported by only four small

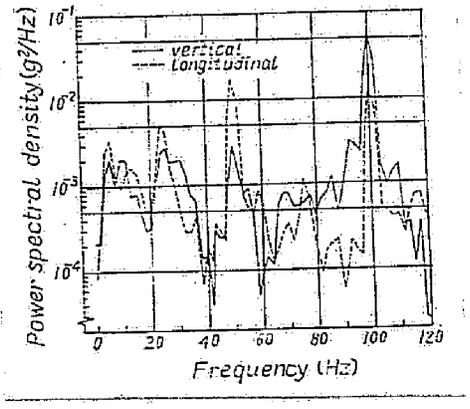

Fig. 4-17 Power Spectra of vibration of Back Rest of the Combine Seat

hard rubbers, it could not be expected to absorb vibration and the seat vibration was caused by the driving endless tracks and espesially by the engine. From these power spectra of the acceierations at the seat and the operator's back, acceleration transmission ratio of the operator could be obtained. The relationship between the power spectral densities of the input and output is given by the following equations[16),17)].

$$P_{yy}(f) = |G(f)|^2 \times P_{xx}(f) \qquad (4\text{-}5)$$

$$P_{xy}(f) = G(f) \times P_{xx}(f) \qquad (4\text{-}6)$$

where $P_{yy}(f)$; Power Spectral Density of Output

$G(f)$; Transmission Ratio or Gain of Frequency Response Function of the System

$P_{xx}(f)$; Power Spectral Density of Input

$P_{xy}(f)$; Cross Power Spectral Density of Input and Output

Eq. (4-5) contains only the gain factor $G(f)$, while Eq. (4-6) is actually a pair of equations containing both the gain factor and the phase factor. Since in this study, the phase factor was not useful, only the gain factor, namely the transmission ratio was calculated. Fig. 4-18 indicates the acceleration transmission ratio in the vertical direction calculated from the values in Fig. 4-16 and Fig. 4-17. For reference, the data given by M. Oshima are indicated in this figure[18)]. It was found that an acceleration transmissibility in the experimented human body in sitting was 8 Hz, while it

was reported that for the sitting man the first resonance was between 4 and 6 Hz and for the standing man resonance peaks occured at about 5 and 12 Hz.[19)]

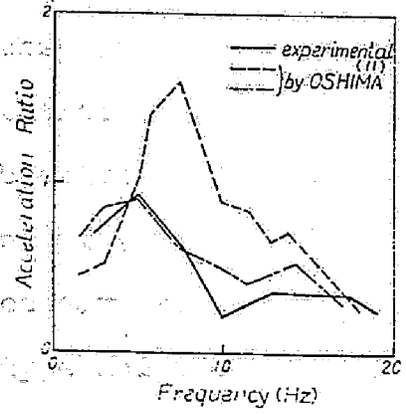

Fig. 4-18 Transmission Ratio of the Vertical Vibration Acceleration of the Combine Operator in Sitting

The magnitude of acceleration on the operator versus its frequency has been considered to examine riding comfort. The magnitudes of the vibrations averaged ten cycles on the oscillograph charts are given in Fig. 4-19. From this figure,

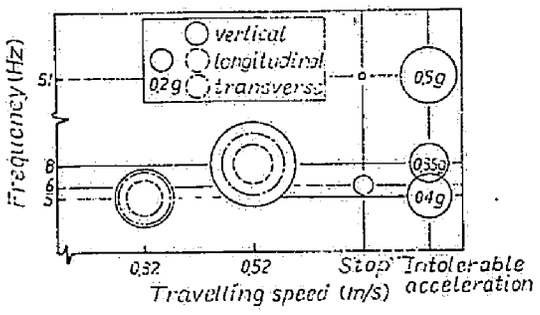

Fig. 4-19 Averaged Peak Accelerations of the Combine Operator and intolerable Accelerations by D.E. Goldman[15)]

it was obvious that the operator suffered from vertical vibration of magnitude about 0.5 g at 5 Hz (driving at 3rd velocity)

and of magnitude about 1.0 g at 8 Hz (at 4th velocity). Some informations have been given on comfort and tolerance levels[15] and they indicated the values of 0.4 g at 5 Hz, 0.35 g at 8 Hz and 0.5 g at 52 Hz. Therefore it was revealed that the operator on the experimented combine suffered from the low frequency vibration which exceeded the physiological limit magnitude of vibration.

From the point of view of ride comfort and operating performance, it is necessary to improve the travelling device of the endless track type and anti-vibration support of the seat.

4-3 Conclusions of This Chapter

Combines used in Japan are required to decrease the ground contact pressure because they must be operated on the soft paddy field. And they are of small size and have many rotating and reciprocating elements, then they have complicated oscillating motions when they are operated. The experiments were produced for the purpose of revealing the above-mentioned travelling and dynamic characteristics. And the following results were obtained.

For the Western-type small rice combine,

1) The contact pressure distribution pattern under the full track combine was never uniform. The maximum pressure was observed under the fore of the track contacting with soil, and reached to 6 times of the average pressure.

2) The torque of the travelling counter shaft fluctuated periodically with pitching of the combine body which was caused by the reciprocating motions of the straw racks.

For the head-feeding type small combine,

1) The ground contact pressure distributions measured by the pressure cell laid in the rubber coating of the track-shoe were not uniform. The peak values of the pressure appeared under each road wheel except the foremost wheel. The maximum value of the pressure was 6 times of the average pressure.

2) The travelling torque and velocity fluctuated at the frequency equal to one ninth of the angular velocity of the driving sprocket shaft. This fluctuation was caused by the intermittent transmission of power from the driving sprocket to the track-shoe.

3) It was revealed by the relative frequency distribution curves of the travelling torque that the maximum value of the travelling torque reached 3 times of the average torque and the mode was approximately 0.0 kg-m because of the above-mentioned intermittent power transmission of the travelling device.

4) The efficiency of the travelling device, especially the driving sprocket and track system, of the experimented combine was remarkably low, namely ranged from 0.1 to 0.5, and was considerably affected by tightness of the endless track.

5) It was revealed that the torques of the driving sprockets were required to be large for steering. Namely, the mean torque for steering reached 2.7 times of the mean torque of the driving sprocket for travelling.

6) The lower frequency vibration of the head-feeding type small combine was caused by the fluctuation of the travelling velocity due to the intermittent power transmission from the driving sprocket to the track.

7) The higher frequency vibration was caused mainly by the engine vibration.

8) The operator on the experimented combine suffered very uncomfortable vibration of great magnitude acceleration at easy transmissible frequency range from the endless track.

As the results of these experiments and discussions, it was necessary to improve the travelling device of the small combine for ride comfort of the operator, strengh of machine and accurate operation of combine.

CHAPTER 5

Automatic Steering of Combine

In the paddy field, the row of rice plant transplanted by the machine meander randomly and the combine must be steered frequently when harvesting in such a paddy field. Therefore the automatic steering system for the combine must be developed for full automatic harvesting.

The automatic steering system presented here had tested two kinds of sensor; one of which detected row of rice plant from both sides of the row by contacting it and another of which detected row from one side. In order to ensure steering accuracy, the former sensor consisted of the double sensors; namely main and supplementary sensors and the electric circuit of the main sensor having the characteristics of delayed reversion to the straight travelling to realize the steering such as the man's steering of the combine. The object of the automatic steering system discussed in this chapter was to correct the course of the combine which harvested in the field travelling straightly, but was not designed to turn at the end of the field and to enter into the unharvested rows of rice plant.

In order to simplify the experimental conditions, to ensure the repeatability of the experiments and to reveal the fundamental problems, the experiments were produced only for the artificially planted row of plant in sinusoidal form.

With using the results of these fundamental experiments, the factors affecting the influences upon the stability and accuracy of the steering system were discussed.

5-1 Experimental Apparatus*,**,***

The principal descriptions of the experimented combine are given in 2-3-1. The steering device consisted of the side clutches, which drove the sprocket wheels for travelling and were disengaged by pulling the steering levers, and the side brakes which were applied upon the sprocket wheel shaft by pulling more the steering levers.

The many detectors of the automatic steering system for the agricultural machinery which sensed the input have been proposed[1) - 6)], and the system represented in this chapter had the input detectors which sensed the row of rice plant by touching it since this contacting detector could be made easily and operated surely. The construction of the sensor which detects the row of rice plant from both sides of the row is shown in Fig. 5-1. It consisted of the contacting links and the sliders. The hydraulic circuit was controlled by the on-off of the electric circuit which were made and broken by the microswitches actuated by the cams fixed on the sliders and the hydraulic cylinder rod. These sensors were equipped at the dividers' position instead of the dividers. The features of the experimented electric-hydraulic circuit were as follows. 1) The relays RR and RL of the electric circuit of the main sensor were driven by the circuit which had the delayed reversion characteristics and so they had the hysteresis. In the man-machine system, when the operator finds out the front obstacles and avoids them, he steers a little over (namely, delays return to the straight travelling). By this method the steering of the combine may be approximated to the steering of man which reduces the number of steering and

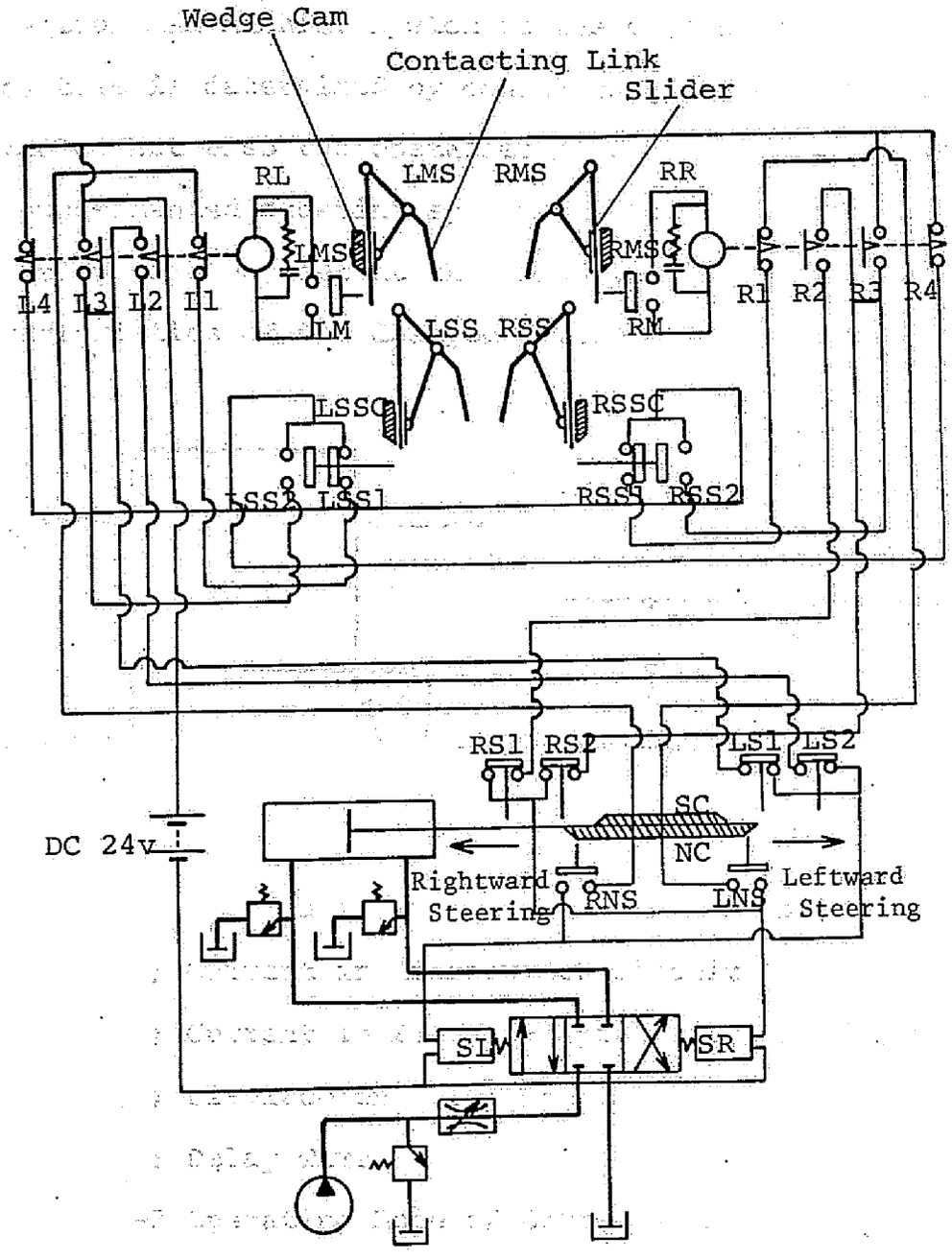

Fig. 5-1 Electric-hydraulic Circuit of Automatic Steering System with Sensors Detecting Row of Plant from both Sides of It

the travelling distance and smoothes the combine movement. However, the actual man-machine system is the closed loop in which the delay time is determined by considering not only the front obstacles but also the obstacles in the steering direction. The experimented steering system was the open loop in which the delay time was set at the fixed value. The operation characteristics of the delayed return is shown in Fig. 5-2.

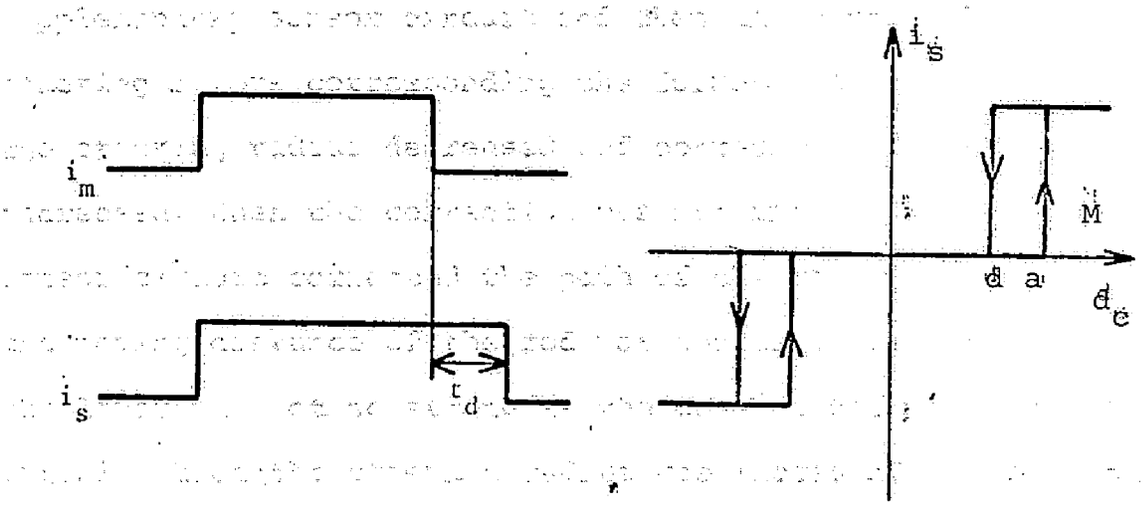

(a) (b)

i_m ; Current in Microswitch Circuit

i_s ; Current in Electro-magnetic Solenoid Circuit

d_c ; Displacement of Wedge Cam

t_d ; Delay Time

Fig. 5-2 Operating Mode of Currents in Microswitch and Electro-magnetic Solenoid Circuit of Main Sensor (a) and Hysteresis Characteristics of Relay Switch in Electro-magnetic Solenoid Circuit of Main Sensor (b)

2) In order to avert the phenomenon that to the sudden change in the input row the sensors could not follow the row of plant, the sensors consisted of the double sensors, namely the main sensors LMS and RMS as well as the supplementary sensors LSS

and RSS. To ensure the accuracy of the following motion the stopper microswitches for the rod of the hydraulic actuator were LS1 and LS2 for the leftward steering and RS1 and RS2 for the rightward steering and the strokes of the rod were different for the main and supplementary sensor citcuits as shown in Fig. 5-1. Therefore the two steering radii were set. The moving distance of the rod for the main sensor circuit was longer than for the supplementary sensor circuit and then the force pulling the steering levers corresponding the former was stronger , then the steering radius decreased and correcting of the path was increased. When the correction was not enough, the supplementary sensor circuit corrected the path of the combine. In this case the moving distance of the rod was shorter, the force pulling the lever was not so strong as the case of the main sensor circuit, then the steering radius was increased and correcting of the path decreased. Therefore, it was possible to follow the row of rice plant precisely.

In Table 5-1, the posssible combination of the input

Table 5-1 Truth Table of Automatic Steering System in Fig. 5-1

Variable / State	Input						Output		Remarks
	RM	LM	RSS1	RSS2	LSS1	LSS2	SR	SL	
1	0	0	1	0	1	0	0	0	Straight Travel
2	1	0	1	0	1	0	1	0	Rightward Steering
3	1	0	0	1	1	0	1	0	"
4	1	0	1	0	0	1	1	0	"
5	0	0	0	1	1	0	1	0	"
6	0	1	1	0	1	0	0	1	Leftward Steering
7	0	1	1	0	0	1	0	1	"
8	0	1	0	1	1	0	0	1	"
9	0	0	1	0	0	1	0	1	"

variables (namely, ON (1) or OFF (0) of the microswitches in the electric circuit of the sensors) and the output variables corresponding to each combination of the input variables (namely, ON (1) or OFF (0) of the electro-magnetic solenoids of the directional control valves in the hydraulic circuit), the so-called truth table, is shown. The leftward steering corresponding to the state 6 in this table was performed as follows. When the main sensor LMS contacted with the row of rice plant and the contacting link was moved over the dead zone width, the wedge cam LMSC closed the microswitch LM, the relay coil was energized, the relay contacts L1 and L4 were OFF, L2 and L3 were ON, the solenoid SL was energized and the valve changed the direction of oil to move the rod rightwards. Although the cam SC fixed on the rod made the stopper LS2 OFF, since LS1 was still ON, SL continued to be energized and the rod continued to move until SC made LS1 OFF and the combine was steered leftwards. After steering, although the contacting link of LMS separated from the row of rice plant and LM was made OFF, the relay coil continued to be energized by the delay circuit and the combine continued to be steered until the delay time was lapsed. When the relay coil finished to be energized, L1 and L4 became ON and L2 and L3 became OFF. Since the rod of the hydraulic actuator was the state where it had been moved to the right, the electric current flowed into the solenoid SR through LNS which was made ON by the wedge cam NC fixed on the rod right after moving of the rod, the rod began to move leftwards, returned to the middle position where LMS was made OFF, the steering was finished and the combine began the straight

travelling again.

The leftward steering by the supplementary sensor circuit corresponding to the state 9 in Table 5-1 was as follows. When the contacting link LSS of the similar construction as the main sensor moved over the dead zone width, the wedge cam LSSL actuated simultaneously the double microswitches LS and LSS1 was made OFF and LSS2 was made ON.Since the main sensor circuit was not made, the electric current flowed into the solenoid SL through the relay contact R4 which was made ON, the rod moved rightwards and stopped to move at the position where SC made LS2 OFF since L2 was OFF. And the combine began to steer leftwards. When the contacting link separated from the row of rice plant, the electric current flowed into SR through LNS which was made ON by NC right after moving of the rod and L4 of the main sensor circuit which was OFF, the rod moved leftwards, stopped at the middle position where LNS was made OFF and the combine began the straight travelling.

The electric-hydraulic circuit of the automatic steering system with the sensors which detected the row of rice plant from one side of it is shown in Fig. 5-3. The circuit for driving the relays had not the delayed reversion. The rear sensor had the extended contacting link which contacted constantly with the row of rice plant under the straight travelling and the front sensor remained to separate from the row under the straight travelling. This steering system was designed for harvesting in the paddy field where the rice plant was not planted in a row. This figure represents the state where the contacting link of the rear sensor is separated from the row of rice plant and

which corresponds to the state 2 in Table 5-2, namely the rightward steering. In this state, since the microswitch RMS was made

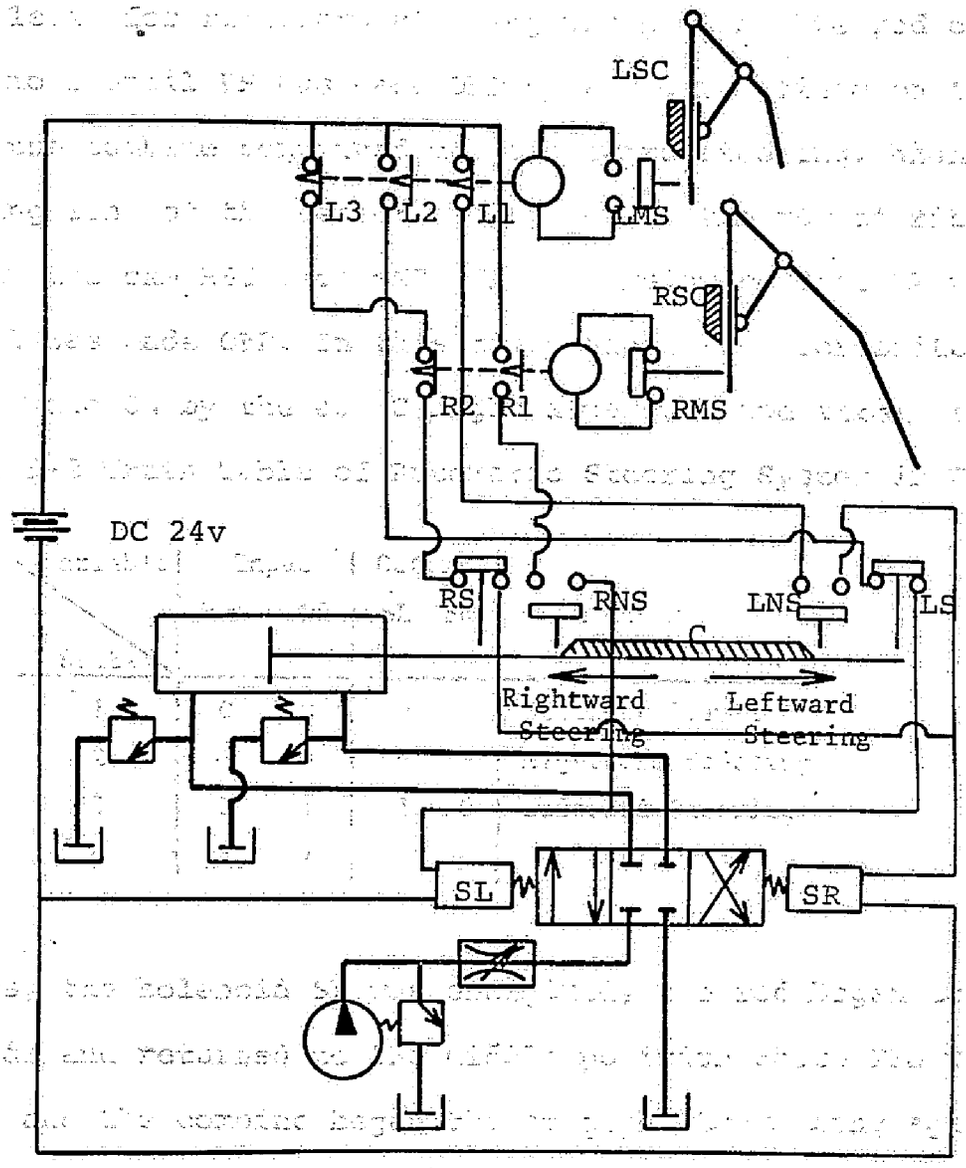

Fig. 5-3 Electric-hydraulic Circuit of Automatic Steering System with Sensors Detecting Row from One Side of It

ON, the relay was energized and the relay contact R1 was made OFF and R2 was made ON. The electric current flowed into SR through L3 which was ON since LMS was OFF, the oil flowed into right cylinder of the hydraulic actuator, the rod moved leftwards and the lever for rightward steering was pulled. The rod continued to move until RS was made OFF by the cam C fixed on the rod and the combine continued the rightward steering. When the contacting link of the sensor was pushed by the row of rice plant and the cam RSC made RMS OFF, the relay contact R1 was made ON and R2 was made OFF. In this time, since the microswitch RNS had been made ON by the cam C right after the rod began to move

Table 5-2 Truth Table of Automatic Steering System in Fig. 5-3

Variable / State	Input RMS	Input LMS	Output SL	Output SR	Remarks
1	0	0	0	0	Straight Travel
2	1	0	0	1	Rightward Steering
3	0	1	1	0	Leftward Steering
4	1	1	1	0	"

leftwards, the solenoid SL was energized, the rod began to move rightwards and returned to the middle position where RNS was made OFF and the combine began the straight travelling again.

5-2 Experimental Methods and Conditions*

Generally, the rows of rice plant transplanted by the machine were meandered randomly as shown in Fig. 5-4. In the usual recutangular paddy field, the power spectra of the plant row are shown in Fig. 5-5. Letting the distance between the adjacent stumps of rice plant be 0.15 m and the travelling

Fig. 5-4 Meandering of Row of Rice Plant Transplanted by Machine

velocity of the combine be 0.15 m/sec, it was found that the upper limit of the equivalent frequencies were about 0.2 Hz. Therefore, the amplitude and wave length of the artificial sinusoidal input row for the fundamental experiments were 0.1 m and 3.6 m, respectively. The equivalent frequency of such sinusoidal input was 0.19 Hz, letting the travelling velocity of the combine be 0.7 m/sec. The artificial rows of plant were made of 200 mm plastic straws thrust into the vinyl chloride tubes which had the inner diameter of 25 mm, and the length of 150 mm. These vynil tubes were layed in the ground at intervals of 0.15 m sinusoidally. The length of these sinusoidal waves was 2.5 times of one cycle. The output paths of the combine were drawn on the ground by the standerdized sand flowing out of the hopper which equipped at the position of the divider.

The variable parameters in the traveling experiments were as follows.

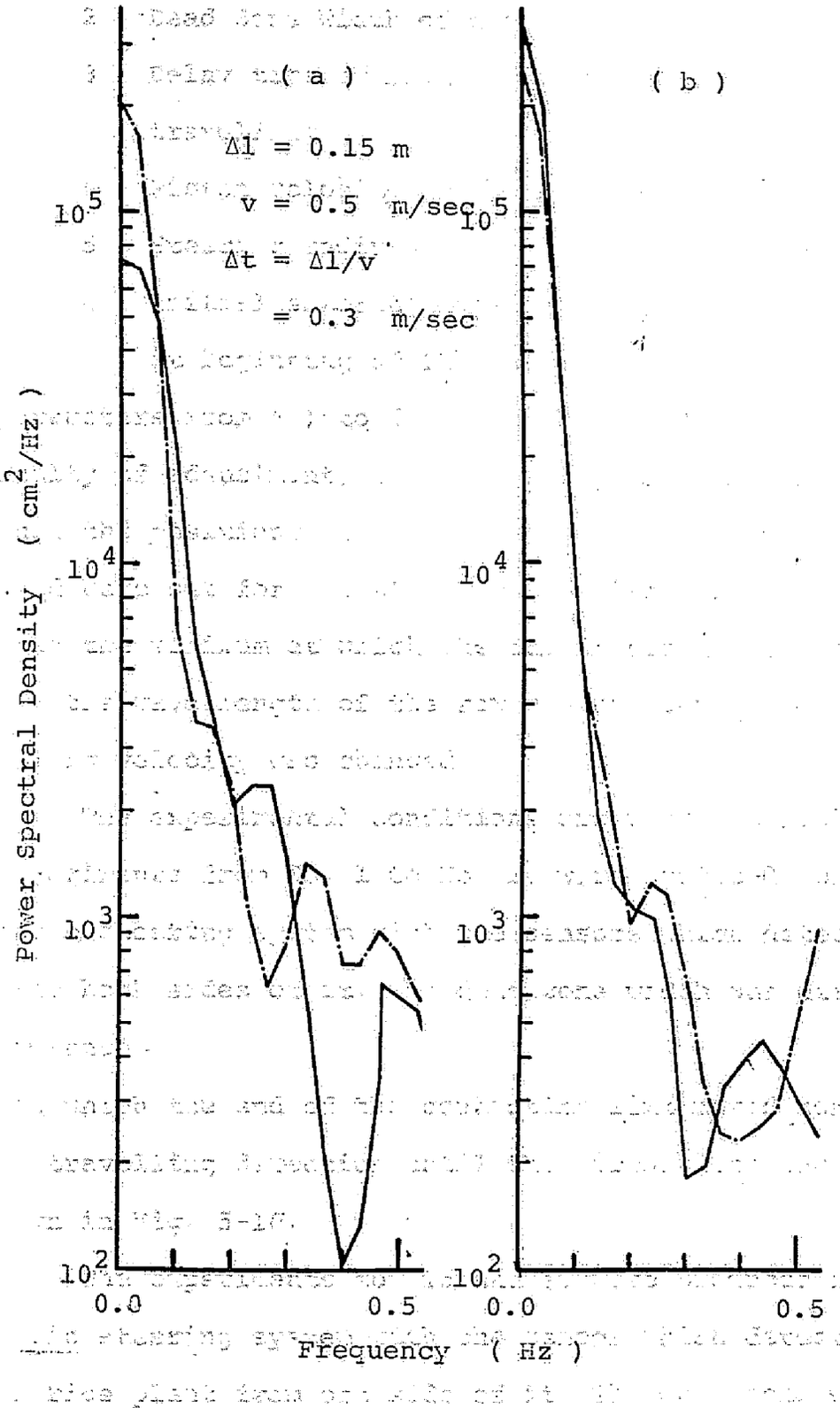

Fig. 5-5 Power Spectral Densities of Meandering of Row of Rice Plant in the Paddy Field

1) Frequency of sinusoidal input

2) Dead Zone Width of the Sensor

3) Delay time of return from steering to straight travelling

4) Piston velocity of the hydraulic actuator for steering

5) Steering radius

6) Initial entering angle against row of rice plant at beginning of the straight travelling

The parameters from 4) to 6) remained constant because of difficulty of adjustment, and especially for the parameter 5) although the positions where the stopper microswitches were actuated were set for two steps, the realized steering radius was only the minimum at which the inside crawler was stopped. For 1) the wave length of the row was not changed but the travelling velocity was changed

The experimental conditions are shown in Table 5-3. The experiments from No. 1 to No. 14 were produced for the antomatic steering system with the sensors which detected the row from the both sides of it. The dead zone width was defined by the distance through which the end of the contacting link moved normally to the travelling direction until the microswitch was actuated as shown in Fig. 5-10.

The experiments No. 15 and 16 were produced for the automatic steering system with the sensor which detected the row of rice plant from one side of it. The dead zone width was defined by the distance between the positions at which the contacting links of the front and rear sensors actuated the

Table 5-3 Experimental Conditions

No.	Delay Time	Travl. Speed	Dead Zone			
			Main Sensor		Suppl. Sensor	
			Right	Left	Right	Left
1	0.0 sec	0.4 m/sec	16 mm	20 mm	17 mm	13 mm
2	0.0	0.65	16	20	17	13
3	0.2	0.4	16	20	17	13
4	0.1	0.4	16	20	17	13
5	0.1	0.4	16	20	17	13
6	0.1	0.65	16	20	17	13
7	0.1	0.4	25	25	13	13
8	0.1	0.4	25	25	13	13
9	0.2	0.65	25	25	13	13
10	0.2	0.4	25	25	13	13
11	0.0	0.4	35	35	5	5
12	0.0	0.65	35	35	5	5
13	0.1	0.4	35	35	5	5
14	0.1	0.65	35	35	5	5
15	0.0	0.35	150 mm			
16	0.0	0.17	150			

microswitches.

5-3 Experimental Results and Discussions - Response to Artificial Input Row -*

5-3-1 Response Paths

The response paths of the combine which was automatically steered by the system with the sensors detecting the row from both sides of it are shown in Figs. 5-6 and 5-7. (a)'s in each figure represent the artificial row.

1) When the travelling velocity and the dead zone width were kept constant, the influences of the changes in the delay time upon the response paths were as follows. When the delay

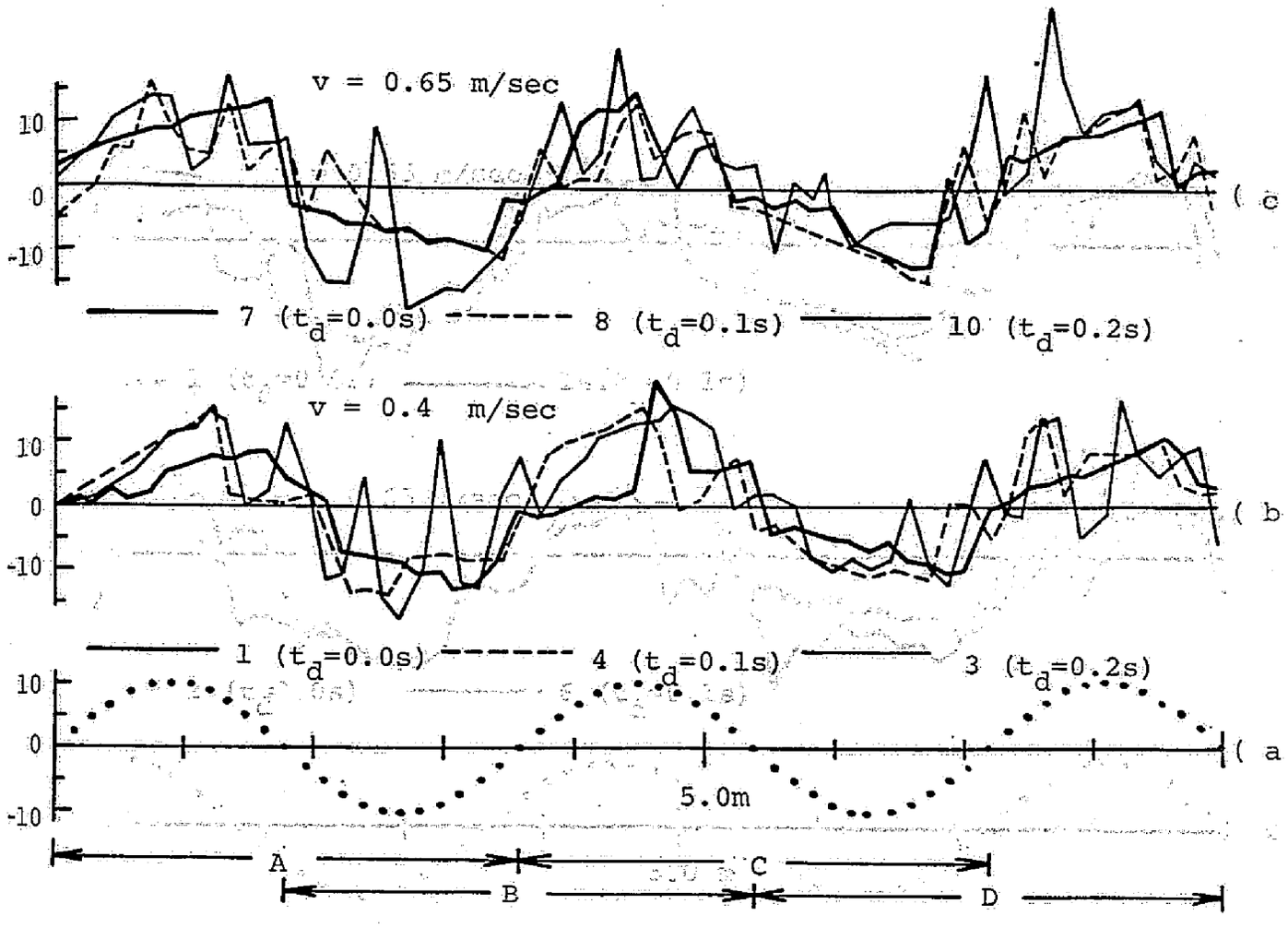

Fig. 5-6 Response Paths of the Automatically Steered Combine with the System in Fig. 5-1

time was too long, the overshoot of the steering was too large and then the response paths were disturbed. This might be caused by the following fact. For example, when the combine was steered rightwards and the contacting link of the left sensor was separated from the row, the steering was too large and then the contacting link of the right sensor came too close to the row, therefore the combine had to begin the rightward

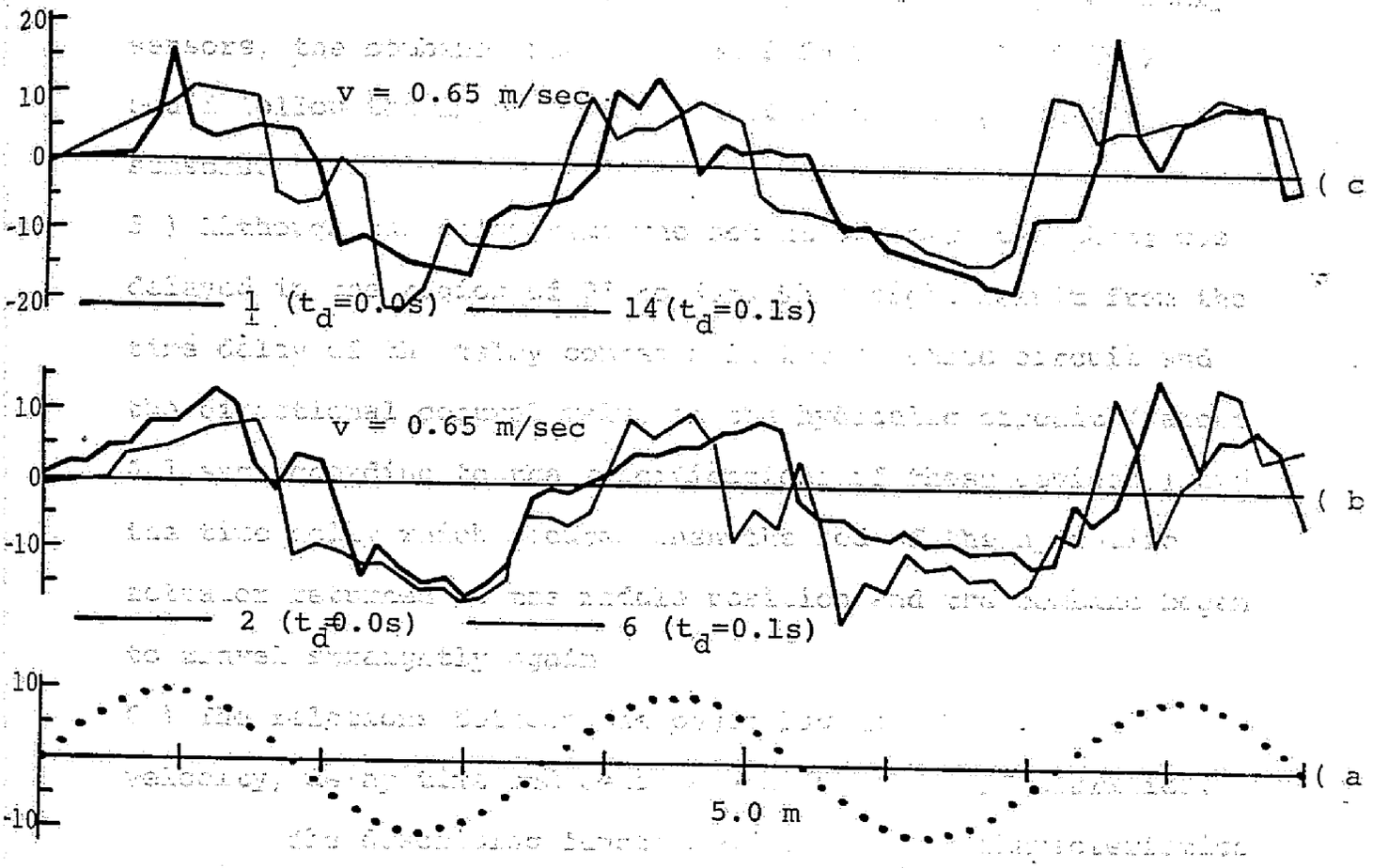

Fig. 5-7 Response Paths of the Automatically Steered Combine with the System in Fig. 5-1

steering just after the beginning of the straight travelling. That is, the number of steering motions was increased and then the distance of the straight travelling was decreased.

2) As the travelling velocity was increased, the response paths were disturbed and the travelling became unstable (Fig. 5-6 (a) and (b)), because the overshoot of the steering caused by the inertia effect of the combine was increased.

3) The influence of the dead zone width upon the travelling stability and following accuracy was not clarified by these

experiments because there existed a great number of combinations of the dead zone widths of the sensors.

4) Since the sensors consisted of the main and supplementary sensors, the combine travelling at 0.65 m/sec (0.18 Hz) could follow the input by the effect of the supplementary sensors.

5) Although the delay time was set at 0.0 sec, the phase was delayed in the region of 0° to 60°. This might result from the time delay of the relay contacts in the electric circuit and the directional control valve in the hydraulic circuit (about 0.1 sec according to the specifications of these devices) and the time delay which occured when the rod of the hydraulic actuator returned to the middle position and the combine began to travel straightly again.

6) The relations between the phase lag and the travelling velocity, delay time and dead zone width were not clarified.

The describing function of hysteresis characteristics (memory type nonlinearity) is given by the following equation[7].

$$K_{eq}(E) = g(E) + jb(E)$$

$$= \frac{2M}{\pi E}\left[\left\{\cos\left(\sin^{-1}\frac{a}{E}\right) + \cos\left(\sin^{-1}\frac{d}{E}\right)\right\}\right.$$

$$\left. - j\left\{\sin\left(\sin^{-1}\frac{a}{E}\right) - \sin\left(\sin^{-1}\frac{d}{E}\right)\right\}\right] \qquad (5\text{-}1)$$

where E represents the amplitude of the sinusoidal input. Therefore, the phase shift is as follow.

$$\tan^{-1}(b/g) = \tan^{-1}\left(\frac{d/a - 1}{\sqrt{E^2/a^2 - d^2/a^2} + \sqrt{E^2/a^2 - 1}}\right) \quad (5\text{-}2)$$

The relationships between d/a and phase shift are shown in Fig. 5-8, letting E/a be the parameters. To increase the delay

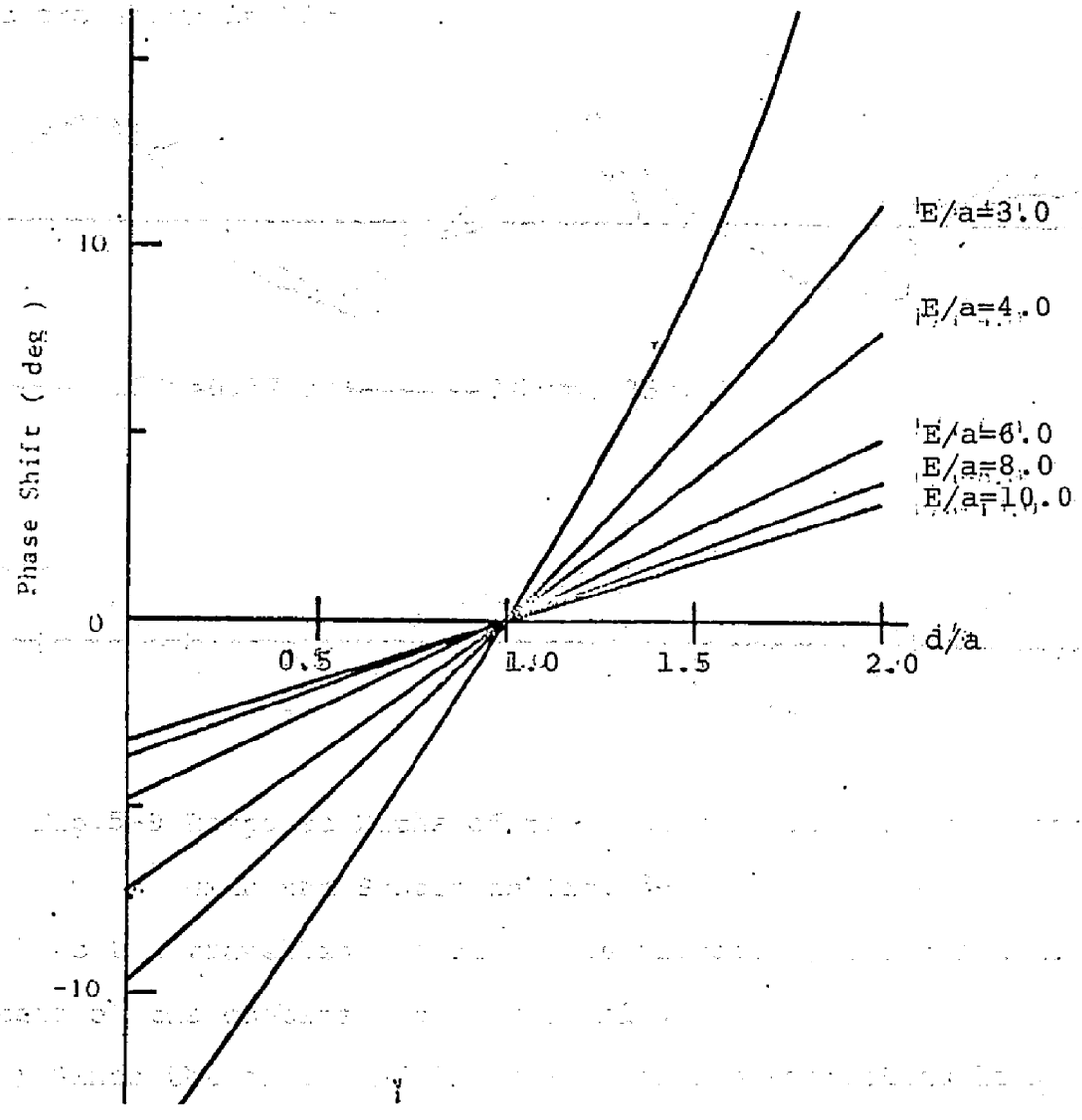

Fig. 5-8 Phase Shift of Memory Type Nonlinear Element

time in the experimental system corresponds to fix a and to move d leftwards (namely, to decrease d). In this case, it is obvious from Fig. 5-8 that the phase lag increases.

On the contrary, when d/a > 1 in Fig.5-8, the phase lead and this corresponds to the state where d goes on the right of a ; therefore the control system has the prediction characteristics rather than memory. The control system possessing such characteristics must be studied in the future.

The response paths of the automatically steered combine by the sensors detecting the row of rice plant from one side of it are shown in Fig. 5-9.

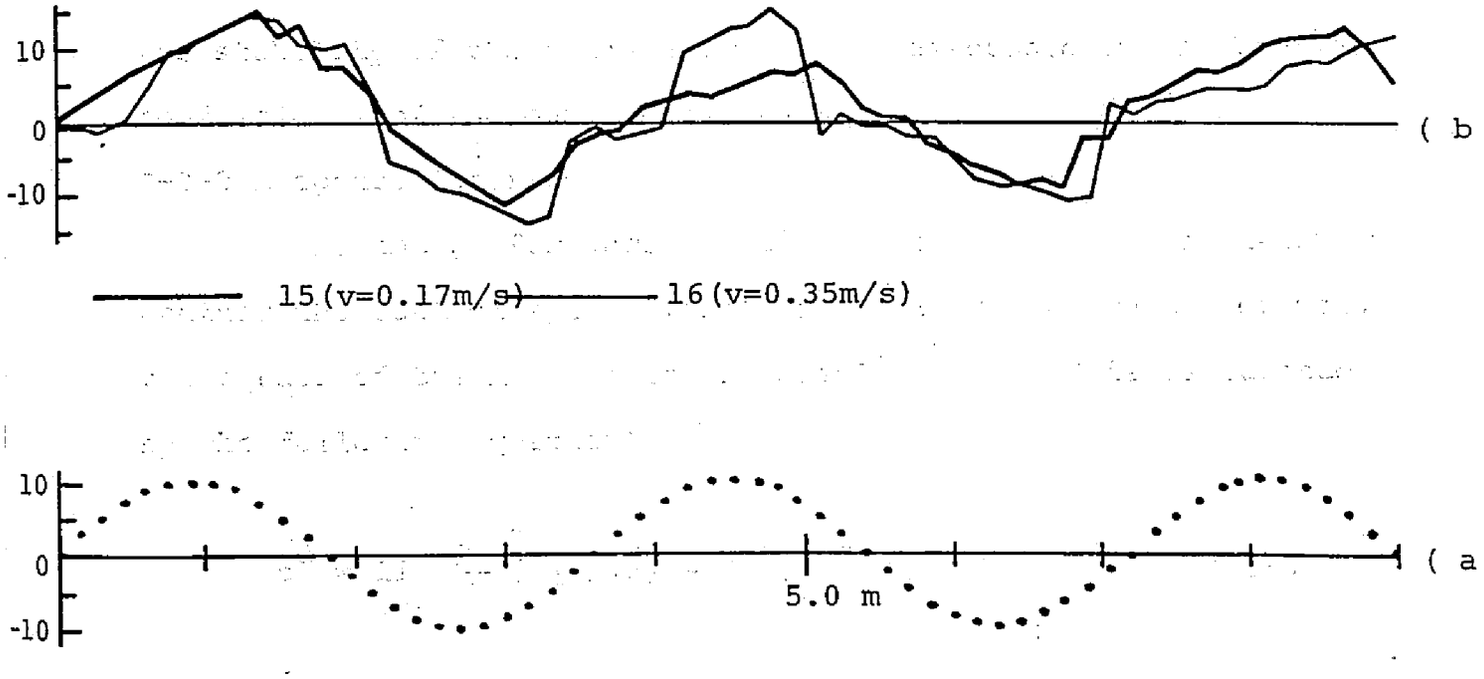

Fig.5-9 Response Paths of the Automatically Steered Combine with the System in Fig. 5- 3

1) As the travelling velocity was increased, the travelling state of the combine became unstable.

2) Since the shape and dimensions of the contacting link of the rear sensor were unsuitable, the combine could not follow the input row at the high velocity. The suitable shape and dimensions of the link must be researched.

3) The response paths were smoother than those of the steering

system mentioned previously (Fig. 5-6 (b) and Fig. 5-9 (b)). This might result from the difference between the characteristics of the sensing mechanism, and possibility of this sensing method was obtained.

The above discussion are qualitative by observing the response paths and the influences of the dead zone width could not be clarified. In the following sections, the response accuracies will be discussed by the squares of the RMS values of the differences between output and input wave forms and the stability of the travelling will be discussed by the Fourier coefficients of the output wave forms.

5-3-2 Response Accuracy

As the performance function which decided quantitatively whether the control system followed the input accurately or not, the square of the RMS values was used[8), 9)] . This is defined by the following equation[10)].

$$\bar{e}^2 = \lim_{T\to\infty} \frac{1}{2T} \int_{-T}^{T} [\, F(t) - f(t) \,]^2 \, dt \qquad (5\text{-}3)$$

where F(t) and f(t) are the input and output, respectively. In this section $\bar{e}^2$ of the input row of plant and the output paths of the combine will be calculated by this equation, and the influence of the travelling velocity of the combine (namely, input frequency), delay time and the dead zone width upon the response accuries will be discussed. The results of calculation are as shown in Fig. 5-10. It was clarified from Fig. 5-10 (a) that as the delay time increased the value of $\bar{e}^2$ increased. Therefore the response accuracy was considerably

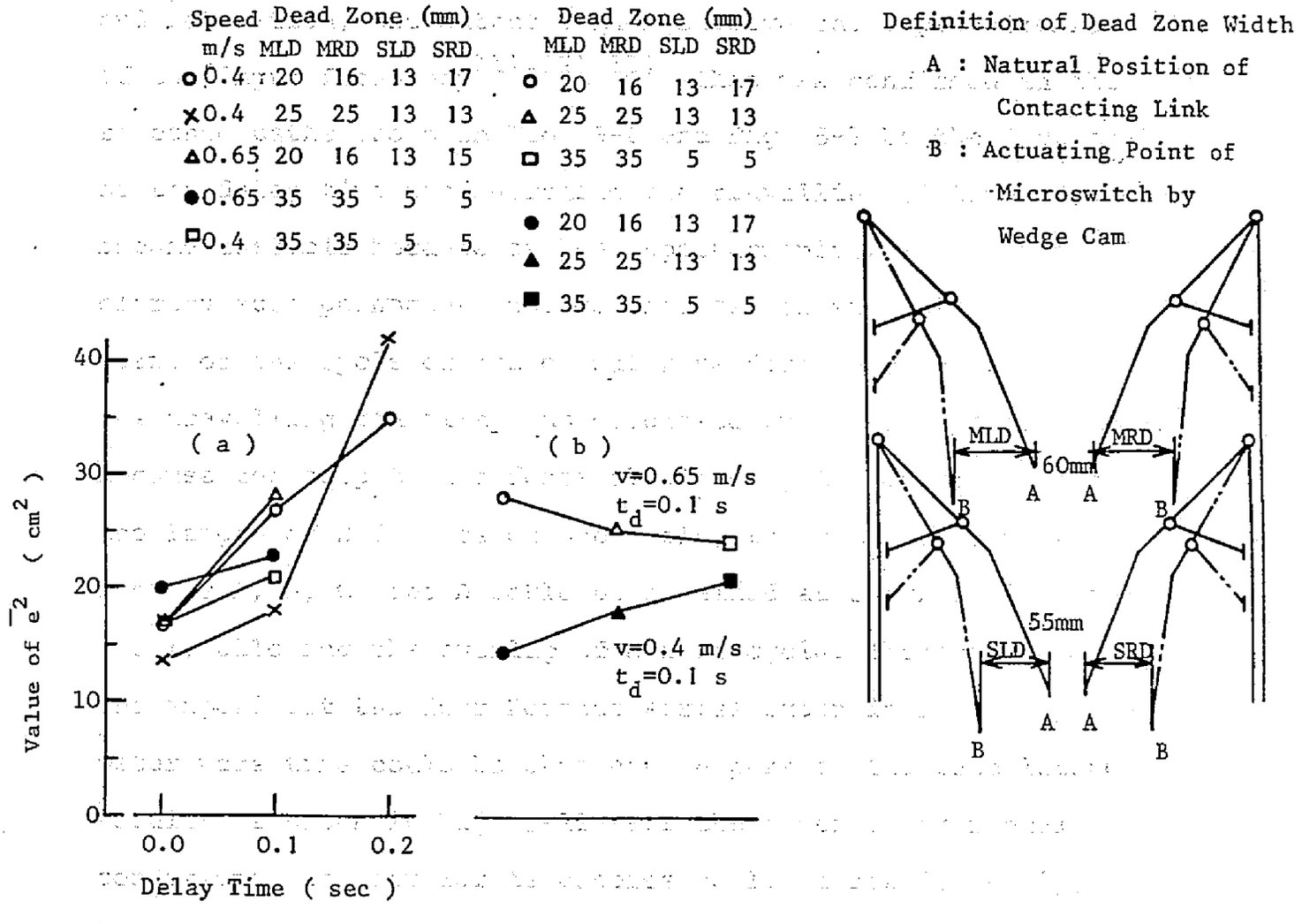

Fig. 5-10 Steering Accuracy of Automatically Steered Combine by Means of Values of $\bar{e}^2$

affected by the delay time. From Fig. 5-10 (b) it was found that the influences of the dead zone width upon the response accuracy were not always similar and the tendency was changed as the travelling velocity varied. That is, the relations between the dead zone width and the response accuracy could not be found. However, when the travelling velocity was increased, the value of $\bar{e}^2$ was increased and the response accuracy was reduced.

5-3-3 Travelling Stability

Since the control system used for the experiments had the nonlinear characteristics such as the dead zone, hysteresis and saturation, the output might involve the superharmonics of the input frequency[11),12),13)]. This was confirmed in the response paths shown in Fig. 5-6 and Fig, 5-7 by the fact that as the delay time was increased the travelling of the combine became unstable because of the superharmonics. In order to clarify such phenomena, the Fourier series expansions of 24 terms of one cycle of the output wave form were obtained and the travelling stability was discussed in the frequency domain. Because the output wave forms obtained by the experiments had the length of 2.5 times of one cycle, the data of four cycles such as A, B, C, and D could be obtained as shown in Fig. 5-6 (a), allowing the overlap of a half cycle. Therefore, for one experiment the four Fourier series expansions whose parameter were time could be obtained. A part of the calculating results is shown in Fig. 5-11. For the other experimental conditions, the similar tendencies could be found. Namely, 1) the response paths were successively disturbed as the time was elapsed after beginning of travelling, and 2) as the delay time was increased the 6th and 7th harmonics grew and the travelling became unstable.

As mentioned above, in the case where the delay time was generated when the combine returned from steering and began the straight travelling, it was found that the response paths became unstable against the initial expectation. This might result from the too long delay time.

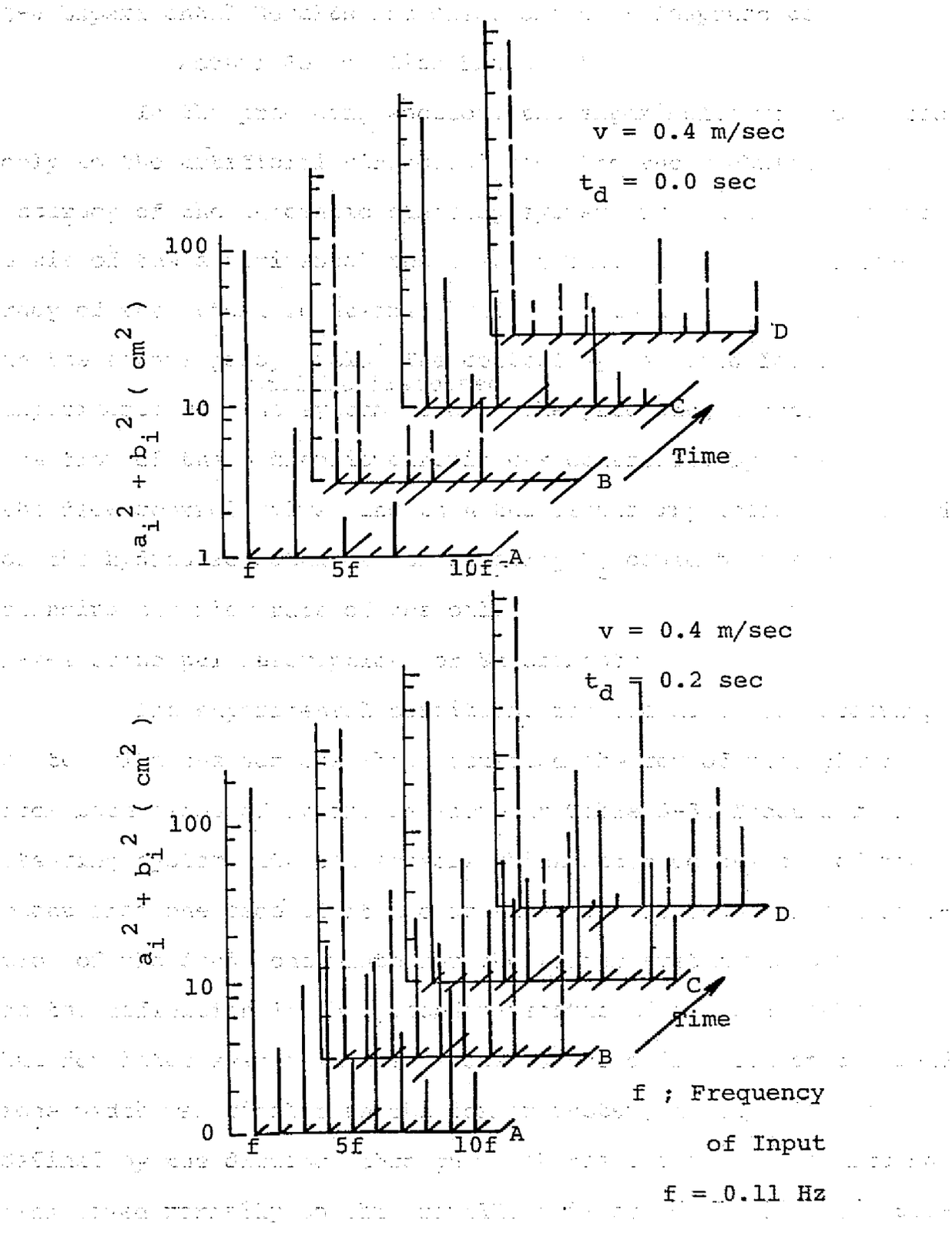

Fig. 5-11 Stability Evaluation by Means of Time-varying Fourier Coefficients of Response Paths of Automatically Steered Combine

5-4 Experimental Results and Discussions - Response to Actual Row of Rice Plant -**

In the preceding section, the experiments were produced only to the artificial sinusoidal row. And the stability and accuracy of the automatic steering system were discussed on the basis of the experimental results. In this section, the accuracy of the automatic steering for the combine which harvested in the actual paddy field. The control system used for the experiments will be discussed was the system used in the preceding section, but the flow of the hydraulic circuit was controlled by means of the flow control valve, and then the displacing speed of the rod of the hydraulic actuator for steering V_c could be varied by changing the flow rate of the oil.

5-4-1 Principal Descriptions of Experiments

The experimental conditions for the automatic steering system with the sensors which detected the row of rice plant from both sides of it are as shown in Table 5-3. Those for the steering system with the sensors which detected the row of rice plant from one side of it are as shown in Table 5-4. The definition of the dead zone width for the former system was similar as the difinition in the preceding section (see Fig. 5-10), but for later system in this section, the definition of the dead zone width was similar as the former system, namely, it was defined by the distance through which the end of the contacting link moved normally to the travelling direction until the microswitch was actuated as shown in Fig. 5-10.

Table 5-3 Experimental Conditions for Automatic Steering System shown in Fig. 5-1

Experiment No.	Dead Zone Width (mm)		Piston Speed (mm/sec)		Delay Time (sec)
	W_{df} *	W_{dr} **	V_{cl} ***	V_{cr} ****	t_d
1	10	10	219.7	205.7	0.0
2	10	10	219.7	205.7	0.1
3	10	10	219.7	205.7	0.2
4	10	10	117.5	157.5	0.0
5	20	20	117.5	157.5	0.1
6	20	20	117.5	157.5	0.2
7	20	20	117.5	157.5	0.5
8	0	0	117.5	157.5	0.0
9	0	0	117.5	157.5	0.1
10	0	0	117.5	157.5	0.2
11	0	0	219.7	205.7	0.0
12	0	0	219.7	205.7	0.1
13	0	0	219.7	205.7	0.2

* Dead Zone Width of the Front Sensor

** Dead Zone Width of the Rear Sensor

*** Speed of Hydraulic Cylinder for Leftward Steering

**** Speed of Hydraulic Cylinder for Rightward Steering

Table 5-4 Experimental Conditions for Automatic Steering System shown in Fig. 5- 3

Experiment No.	Dead Zone Width (mm)		Piston Speed (mm/sec)		Delay Time (sec)
	W_{df}	W_{dr}	V_{cl}	V_{cr}	t_d
21	20	35	117.5	157.5	0.0
22	20	20	117.5	157.5	0.0
23	30	55	117.5	157.5	0.0
24	30	55	219.5	205.7	0.0
25	20	35	219.7	205.7	0.0

5-4-2 Response Paths and Following Accuracy

A part of the response paths of the automatically steered combine are shown in Fig. 5-12, the control system of which are shown in Fig. 5-1.

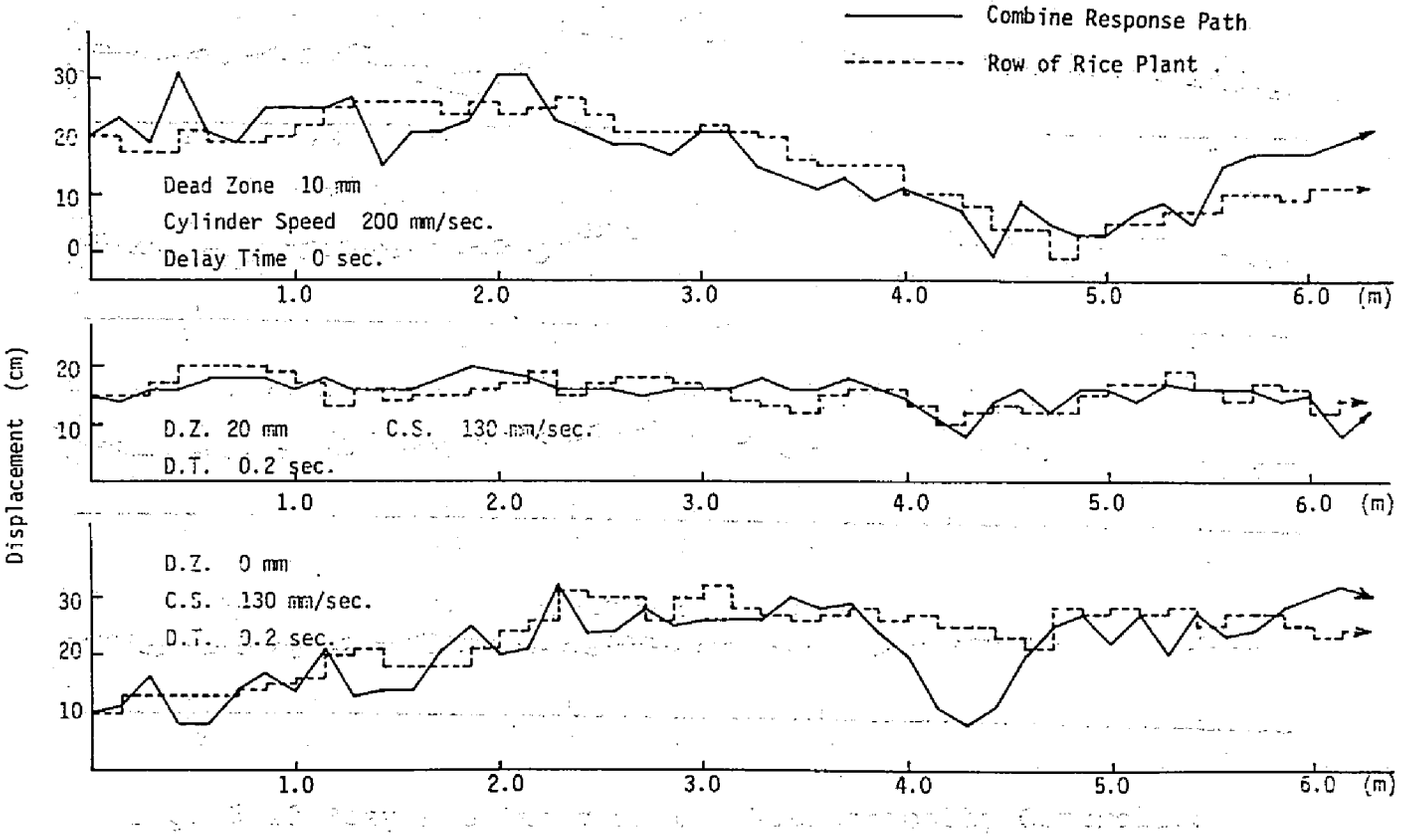

Fig. 5-12 Response Paths of the Automatically Steered Combine with the System shown in Fig. 5-1

The response paths of the automatically steered combine with the system in Fig. 5- 3 are shown in Fig. 5-13. In the almost all experiments, the combine could travel smoothly, but for the low speed of the hydraulic actuator rod for steering, the narrow dead zone width of the sensors and the too long delay time the response paths showed the self-excited oscillation as shown in Fig. 5-14 which obtained for the experiment No. 2. The amplitude and the wave length of this self-excited oscillation was 8.5 cm and 11.5 cm, respectively. In order to discuss the

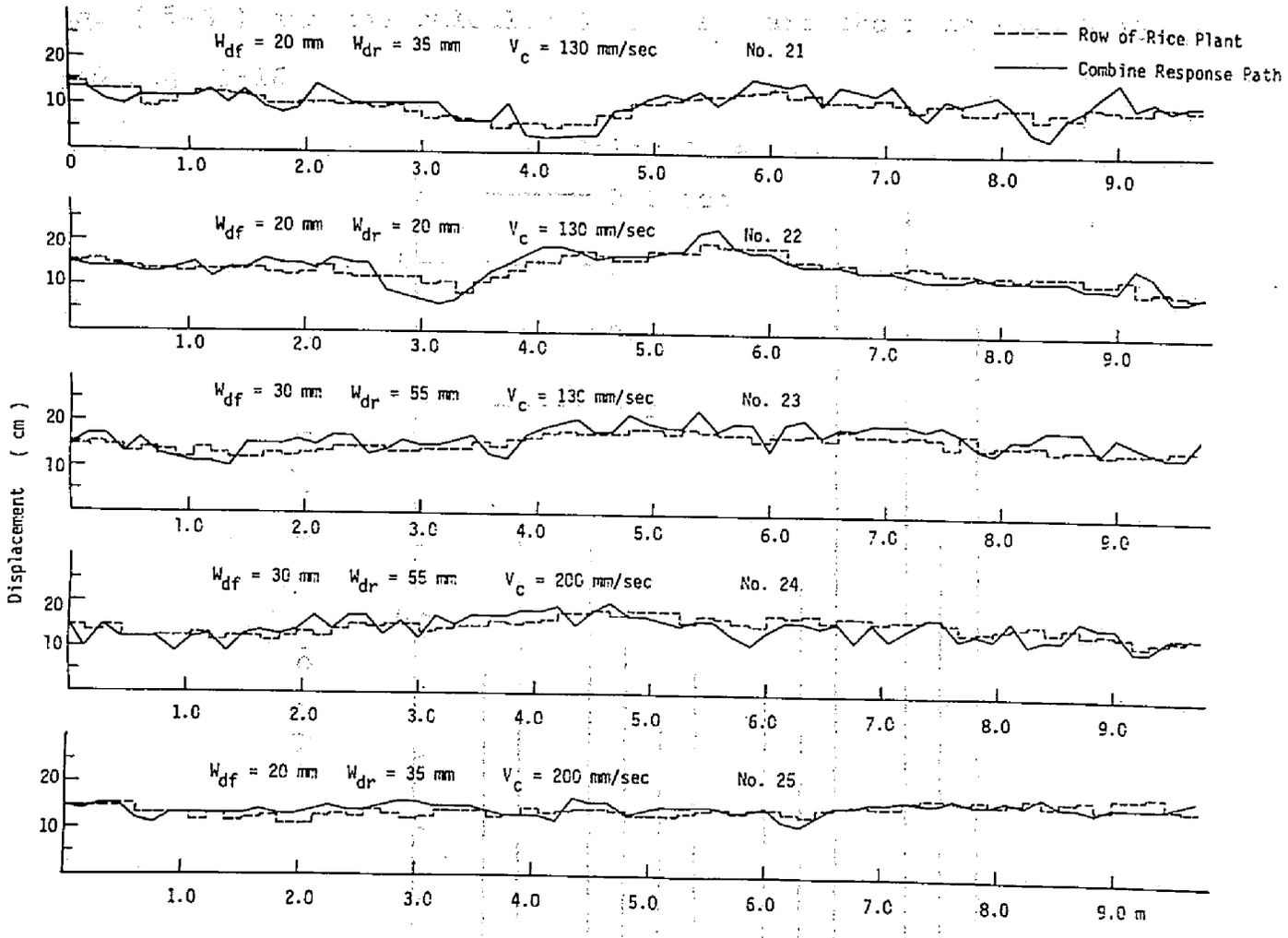

Fig. 5-13 Response Paths of the Automatically Controlled Combine with the Sensors shown in Fig. 5-3

Fig. 5-14 An Example of the Unstable Response Paths

following accuracy of the autamatically steered combine, the squares of RMS values $\overline{e^2}$ were calculated from the input and

output paths of the combine by means of Eq. (5-3) and the calculated results are shown in Fig. 5-15 and Fig. 5-16.

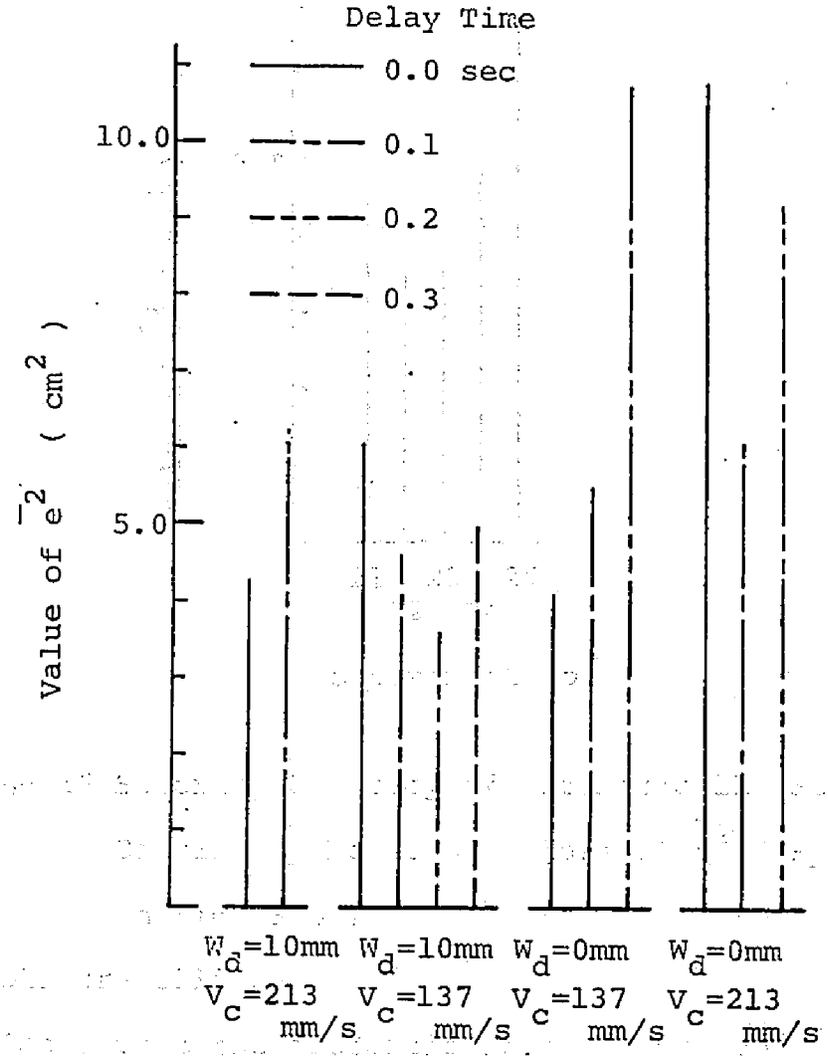

Fig. 5-15 Steering Accuracy of Automatically Steered Combine by Means of Values of $\bar{e}^2$ (System in Fig. 5-1)

From these figures the followings were clarified.

1) The delay time of about 0.2 sec was suitable, and for the too long delay time the stability of the control was decreased.

2) The suitable dead zone width was about 20 mm.

3) The lower speed of the hydraulic cylinder rod was suitable

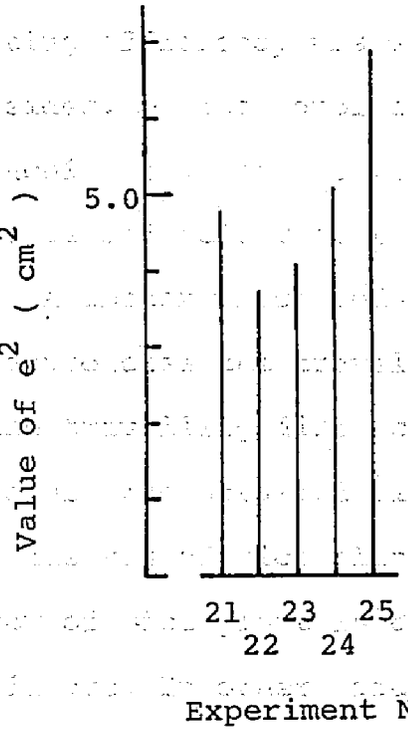

Fig. 5- 16 Steering Accuracy of Automatically Steered Combine by Means of Values of $\bar{e}^2$ (System in Fig. 5-3)

for the stable travelling.

4) It was found that the automatic steering system with the sensors which detected the row of rice plant from one side of it operated sufficiently.

6-5 Concluding Remarks

The following (or steering) accuracies were evaluated by the squares of the RMS values $\bar{e}^2$ of the deference between the input and output, however, the output which made the value $\bar{e}^2$ zero was not necessarily optimal. Namely, since the distance between the adjacent dividers was about 30 cm, the cutting

operation could be done without following the row of rice plant accurately. From the point of view of the operating efficiency, on the contrary, it might be thought that the travelling distance increased and operating efficiency was decreased due to the accurate follow. Besides, if the combine was steered frequently, the motion of the machine body became violent and the life time of the combine might be reduced. Therefore, to determine the combination of each parameter which reduces the steering motion as far as possible approaches the travelling paths to a straight line and shortens the travelling distance (namely, decreases the values of $\bar{e}^2$ against the straight line) and which the combine can follow the row of rice plant (namely, the value of $\bar{e}^2$ against the row of rice plant is decreased) will become the problem in the future. In other wards, such problem is to determine the optimal path in the meaning of the minimum travelling distance and the minimum error.

In order to develope the stability of travelling, the experimented steering system had the characteristics of the delayed reversion from steering to straight travelling simulating the situation when the man operated the combine, but the travelling of the combine became unstable for the too long delay time. However, in order to realize the smooth travelling, it is necessary to discuss the suitable delay time in connection with the dead zone width. Besides, as the furture problem, the system which determine the delay time referring the distance between the sensors and the row of rice plant, namely the closed system, must be developed.

5-6 Conclusions of This Chapter

The automatic steering system which had two kinds of sensor for detecting the row of rice plant by contacting it was examined, the response paths of the combine with the above system to the artificial sinusoidal row as the input were determined experimentally and the fundamental problems and the future principles were discussed.

The results of experiments are as follows.

For the automatic steering system with the sensors detecting the row of rice plant from both sides of the row by contacting it,

1) As the delay time for restoring from steering motion to straight travel was increased, the response path of the combine was disturbed because of the excessive corrections of errors.

2) As the travelling velocity was increased, the path of the combine was disturbed because of inertia effect of the mass of the combine.

3) Because of the double sensing device consisting of the main and supplementary sensors, the combine travelling at the top speed was able to track the input row by means of the effect of the supplementary sensors.

4) The relationships between the dead zone width of the sensor and travelling stability and tracking accuracy could not be found because the experiments were not produced so many.

5) The influence of the delay time, travelling velocity and dead zone width upon the phase shift between the input and output paths were not found.

For the automatic steering system with the sensors

detecting the row of rice plant from one side of it, the possibility of this type of sensor was found and the experimental results are as follows.

1) As the travelling velocity was increased, the paths of the combine was disturbed.

2) The combine travelling at the relatively high speed could not track the input row because of the unsuitable shape and dimensions of the constantly contacting link of the later sensor.

3) The path of the combine travelling at lower speed was more smooth than the path of the combine with the sensors detecting the row of rice plant from both sides of it, may be because of difference of the mode of sensing.

The response paths of the combine with the systems mentioned above to the row of rice plant in the actual paddy field were determined and the following results were obtained.

1) The delay time of about 0.2 sec was suitable, and for the too long delay time the stability of the control system was decreased.

2) The suitable dead zone width was about 20 mm.

3) The lower speed of the hydraulic cylinder rod was suitable for the stable travelling.

4) It was found that the automatic steering system with the sensors which detected the row of rice plant from one side of it operated sufficiently.

CHAPTER 6

Digital Simulation of the Automatically Steered Combine

The automatic steering system used for the experiments had the nonlinearity such as the dead zone in order to stabilize the motion of the combine, and the asymmetry of the combine body (see Fig. 6-1) had to be considered since the exparimented combine cut the plant diagonally forwards. Therefore, the theoretical consideration of this control system was very difficult and then the analytical description of the behavior of the system was complicated. And the optimal combination of the parameters such as the dead zone width, delay time, travelling velocity and the speed of the rod of the hydraulic actuator, as suggested in 6-5, became impossible by means of the theoretical analysis. In such a case, the digital simulation technique become effective. That is, the behavior of the system is taken apart and can be described by a number of the comparatively simple equations, and the initial conditions and the variable parameters are given previously and the numerical prediction of the combine response is achieved by the computer. And thus the optimal path of the combine could be decided by the method of trial and error through the digital computer experiments.

In this chapter, the response paths of the combine which has the automatic steering systems shown in Fig. 5-1 and Fig. 5-3 are predicted by the digital simulation technique. And their applicability in the actual paddy field are deduced. Moreover, the response paths by the prediction and experiment are compared and the reliability of mathematical models for the steering system is discussed.

6-1 Equation of Motion of Combine*,**,***,

The reports on the analysis of the tracked vehicle were restricted to the geometric problems[2)3)4)]. However, for the digital simulation of the automatically steered combine the dynamic analysis of the tracked vehicle is necessary. In this section, the dynamic behavior of the combine which begins steering and straight travelling will be discussed and the equation of motion of the combine will be obtained.

The assumptions to find the equations are as follows.

1) The travelling resistence of the combine for the straight travel is proportional to the travelling velocity. Namely, the equivalent viscous damping is introduced.

2) The pitching, rolling and yawing motions of the combine are neglected since these motions increase the degree-of-freedom, and then the motion of the combine is complicated. Besides, since the equations are concerned with the plane motion, it is possible to neglect these oscillating motions.

3) When steering, the center of turning is fixed and located on the center line of the inside track. This was confirmed by the experiments.

4) The resistance of the ground to turning is proportional to the turning angular velocity.

6-1-1 Equation of Motion for Straight Travel

The geometry of the experimented combine is shown in Fig. 6-1. Note the asymmetry of the sensors and the turning centers. In this figure, the turning center CR and CL are defined by the point about which the combine is turned. The center of gravity CG was determined by the

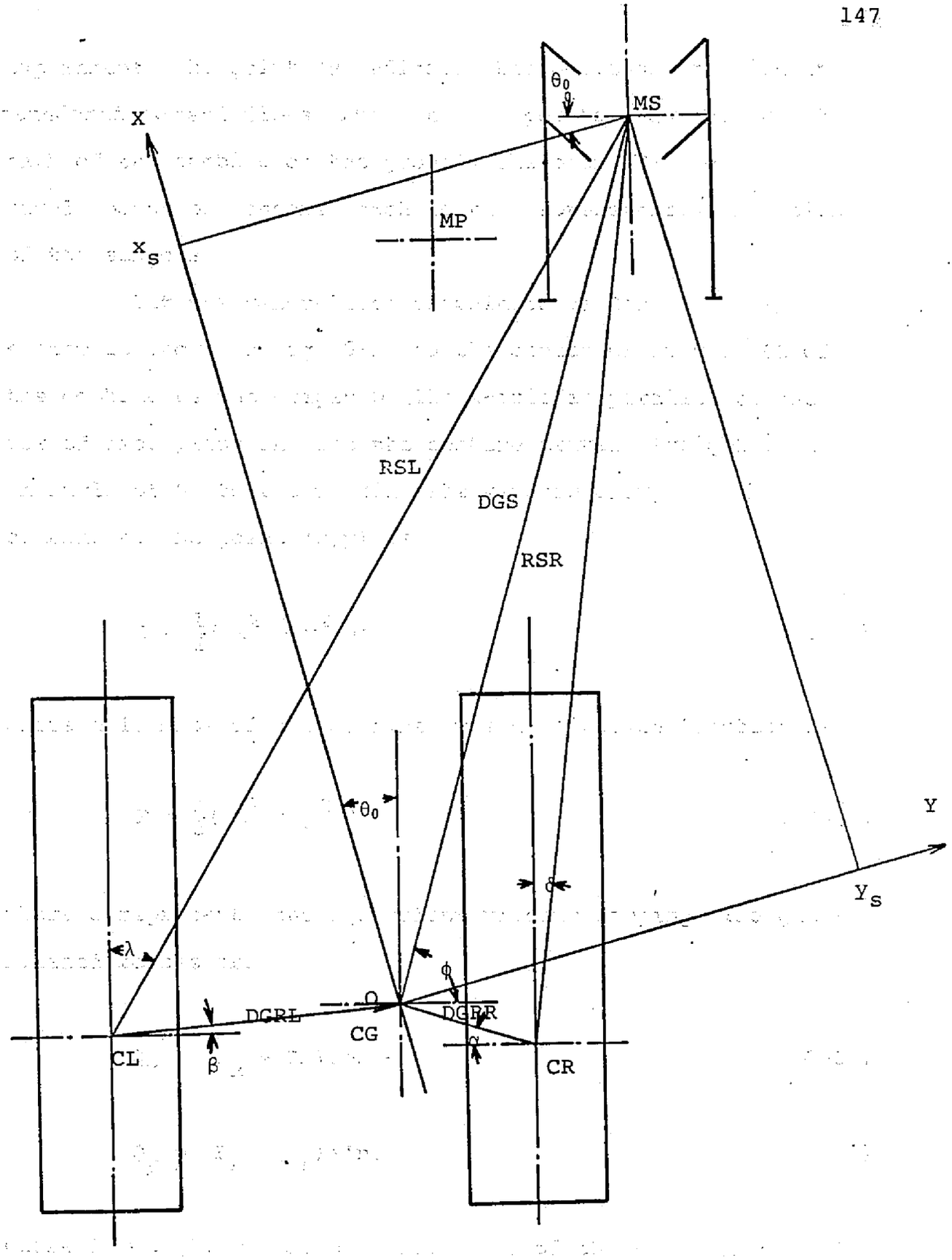

Fig. 6-1 Geometry of the Experimented Combine

experiment. The point MP indicates the position at which the standardised sand flows from the hopper to draw the output path of the combine on the ground. The point MS shows the middle point of sensors which is the representative position of the sensors.

Let the generalized coordinate be Cartesian x-y system as shown in Fig. 6-1 and the center of gravity CG of the combine be the origin O. The x-axis is parallel to the row of rice plant and let the combine travel straightly at an angle of θ_0 to the x-axis. The kinetic energy of the combine at the point (x,y) is

$$T = \frac{1}{2}(\dot{x}^2 + \dot{y}^2)m \qquad (6\text{-}1)$$

where m is mass of the combine. The dissipation function is

$$F = \frac{1}{2}(\dot{x}^2 + \dot{y}^2)c \qquad (6\text{-}2)$$

where c represents the equivalent viscous damping. The generalized forces are

$$Q_x = (F_R + F_L)\cos\theta_0 \qquad (6\text{-}3)$$

$$Q_y = (F_R + F_L)\sin\theta_0 \qquad (6\text{-}4)$$

where $F_R = M_R/R$ is the driving force of the right track and $F_L = M_L/R$ is the driving force of the left track. M_R and M_L are the travelling torques of the right and left drive sprocket

shafts, respectively. R is the pitch radius of the drive sprocket. Substituting the Eqs. (6-1) through (6-4) into Lagrange's equation of motion, the following differential equations are obtained.

$$m\ddot{x} + c\dot{x} = (F_R + F_L)\cos\theta_0 \qquad (6\text{-}5)$$

$$m\ddot{y} + c\dot{y} = (F_R + F_L)\sin\theta_0 \qquad (6\text{-}6)$$

Taking the Laplace transformations of both sides of these equations with the initial conditions, $x(0) = y(0) = \dot{x}(0) = \dot{y}(0) = 0$, gives

$$ms^2X(s) + csX(s) = \frac{1}{s}(F_R + F_L)\cos\theta_0 \qquad (6\text{-}7)$$

$$ms^2Y(s) + csY(s) = \frac{1}{s}(F_R + F_L)\sin\theta_0 \qquad (6\text{-}8)$$

Solving for X(s) and Y(s), respectively, gives

$$X(s) = \frac{\frac{F_L + F_R}{m}\cos\theta_0}{s^2(s + c/m)} \qquad (6\text{-}9)$$

$$Y(s) = \frac{\frac{F_L + F_R}{m}\sin\theta_0}{s^2(s + c/m)} \qquad (6\text{-}10)$$

Performing the inverse Laplace transformation the both sides of these equations gives the coordinates of the center of gravity of the combine, namely

$$x(t) = \frac{(F_R + F_L)}{m}\cos\theta_0\frac{m^2}{c^2}\left(e^{-\frac{c}{m}t} + \frac{c}{m}t - 1\right) \qquad (6\text{-}11)$$

$$y(t) = \frac{(F_R + F_L)}{m}\sin\theta_0 \frac{m^2}{c^2}\left(e^{-\frac{c}{m}t} + \frac{c}{m}t - 1\right) \qquad (6\text{-}12)$$

By the results of experiments on the combine starting on the straight travel, it was found that the starting torque of the drive sprocket shaft was as shown in Fig. 6-2. From this figure, it may be appropriate that this

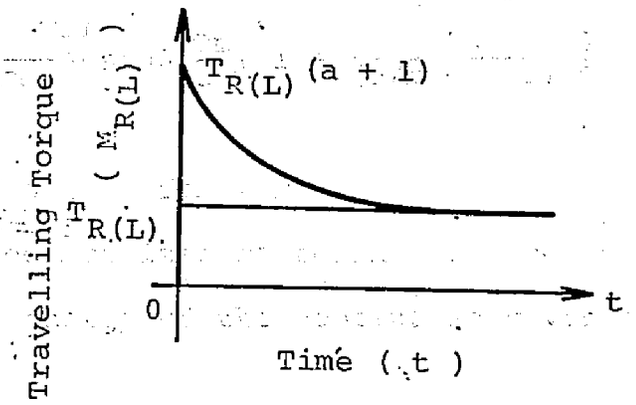

Fig. 6-2 Travelling Torque of Combine at Starting on Straight Travel

real torque is assumed to be given by the following equation

$$M_{R(L)} = T_{R(L)}\left(a \cdot e^{-\frac{t}{T}} + 1.0\right) \qquad (6\text{-}13)$$

where a and T must be determined by the experiments. The constant a is non-dimensional and its value is 2.0 and T is 0.5 sec.

If the driving forces given by Eq. (6-13) are used instead of the stepwise driving forces F_R and F_L, which are used in Eq. (6-11) and Eq. (6-12), the coordinate of the center of gravity of the combine are given by the following equations. Using $F_R = M_R/R$ and $F_L = M_L/R$,

$$x(t) = \frac{(T_R + T_L)}{Rm}\cos\theta_0\frac{m^2}{c^2}(e^{-\frac{c}{m}t} + \frac{c}{m}t - 1)$$

$$+\frac{a(T_R + T_L)}{Rm}\cos\theta_0\frac{Tm}{c}[\,1 + \frac{1}{(c/m - 1/T)}(\frac{1}{T}e^{-\frac{c}{m}t} - \frac{c}{m}e^{-\frac{t}{T}})\,]$$

$$y(t) = \frac{(T_R + T_L)}{Rm}\sin\theta_0\frac{m^2}{c^2}(e^{-\frac{c}{m}t} + \frac{c}{m}t - 1)$$

$$+\frac{a(T_R + T_L)}{Rm}\sin\theta_0\frac{Tm}{c}[\,1 + \frac{1}{(c/m - 1/T)}(\frac{1}{T}e^{-\frac{c}{m}t} - \frac{c}{m}e^{-\frac{t}{T}})\,]$$

6-1-2 Equation of Motion for Turning

Let the generalized coordinate be the turning angle θ. The total kinetic energy of the combine is given by

$$T = \frac{1}{2}J_R\dot{\theta}^2 \qquad (6\text{-}14)$$

where J represents the mass moment of inertia about the axis through the turning center and the subscript R or L indicates that the steering is rightward or leftward. The equation of the rightward turning motion of the combine is as follows. The dissipation function F is

$$F = \frac{1}{2}c_{rR}\dot{\theta}^2 \qquad (6\text{-}15)$$

where c_{rR} is the equivalent turning resistance. The generalized force Q_θ is

$$Q_\theta = F_L \cdot B = M_R \qquad (6\text{-}16)$$

where F_L is the driving force of the leftside track for rightward steering and M_R is the rightward turning torque by F_L. B is a tread.

Substituting Eqs. (6-15) and (6-16) into Lagrange's equation gives

$$J_R\ddot{\theta} + c_{rR}\dot{\theta} = M_R \qquad (6\text{-}17)$$

Taking the Laplace transformation of both sides of Eq. (6-17) with the initial conditions; $\theta(0) = \theta_0$ and $\dot{\theta}(0) = 0$, we have

$$J_R s^2\theta(s) - s J_R\theta_0 + sc_{rR}\theta(s) = \frac{M_R}{s} \qquad (6\text{-}18)$$

Solving for $\theta(s)$ gives

$$\theta(s) = \frac{M_R/J_R}{s^2(s + c_{rR}/J_R)} + \frac{\theta_0}{(s + c_{rR}/J_R)} \qquad (6\text{-}19)$$

The turning (or steering) angle after t sec is given by the inverse Laplace transform of Eq. (6-19). Namely

$$\theta(t) = \left(\frac{M_R J_R}{c_{rR}^2} + \theta_0\right)e^{\frac{-c_{rR}}{J_R}t} + \frac{M_R}{c_{rR}}t - \frac{M_R J_R}{c_{rR}^2} \qquad (6\text{-}20)$$

The value of $\theta(t)$ at the instance when the turning has finished becomes the initial value of the next step. Therefore, for the rightward steering the coordinate $x(t)$ and $y(t)$ of the center of gravity can be given as the function of the above-mentioned $\theta(t)$. Namely, from Fig. 6-3, they are

$$x(t) = DGRR\{\sin(\alpha + \theta_0 + \theta(t)) - \sin(\alpha + \theta_0)\} \quad (6\text{-}21)$$

$$y(t) = DGRR\{\cos(\alpha + \theta_0) - \cos(\alpha + \theta_0 + \theta(t)\} \quad (6\text{-}22)$$

In the similar manner, for the leftward steering the turning angle after t sec is given by

$$\theta(t) = (\frac{M_L J_L}{c_{rL}} + \theta_0) e^{\frac{-c_{rL}}{J_L} t} + \frac{M_L}{c_{rL}} t - \frac{M_L J_L}{c_{rL}^2} \quad (6\text{-}23)$$

The coordinate x(t) and y(t) of the center of gravity are given as the function of this θ(t) from Fig. 6-4. Namely,

$$x(t) = DGRL\{\sin(\theta(t) + \beta - \theta_0) - \sin(\beta - \theta_0)\} \quad (6\text{-}24)$$

$$y(t) = DGRL\{\cos(\theta(t) + \beta - \theta_0) - \cos(\beta - \theta_0)\} \quad (6\text{-}25)$$

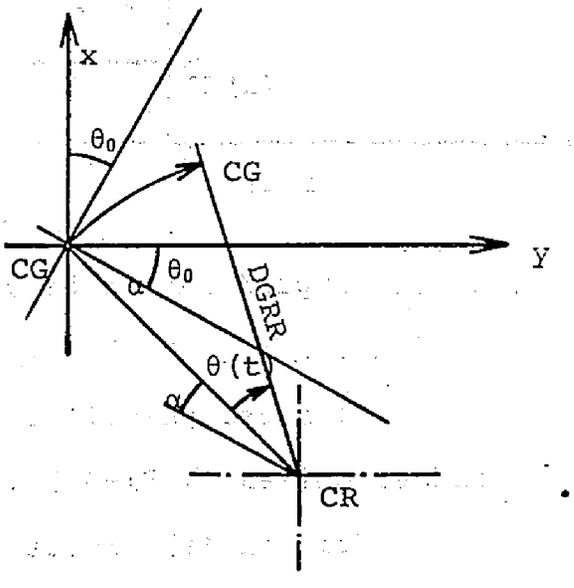

Fig. 6-3 Geometry for Rightward Steering

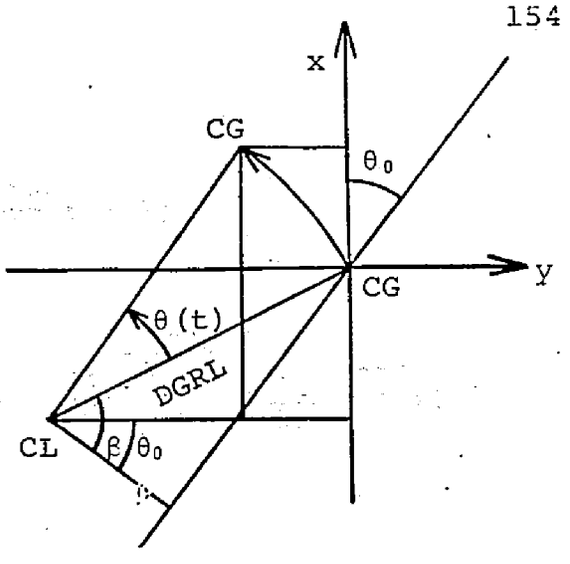

Fig. 6-4 Geometry for Leftward Steering

From the experimental results, the actual torque of the drive sprocket shaft is as shown in Fig. 6-5, and is governed by the following equation for turning.

$$M_{R(L)} = T_{R(L)} + RT_{R(L)}\left(1 - e^{-\frac{t}{T}}\right), \qquad (6\text{-}26)$$

namely, as shown in Fig. 6-5.

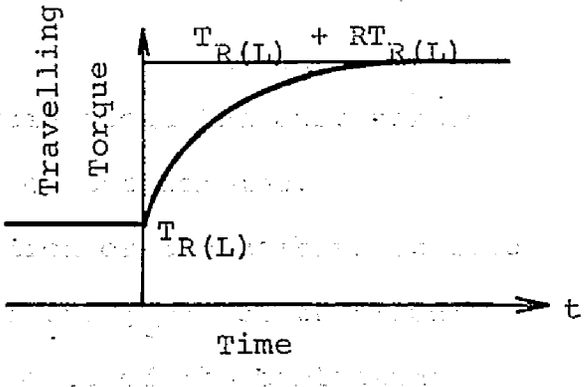

Fig. 6-5 Travelling Torque of Combine at Starting on Steering

If this actual torque is used instead of the torque M_R, which is used in Eq. (6-17) through Eq. (6-20), the turning angle after t sec is given by the following equation. Substituting Eq. (6-26) into Eq. (6-17), taking Laplace transform of this result, solving about θ(s) and taking inverse Laplace transform, then θ(t) is,

$$\theta(t) = \frac{T_R + RT_R}{J_R}\frac{J_R^2}{c_{rR}^2}\left(e^{-\frac{c_{rR}}{J_R}t} + \frac{c_{rR}}{J_R}t - 1\right)$$

$$-\frac{J_R T}{c_{rR}}\left[1 + \frac{1}{c_{rR}/J_R - 1/T}\left(\frac{1}{T}e^{-\frac{c_{rR}}{J_R}t} - \frac{c_{rR}}{J_R}e^{-\frac{1}{T}t}\right)\right]$$

$$+ \theta_0 e^{-\frac{c_{rR}}{J_R}t}$$

The moments of inertia J_R and J_L are given by

$$J_R = J_G + \frac{1}{2}m(DGRR)^2 \qquad (6\text{-}27)$$

$$J_L = J_G + \frac{1}{2}m(DGRL)^2 \qquad (6\text{-}28)$$

where J_G is the mass moment of inertia about the axis through the center of gravity and m is mass of the combine.

In order to predict the motion of the combine steered automatically, the coordinates $x_s(t)$ and $y_s(t)$ of the middle point of the sensors and the coordinates of the contacting points of the links with the row of rice plant are necessary. And the equation giving these coordinates are different between the sensing systems as well as the turning directions.

1) The control system shown in Fig. 5-1

a) Straight travel

As shown in Fig. 6-1, the coordinates $x_s(t)$ and $y_s(t)$ of the middle point of the sensors are given by

$$x_s(t) = x(t) + DGS\ \sin(\phi - \theta_0) \qquad (6\text{-}29)$$

$$y_s(t) = y(t) + DGS\ \cos(\phi - \theta_0) \qquad (6\text{-}30)$$

Referring Fig. 6-6 gives the coordinates of the contacting points of the links with the row of rice plant.

i) Front right sensor

$$x_{MR}(t) = x_s(t) + \tfrac{1}{2}MS\cos\theta_0 - \tfrac{1}{2}MW\sin\theta_0 \qquad (6\text{-}31)$$

$$y_{MR}(t) = y_s(t) + \tfrac{1}{2}MS\sin\theta_0 + \tfrac{1}{2}MW\cos\theta_0 \qquad (6\text{-}32)$$

ii) Front left sensor

$$x_{ML}(t) = x_s(t) + \tfrac{1}{2}MS\cos\theta_0 + \tfrac{1}{2}MW\sin\theta_0 \qquad (6\text{-}33)$$

$$y_{ML}(t) = y_s(t) + \tfrac{1}{2}MS\sin\theta_0 - \tfrac{1}{2}MW\cos\theta_0 \qquad (6\text{-}34)$$

iii) Rear right sensor

$$x_{SR}(t) = x_s(t) - \tfrac{1}{2}MS\cos\theta_0 - \tfrac{1}{2}SW\sin\theta_0 \qquad (6\text{-}35)$$

$$y_{SR}(t) = y_s(t) - \tfrac{1}{2}MS\sin\theta_0 + \tfrac{1}{2}SW\cos\theta_0 \qquad (6\text{-}36)$$

iv) Rear left sensor

$$x_{SL}(t) = x_s(t) - \tfrac{1}{2}MS\cos\theta_0 + \tfrac{1}{2}SW\sin\theta_0 \qquad (6\text{-}37)$$

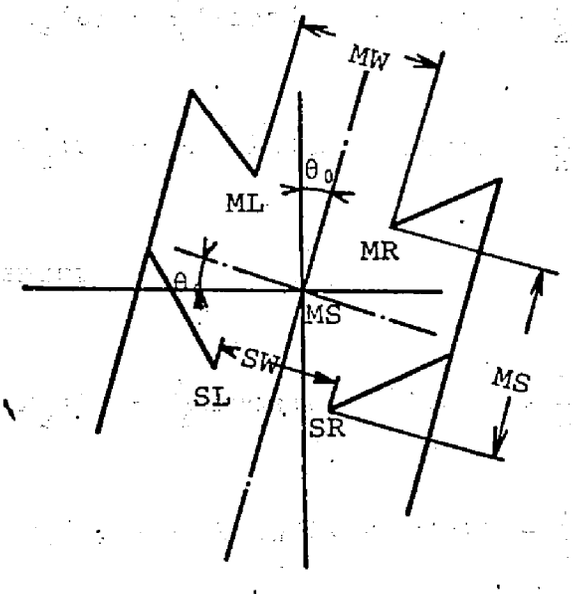

Fig.6-6 Locations of Contacting Points of Links with Row of Rice Plant

$$y_{SL} = y_s(t) - \frac{1}{2}MS\sin\theta_0 - \frac{1}{2}SW\cos\theta_0 \qquad (6\text{-}38)$$

b) Rightward steering

The coordinate $x_s(t)$ and $y_s(t)$ are given by

$$x_s(t) = RSL\cos(\lambda + \theta_0 - \theta(t)) - DGRL\sin(\beta - \theta_0) \qquad (6\text{-}39)$$

$$y_s(t) = RSL\sin(\lambda + \theta_0 - \theta(t)) - DGRL\cos(\beta - \theta_0) \qquad (6\text{-}40)$$

The coordinates of the contacting points of the links with the row of rice plant are given as follows.

i)Front right sensor

$$x_{MR}(t) = x_s(t) + \frac{1}{2}MS\cos(\theta_0 + \theta(t)) - \frac{1}{2}MW\sin(\theta_0 + \theta(t)) \quad (6\text{-}41)$$

$$y_{MR}(t) = y_s(t) + \frac{1}{2}MS\sin(\theta_0 + \theta(t)) + \frac{1}{2}MW\cos(\theta_0 + \theta(t)) \quad (6\text{-}42)$$

ii) Front left sensor

$$x_{ML}(t) = x_s(t) + \frac{1}{2}MS\cos(\theta_0 + \theta(t)) + \frac{1}{2}MW\sin(\theta_0 + \theta(t)) \quad (6\text{-}43)$$

$$y_{ML}(t) = y_s(t) + \frac{1}{2}MS\sin(\theta_0 + \theta(t)) - \frac{1}{2}MW\cos(\theta_0 + \theta(t)) \quad (6\text{-}44)$$

iii) Rear right sensor

$$x_{SR}(t) = x_s(t) - \frac{1}{2}MS\cos(\theta_0 + \theta(t)) - \frac{1}{2}SW\sin(\theta_0 + \theta(t)) \quad (6\text{-}45)$$

$$y_{SR}(t) = y_s(t) - \frac{1}{2}MS\sin(\theta_0 + \theta(t)) + \frac{1}{2}SW\cos(\theta_0 + \theta(t)) \quad (6\text{-}46)$$

iv) Rear left sensor

$$x_{SL}(t) = x_s(t) - \frac{1}{2}MS\cos(\theta_0 + \theta(t)) + \frac{1}{2}SW\sin(\theta_0 + \theta(t)) \quad (6\text{-}47)$$

$$y_{SL}(t) = y_s(t) - \frac{1}{2}MS\sin(\theta_0 + \theta(t)) + \frac{1}{2}SW\cos(\theta_0 + \theta(t)) \quad (6\text{-}48)$$

c) Leftward steering

Substituting $\{\theta_0 - \theta(t)\}$ into $\{\theta_0 + \theta(t)\}$ into Eqs.(6-41) through (6-48) gives the coordinates of the contacting points of the links with the row of rice plant for leftward steering.

2) The control system shown in Fig. 5-3

a) Straight travel

The contacting points of the links with the row of rice plant are given by referring Fig. 6-7.

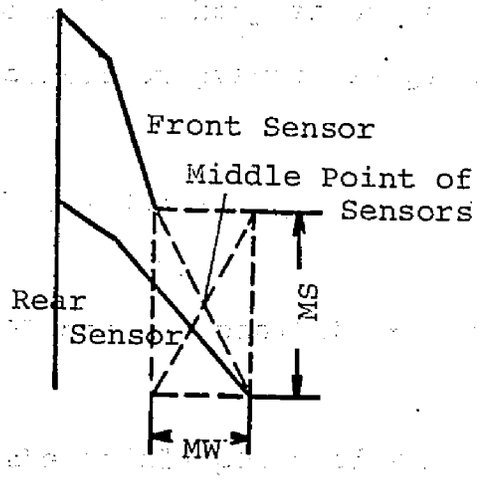

Fig. 6-7 Location of Contacting Points of Links with Row of Rice Plant

i) Front sensor

$$x_{MF}(t) = x_s(t) + \frac{1}{2}MS\cos\theta_0 + \frac{1}{2}MW\sin\theta_0 \qquad (6\text{-}49)$$

$$y_{MF}(t) = y_s(t) + \frac{1}{2}MS\sin\theta_0 - \frac{1}{2}MW\cos\theta_0 \qquad (6\text{-}50)$$

ii) Rear sensor

$$x_{MR}(t) = x_s(t) - \frac{1}{2}MS\cos\theta_0 - \frac{1}{2}MW\sin\theta_0 \qquad (6\text{-}51)$$

$$y_{MR}(t) = y_s(t) - \frac{1}{2}MS\sin\theta_0 + \frac{1}{2}MW\cos\theta_0 \qquad (6\text{-}52)$$

The coordinates of the middle point of the sensors $x_s(t)$ and

$y_s(t)$ are given by Eqs. (6-29) and (6-30).

b) Rightward steering

It is assumed that the turning centers are not located on the center lines of the tracks as shown in Fig. 6-1 but located outside the combine body as shown in Fig. 6-8. The coordinate of the center of gravity is given by

$$x(t) = DGRR\{\sin(\theta(t) - \theta_0) - \sin\theta_0\} \qquad (6\text{-}53)$$

$$y(t) = DGRR\{\cos\theta_0 - \cos(\theta(t) - \theta_0)\} \qquad (6\text{-}54)$$

The coordinate of the middle point of the sensor is given by

$$x_s(t) = RSR\{\cos(\delta + \theta_0 - \theta(t)) - \cos(\delta - \theta_0)\} \qquad (6\text{-}55)$$

$$y_s(t) = RSR\{\sin(\delta - \theta_0) - \sin(\delta + \theta_0 - \theta(t))\} \qquad (6\text{-}56)$$

The coordinates of the contacting points of the links with the row of rice plant are given by the following equations.

i) Front sensor

$$x_{MF}(t) = x_s(t) + \frac{1}{2}MS\cos(\theta_0 + \theta(t)) + \frac{1}{2}MW\sin(\theta_0 + \theta(t)) \qquad (6\text{-}57)$$

$$y_{MF}(t) = y_s(t) + \frac{1}{2}MS\sin(\theta_0 + \theta(t)) - \frac{1}{2}MW\cos(\theta_0 + \theta(t)) \qquad (6\text{-}58)$$

ii) Rear sensor

$$x_{MR}(t) = x_s(t) - \frac{1}{2}MS\cos(\theta_0 + \theta(t)) - \frac{1}{2}MW\sin(\theta_0 + \theta(t)) \qquad (6\text{-}59)$$

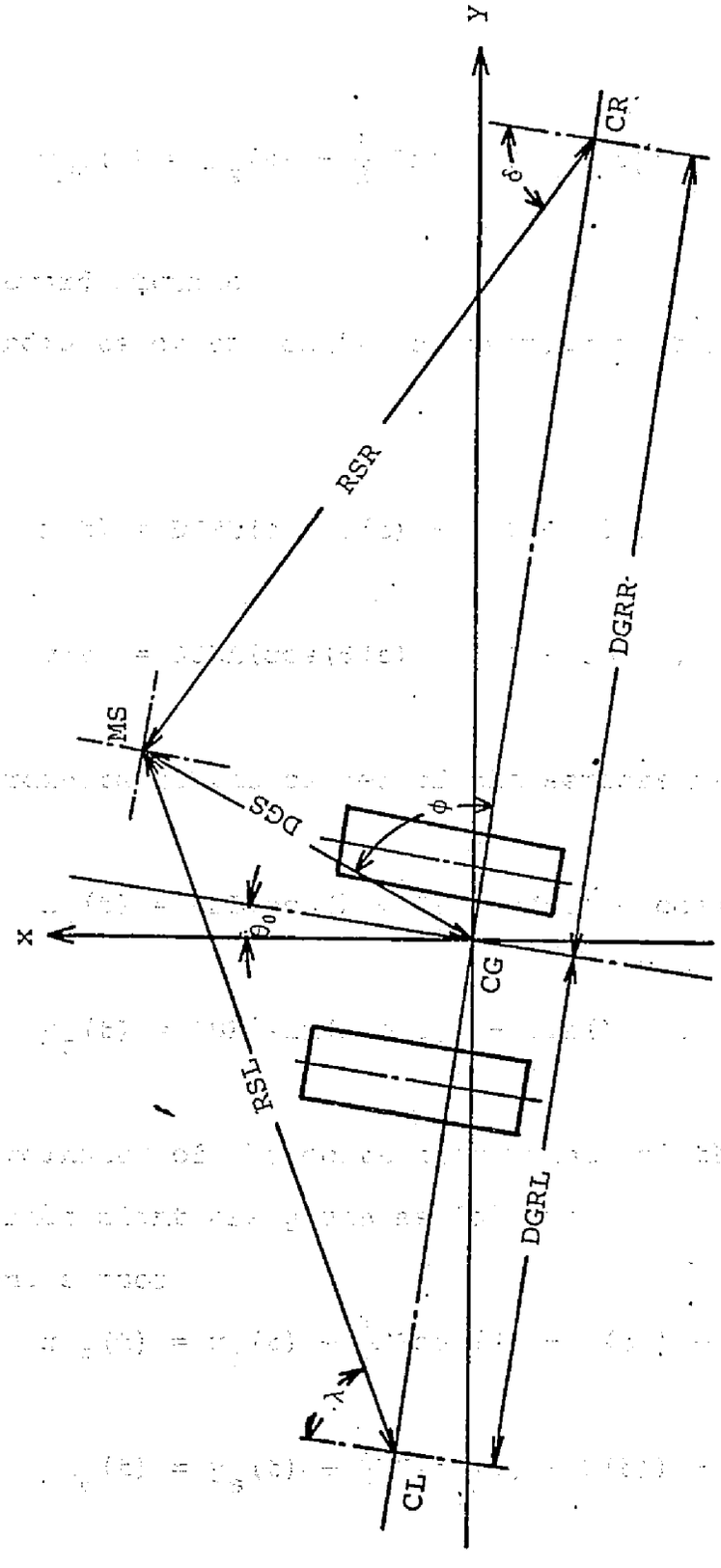

Fig. 6-8 Geometry of the Experimented Combine with the Control System shown in Fig. 5-3

$$y_{MR}(t) = y_s(t) - \frac{1}{2}MS\sin(\theta_0 + \theta(t)) + \frac{1}{2}MW\cos(\theta_0 + \theta(t)) \quad (6\text{-}60)$$

c) Leftward steering

The coordinate of the center of gravity of the combine is given by

$$x(t) = DGRL(\sin(\theta(t) - \theta_0) + \sin\theta_0) \quad (6\text{-}61)$$

$$y(t) = DGRL(\cos(\theta(t) - \theta_0) + \cos\theta_0) \quad (6\text{-}62)$$

The coordinate of the center of the sensors is given by

$$x_s(t) = RSL\{\cos(\lambda + \theta_0 - \theta(t)) - \cos(\lambda + \theta_0)\} \quad (6\text{-}63)$$

$$y_s(t) = RSL\{\sin(\lambda + \theta_0) - \sin(\lambda + \theta_0 - \theta(t)) \quad (6\text{-}64)$$

The coordinates of the contacting points of the links with the row of ride plant are given as follows.

i) Front sensor

$$x_{MF}(t) = x_s(t) + \frac{1}{2}MS\cos(\theta_0 - \theta(t)) + \frac{1}{2}MW\sin(\theta_0 - \theta(t)) \quad (6\text{-}65)$$

$$y_{MF}(t) = y_s(t) + \frac{1}{2}MS\sin(\theta_0 - \theta(t)) - \frac{1}{2}MW\cos(\theta_0 - \theta(t)) \quad (6\text{-}66)$$

ii) Rear sensor

$$x_{MR}(t) = x_s(t) - \frac{1}{2}MS\cos(\theta_0 - \theta(t)) - \frac{1}{2}MW\sin(\theta_0 - \theta(t)) \quad (6\text{-}67)$$

$$y_{MR}(t) = y_s(t) - \frac{1}{2}MS\sin(\theta_0 - \theta(t)) + \frac{1}{2}MW\cos(\theta_0 - \theta(t)) \qquad (6\text{-}68)$$

Using the mathematical model of the control system which was constructed by the above-mentioned equations and the logical flowchart represented in the next section, the digital simulation of the response paths of the automatically steered combine was performed by the FACOM 230-60 digital computer at Kyoto University Data Processing Center.

6-2 Logical Flowchart for Automatic Steering System Simulation

6-2-1 System with the Sensors Detecting the Row of Rice Plant from Both Sides of It*

The process in which the sensors detect the row of rice plant and determine the steering direction is represented by the flowchart of the upper part in Fig. 6-9. In this process, the combine is determined its steering direction (that is, rightward or leftward turning) by the sign of deviation of the contacting links. The flow chart in the lower part represents the action of the main circuit. In this flowchart, the first dicision process compares the deviation of the contacting link of the main sensor (MLD) with the deviation of the supplementary sensor (SLD) and when MLD is larger than SLD the steeing is performed by the main sensor circuit. When SLD is larger than MLD on the contrary, the steering is performed by the supplementary circuit as shown in Fig. 6-10. As soon as MLD is occured in this case, the steering is performed by the main sensor circuit instead of the supplementary circuit. In Fig. 6-9, MPSWL indicates the dead zone width of the main sensor and MSL1 is the stroke of the rod of hydraulic actuator controlled by the main sensor circuit. In Fig. 6-10, SPSWL indicates the dead zone width of the supplementary sensor and MSL2 is the stroke of the rod of hydraulic actuator controlled by the supplementary sensor circuit. In this experiment, since MSL1 is larger than MSL2, the turning radius by the main sensor circuit is smaller. But, since the difference between the radii of the steering by those circuits was not confirmed according to the experiments, the

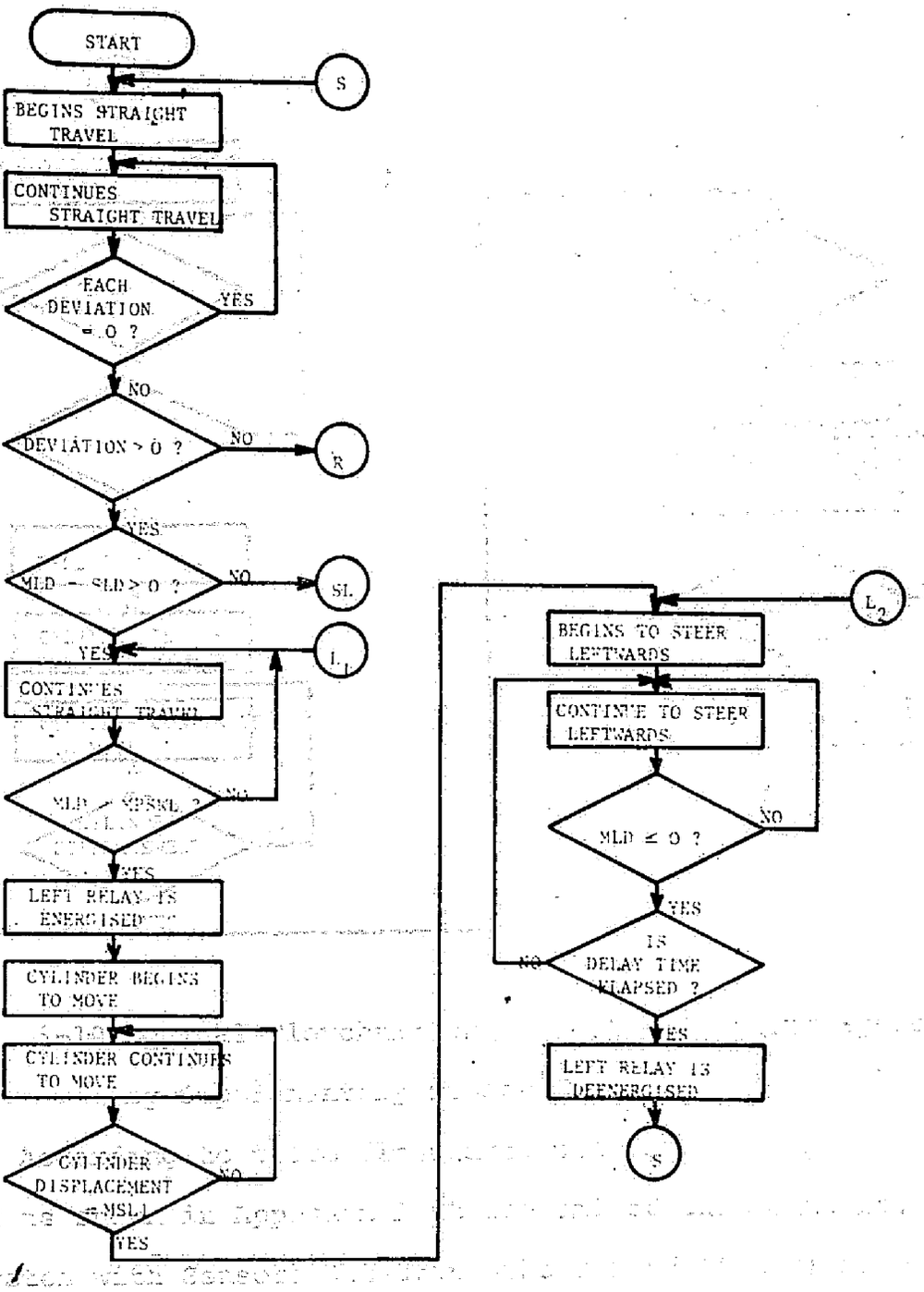

Fig. 6-9 Logical Flowchart of Steering System for Searching Row of Rice Plant and Determining Steering Direction and Automatic Steering by Main Sensor

equal radii of the steering were used for the digital simulation.

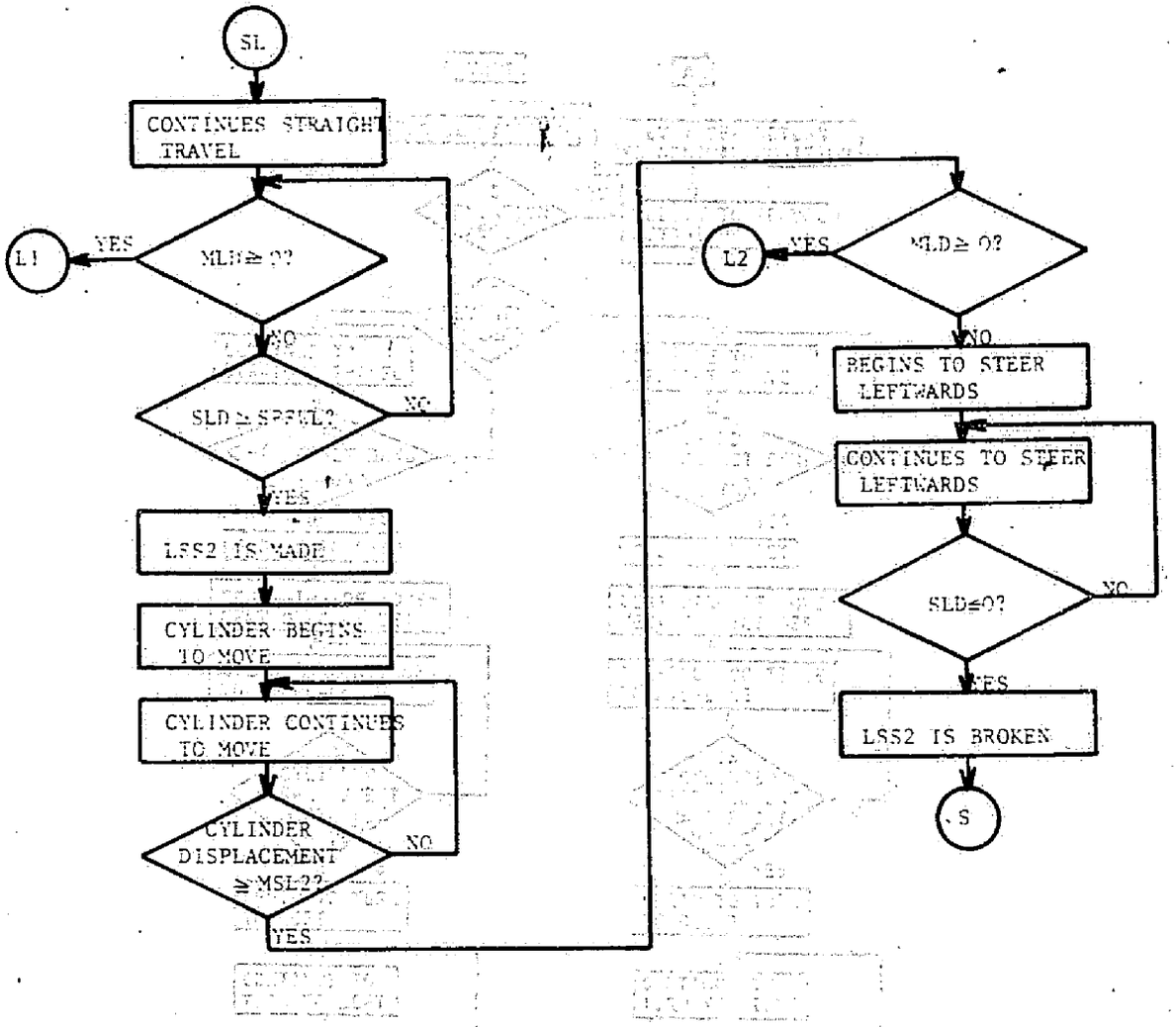

Fig. 6-10 Logical Flowchart of Automatic Steering System by Supplementary Sensor Circuit

According to these flowchart, the simulatin programm was obtained as shown in Appendix A at the end of this chapter.

6-2-2 System with Sensors Detecting the Row of Rice Plant from One side of It**

The logical flowchart for the automatic steering system is shown in Fig. 6-11. In this flowchart, FMS and RMS represent the microswitches of the front and rear sensors, respectively. FD indicates the difference between the y-coordinates of the

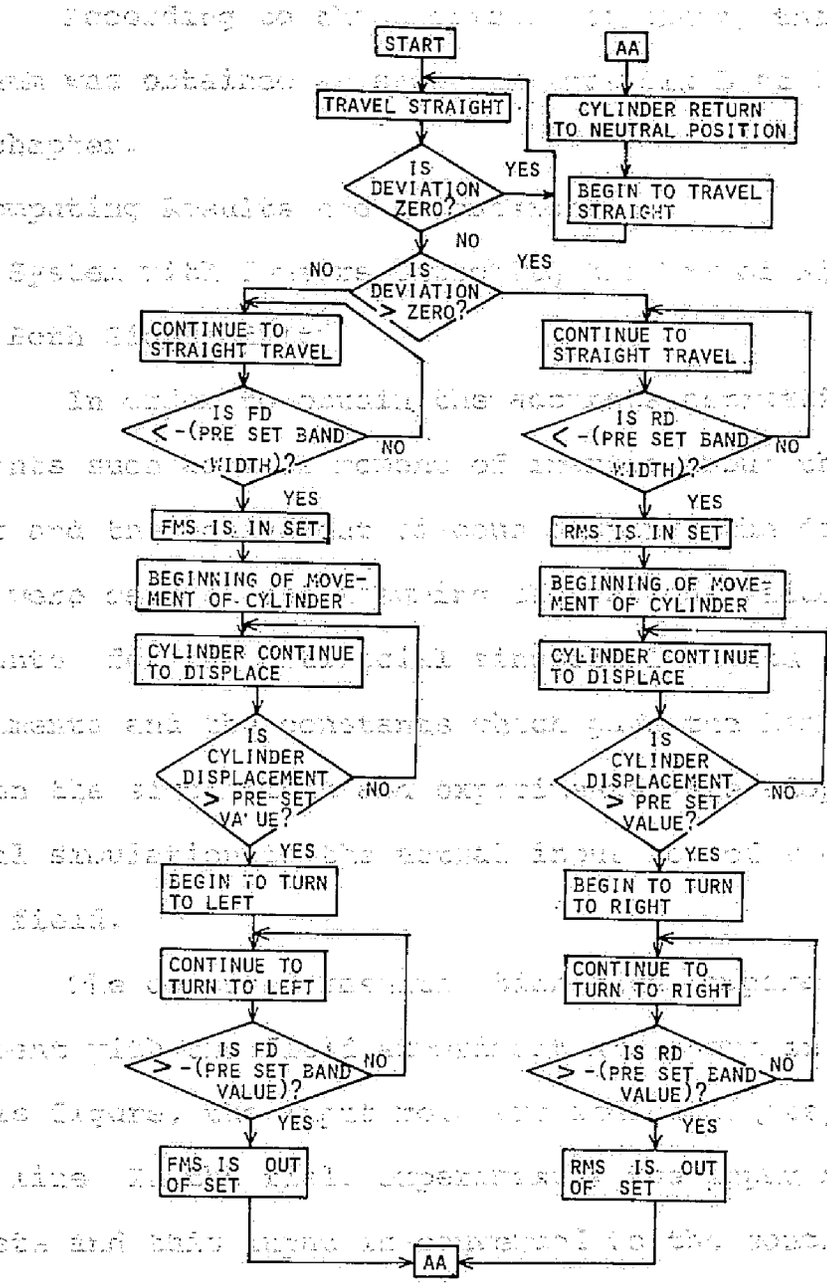

Fig 6-11 Logical Flowchart for Digital Simulation of the Automatic Steering System Shown in Fig. 5-3

contacting point given by Eqs. (6-50), (6-58) and (6-66) and of the stump of rice plant. RD indicates the difference between the y-coordinates of the contacting point given by

Eqs. (6-52), (6-60) and (6-68) and of the stump of rice plant.

According to this logical flowchart, the simulation programm was obtained as shown in Appendix B at the end of this chapter.

6-3 Computing Results and Discussions

6-3-1 System with Sensors Detecting the Row of Rice Plant from Both Sides of It*

In order to obtain the accurate estimations of the constants such as mass moment of inertia about the steering center and the equivalent viscous damping, the digital simulations were carried out assuming the various values of these constants for the artificial sinusoidal inputs used for the experiments and the constants which gave the least difference between the simulations and experiments were adopted for the digital simulation to the actual input row of rice plant in the paddy field.

The computed results which gave comparatively good agreement with the field experiment are shown in Fig. 6-12. In this figure, the input rows are indicated stepwise with the solid line. In the field experiments, the input row of plant is discrete and this input is converted to the continuous input by using the contacting link of the finite length longer than the distance between the adjacent stumps. In the digital simulation of this chapter, the sensing method mentioned above could be considered as the 0-order hold in the sampled-data control system and then the input was shown by the series of steps. The paths represented by the broken and the dot-dash

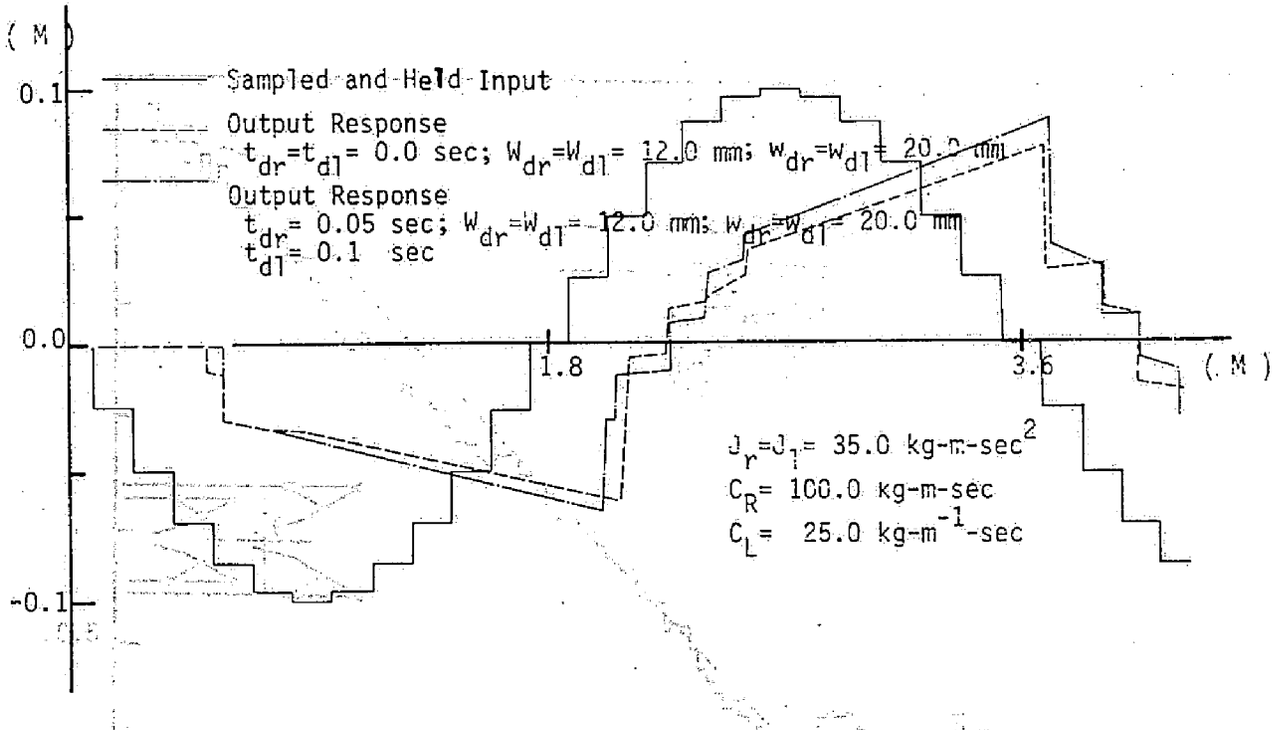

Fig. 6-12 Predicted Response Paths to the Artificial Sinusoidal Input Row of Plant by Digital Simulation

lines are the predicted loci of the middle point of the sensors. From these results, it may be appropriate to assume that mass moments of inertia J_R and J_L about the centers of the rightward and leftward steering are equal and 35 kg-m-sec^2 and the equivalent viscous damping factors are 100 kg-m^{-1}-sec for turning and 25 kg-m^{-1}-sec for straight travel. These constants take different values for the different soil conditions and machines.

Therefore, in the future the accurate values must be determined by the experiments.

Fig. 6-13 indicates the digital simulation results

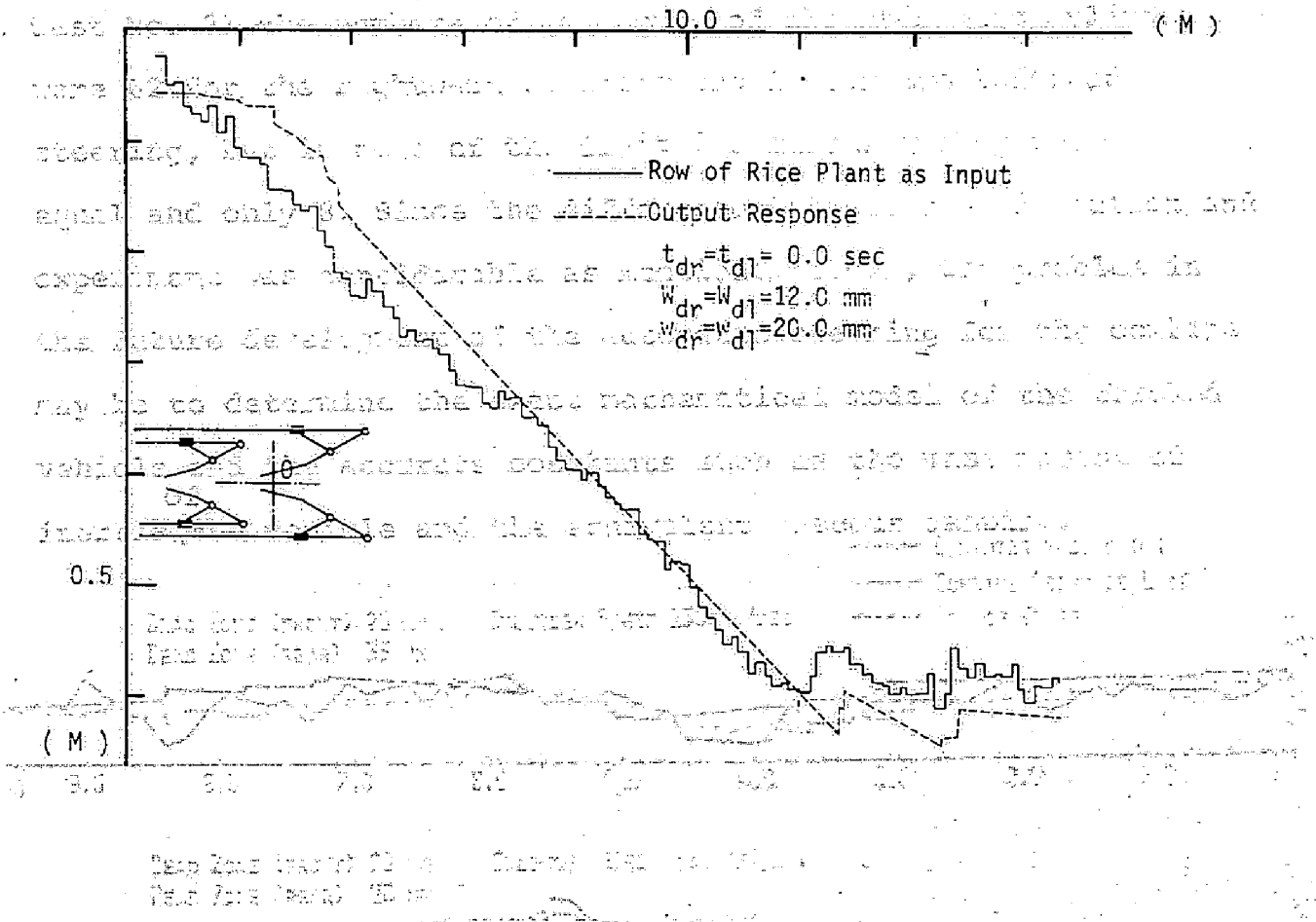

Fig. 6-13 Predicted Response Paths to the Actual Row of Rice Plant in the Paddy Field by Digital Simulation

carried out for the actual row of rice plant which showed the most considerable meandering of the data obtained in the field. This figure suggests the applicability of the automatic steering system in the actual paddy field.

6-3-2 System with Sensors Detecting the Row of Rice Plant from One Side of It**

The simulation results carried out for the actual data in the field are shown in Fig. 6-14 by the solid lines. From these figures, it was found that the digital simulated combine was steered less than the experimented combine. For example, in Test No. 21 the numbers of movements of the hydraulic cylinder were 62 for the rightward steering and 27 for the leftward steering, but in case of the digital simulation they were equal and only 8. Since the difference between the simulation and experiment was considerable as mentioned above, the problem in the future development of the automatic steering for the combine may be to determine the exact mathematical model of the tracked vehicle and the accurate constants such as the mass moment of inertia of the vehicle and the equivalent viscous damping.

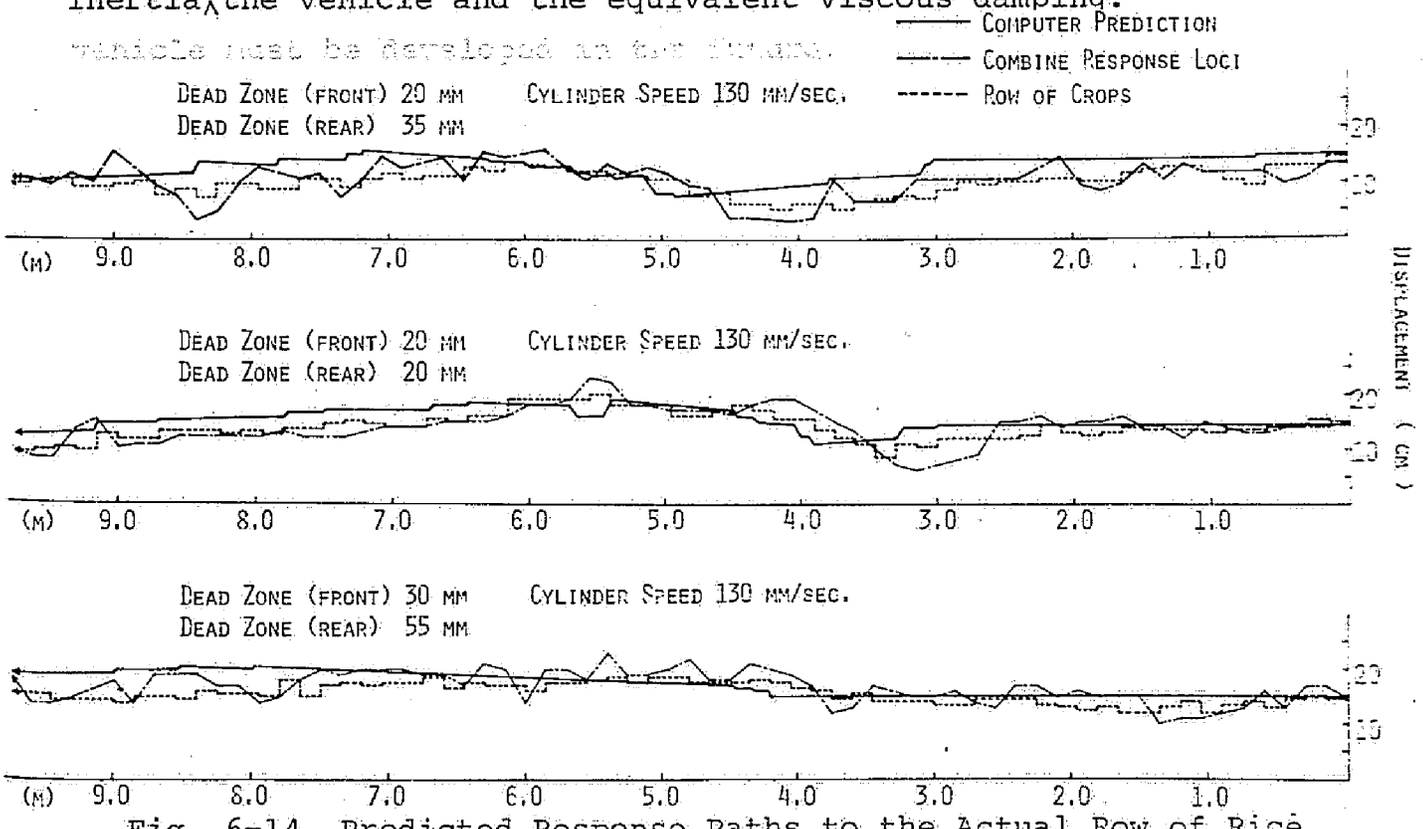

Fig. 6-14 Predicted Response Paths to the Actual Row of Rice Plant in the Field by Digital Simulation

6-3 Conclusions of This Chapter

In order to determine the optimal combination of the parameters in the nonlinear control system, the digital simulation technique may be effective. In this chapter, the mathematical model of the automatically steered combine is proposed and the applicability of the automatic steering system is discussed in the field by this technique. Moreover, the reliability of the model is discussed comparing simulation and experiment results. The following results were obtained.

1) The digital simulation of the automatic steering of the combine suggested the possibility of the utilization of the experimented system in the actual field.

2) The predicted paths of the automatically steered combine were smoother than the experimental results. Therefore, the appropriate mathematical model for the dynamics of the tracked vehicle must be developed in the future.

Appendix A Simulation Programm for Automatically Steered Combine with Sensors Detecting Row of Rice Plant from Both Sides of It

The constants used in this simulation programm are as follows.

N = 1500	DT = 0.02 sec	DRIVE = 0.0 rad
TR = 8.5 kg-m	AMP = 0.1 m	T = 3.6 m
PSI = 0.0 rad	CVR = 0.065 m/sec	AMR = 0.1 m
MPSWR = 0.012 m	SPSWL = 0.02 m	AMP = 0.1 m
T = 3.6 m	PSI = 0.0 rad	CVL = 0.055 m
AML = 11.0 kg-m	MPSWL = 0.012 m	SPSWL = 0.02 m
TL = 8.5 kg-m	GM = 76.5 $kg\text{-}m^{-1}\text{-}sec^{2}$	
C = 25 $kg\text{-}m^{-1}$	CR = 100.0 kg-m-sec	
MSR = 0.02 m	SSR = 0.018 m	AJR = 35.0$kg\text{-}m\text{-}s^{2}$
MSL = 0.02 m	SSL = 0.018 m	AJL = 35.0$kg\text{-}m\text{-}s^{2}$

```
C     SIMULATION OF MOTION OF AUTOMATIC STEERED COMBINE
      REAL MYSL,MYSR,MDSL,MDSR,MRY,MRDSL,MRDSR,MXSL,MXSR,MPSWR,MPSWL,MSL
     1,MSR,Mw,MS,MWCT,MSST,MSCT,MRX,MYSRO,MYSLO,MXSRO,MXSLO,MWST
      DIMENSION X(2000),Y(2000),XS(2000),YS(2000),MYSL(2000),MYSR(2000),
     1MDSL(2000),MDSR(2000),SDSL(2000),SDSR(2000),THETA(2000),MRY(2000),
     2MRDSL(2000),MRDSR(2000),SRDSL(2000),SRDSR(2000),SYSL(2000),SYSR(2C
     300),MXSL(2000),MXSR(2000),SXSL(2000),SXSR(2000),SRY(2000),XSL(200C
     4),RMDSL(2000),RMDSR(2000),RSDSL(2000),RSDSR(2000),CP(200),MRX(200C
     5),SRX(2000)
C     CP IS MEASURED Y COORDINATE OF RICE PLANT ROW
C     N IS NUMBER OF DATA
C     NR IS DELAY TIME FOR RIGHT STEERING
C     NL IS DELAY TIME FOR LEFT STEERING
C     KK IS TEST NO.
C     AMP IS AMPLITUDE OF ROW AS INPUT
C     T   IS PERIOD OF ROW AS INPUT
C     PSI IS PHASE OF ROW
      DRIVE IS ANGLE OF INITIAL TRAVEL
      DGS   IS DISTANCE FROM CENTER OF GRAVITY TO CENTER OF SENSER
      CVR   IS SPEED OF HYDRAULIC CYLINDER FOR RITHT STEERING
      CVL   IS SPEED OF HYDRAULIC CYLINDER FOR LEFT TRAVEL
      MSR   IS PRESET RANGE OF DISPLACEMENT OF CYLINDER FOR RIGHT STEERI
      NG BY MAIN  SENSING POINT
      MSL   IS  PRESET RANGE OF DISPLACEMENT OF CYLINDER FOR LEFT STEERI
      G BY MAIN  S.P.
      SSR   IS PRESET RANGE OF DISPLACEMENT OF CYLINDER BY SUB  S.P.
      SSL   IS PRESET RANGE OF DISPLACEMENT OF CYLINDER BY SUB  S.P.
      TR    IS TORQUE OF RIGHT READ AXLE
      TL    IS TORQUE OF LEFT READ AXLE
      GM  IS MASS OF COMBINE
      C   IS EQUIVALENT VISCOUSITY TO STRAIGHT TRAVEL
      AJR IS MASS MOMENT OF INERTIA ABOUT AXIS THROUGH CENTER OF ROTATIC
      NAT RIGHT STEERING
      AJL IS MASS MOMENT OF INERTIA ABOUT AXIS THROUGH CENTER OF ROTATIC
      N AT LEFT STEERING
      CR  IS EQUIVALENT VISCOUSITY TO STEERING
      AMR IS MOMENT OF RIGHT STEERING
      AML IS MOMENT OF LEFT STEERING
      MPSWR IS PRE-SET BAND WIDTH OF DEAD ZONE OF MAIN  SENSOR FOR RIGHT
      STEERING
      MPSWL IS PRE-SET BAND WIDTH OF DEAD ZONE OF MAIN SENSOR FOR LEFT
      STEERING
C     SPSWR IS PRE-SET BAND WIDTH OF DEAD ZONE OF SUB  SENSOR FOR RIGHT
C     STEERING
C     SPSWL IS PRE-SET BAND EIDTH OF DEAD ZONE OF SUB  SENSOR FOR LEFT S
C     TEFRING
C     X   IS X-COORDINATE OF THE POSITION OF THE CENTER OF GRAVITY
C     Y   IS Y-COORDINATE OF THE POSITION OF THE CENTER OF GRAVITY
C     XS  IS X-COORDINATE OF MIDPOINT OF THE SENSOR
C     YS  IS Y-COORDINATE OF MIDPOINT OF THE SENSOR
C     MYSL IS Y-COORDINATE OF LEFT CONTACTING POINT OF THE MAIN SENSOR
C     MYSR IS Y-COODINATE OF RIGHT CONTACTING POINT OF THE MAIN SENSOR
C     SYSL IS Y-COORDINATE OF LEFT CONTACTING POINT OF THE SUB SENSOR
C     SYSR IS Y-COORDINATE OF RIGHT CONTACTING POINT OF THE SUB SENSOR
C     MXSL IS X-COORDINATE OF LEFT CONTACTING POINT OF THE MAIN-SENSOR
```

```
)*
C      MXSR IS X-COORDINATE OF RIGHT CONTACTING POINT OF THE MAIN SENSOR
C      SXSL IS X-COORDINATE OF LEFT CONTACTING POINT OF THE SUB SENSOR
C      SXSR IS X-COORDINATE OF RIGHT CONTACTING POINT OF THE MAIN SENSOR
C      WM  IS DISTANCE OF CONTACTING POINTS OF MAIN SENSOR
C      WS  IS DISTANCE OF CONTACTING POINTS OF SUB SENSOR
C      MS  IS DISTANCE FROM MAIN CONTACTOR TO SUB CONTACTOR
C      MRY  IS Y-COORDINATE OF THE ROW OF CROP AT MAIN SENSOR
C      SRY  IS Y-COORDINATE OF THE ROW OF CROP  AT MAIN SENSOR
  111 READ(5,100)N,KK,AMP,DT,T,NR,NL
  100 FORMAT(2I8,3F10.0,2I8)
      IF(KK.EQ.0)GO TO 112
      READ(5,123)PSI,DRIVE,DGS,CVR,CVL,MSR,MSL,SSR,SSL,ALPHA,BETA,DELTA,
     1ALAMDA,PHI,TR,TL,GM,C,AJR,AJL,CR,AMR,AML,RSL,RSR,DGRR,DGRL,MPSWR,M
     2PSWL,SPSWR,SPSWL,MW,SW,MS
  123 FORMAT(7F10.0)
      DO 334 I=1,192
  334 CP(I)=100.0*SIN(FLOAT(I-1)*0.2618+3.14159)
      EY=0.444-CP(1)/1000.0
      WRITE(6,101)
  101 FORMAT(1H1,39HSIMURATION OF AUTOMATIC STEERED COMBINE)
      WRITE(6,1)
    1 FORMAT(1H0,5X,16HSINUSOIDAL INPUT)
      WRITE(6,102)N,KK,DT,DRIVE,TR,TL,GM,C,CR
  102 FORMAT(1H0,2HN=I8,1X,3HKK=I8,1X,3HDT=F10.5,1X,6HDRIVE=F10.5,1X,3HT
     1R=F10.5,1X,3HTL=F10.5,1X,3HGM=F10.5,1X,2HC=F10.5,1X,3HCR=F10.5)
      WRITE(6,103)AMP,T,PSI,CVR,MSR,SSR,AJR,AMR,MPSWR,SPSWR,NR,RSR
  103 FORMAT(1H0,2X,4HAMP=F10.5,4X,2HT=F10.5,4X,4HPSI=F10.5,4X,4HCVR=F10
     1.5,4X,4HMSR=F10.5,4X,4HSSR=F10.5,4X,4HAJR=F10.5///,1H ,4HAMR=F10.5
     2,4X,6HMPSWR=F10.5,4X,6HSPSWR=F10.5,4X,3HNR=I8,4X,4HRSR=F10.5)
      WRITE(6,104)AMP,T,PSI,CVL,MSL,SSL,AJL,AML,MPSWL,SPSWL,NL,RSL
  104 FORMAT(1H0,2X,4HAMP=F10.5,4X,2HT=F10.5,4X,4HPSI=F10.5,4X,4HCVL=F10
     1.5,4X,4HMSL=F10.5,4X,4HSSL=F10.5,4X,4HAJL=F10.5///,1H ,4HAML=F10.5
     2,4X,6HMPSWL=F10.5,4X,6HSPSWL=F10.5,4X,3HNL=I8,4X,4HRSL=F10.5)
      WRITE(6,107)
  107 FORMAT(1H0,5X,1HL,6X,1HX,6X,1HY,6X,2HXS,5X,2HYS,3X,4HMXSL,3X,4HMYS
     1L,3X,4HMXSR,3X,4HMYSR,3X,4HSXSR,3X,4HSYSR,3X,4HSXSL,3X,4HSYSL,2X,6
     2HTHETA0,3X,3HMRX,4X,3HMRY,4X,3HSRX,4X,3HSRY)
      AK=6.2831/T
      X0=0.0
      Y0=0.0
      XS0=0.0
      YS0=0.0
      THETA0=DRIVE
      L=0
      M=2
   11 I=1
      WRITE(6,204)
  204 FORMAT(1H ,31HBEGINNING OF STRAIGHT TRAVELING)
      CT=COS(THETA0)
      ST=SIN(THETA0)
      GC=GM/(C*C)
      CG=C/GM
      PT=PHI-THETA0
      DSP=DGS*SIN(PT)
      DCP=DGS*COS(PT)
```

```
      CGDT=CG*DT
      CTCG=CT*GC
      STCG=ST*GC
      MWCT=MW*CT/2.0
      SWCT=SW*CT/2.0
      MSST=MS*ST/2.0
      MWST=MW*ST/2.0
      SWST=SW*ST/2.0
      MSCT=MS*CT/2.0
   12 CI=-2.0*FLOAT(I)
      FR=TR*(2.0*EXP(CI)+1.0)
      FL=TL*(2.0*EXP(CI)+1.0)
      FRLC=(FR+FL)*CTCG
      FRLS=(FR+FL)*STCG
      AI=-CGDT*FLOAT(I)
      L=L+1
      X(L)=X0+FRLC*(EXP(AI)+CGDT*FLOAT(I)-1.0)
      Y(L)=Y0+FRLS*(EXP(AI)+CGDT*FLOAT(I)-1.0)
      XS(L)=X(L)+DSP
      YS(L)=Y(L)+DCP
      MYSL(L)=YS(L)+MSST-MWCT
      MYSR(L)=YS(L)+MSST+MWCT
      SYSL(L)=YS(L)-MSST-SWCT
      SYSR(L)=YS(L)-MSST+SWCT
      MXSL(L)=XS(L)+MSCT+MWST
      MXSR(L)=XS(L)+MSCT-MWST
      SXSL(L)=XS(L)-MSCT+SWST
      SXSR(L)=XS(L)-MSCT-SWST
      MRX(L)=XS(L)+0.08*CT
      SRX(L)=XS(L)-0.08*CT
      DNN=0.15*(FLOAT(M))+1.587
      IF(MRX(L).GE.DNN)GO TO 35
      IF(MRX(L).LT.DNN)GO TO 36
   35 M=M+1
      IF(M.EQ.290)GO TO 112
   36 MRY(L)=CP(M)/1000.0+EY
      SRY(L)=CP(M-1)/1000.0+EY
      MDSL(L)=MRY(L)-MYSL(L)
      MDSR(L)=MRY(L)-MYSR(L)
      SDSL(L)=SRY(L)-SYSL(L)
      SDSR(L)=SRY(L)-SYSR(L)
      WRITE(6,108)L,X(L),Y(L),XS(L),YS(L),MXSL(L),MYSL(L),MXSR(L),MYSR(L
     1),SXSR(L),SYSR(L),SXSL(L),SYSL(L),THETA0,MRX(L),MRY(L),SRX(L),SRY(
     2L)
  108 FORMAT(1H ,2X,I6,17F7.4)
      IF(L.EQ.N)GO TO 111
      IF(MDSR(L).GE.0.0)GO TO 200
      IF(MDSL(L).LE.0.0)GO TO 600
      IF(SDSR(L).GE.0.0)GO TO 1000
      IF(SDSL(L).LE.0.0)GO TO 2000
      I=I+1
      GO TO 12
  200 WRITE(6,201)
  201 FORMAT(1H0,50HBEGINNING OF CONTACT OF RIGHT MAIN SENSOR WITH ROW)
  202 I=I+1
```

```
)*
      L=L+1
      AI=-CGDT*FLOAT(I)
      X(L)=X0+FRLC*(EXP(AI)+CGDT*FLOAT(I)-1.0)
      Y(L)=Y0+FRLS*(EXP(AI)+CGDT*FLOAT(I)-1.0)
      XS(L)=X(L)+DSP
      YS(L)=Y(L)+DCP
      MYSL(L)=YS(L)+MSST-MWCT
      MYSR(L)=YS(L)+MSST+MWCT
      SYSL(L)=YS(L)-MSST-SWCT
      MRX(L)=XS(L)+0.08*CT
      SRX(L)=XS(L)-0.08*CT
      DNN=0.15*(FLOAT(M))+1.587
      IF(MRX(L).GE.DNN)GO TO 40
      IF(MRX(L).LT.DNN)GO TO 41
   40 M=M+1
      IF(M.EQ.190)GO TO 112
   41 MRY(L)=CP(M)/1000.0+EY
      SRY(L)=CP(M-1)/1000.0+EY
      SYSR(L)=YS(L)-MSST+SWCT
      MXSL(L)=XS(L)+MSCT+MWST
      MXSR(L)=XS(L)+MSCT-MWST
      SXSL(L)=XS(L)-MSCT+SWST
      SXSR(L)=XS(L)-MSCT-SWST
      WRITE(6,108)L,X(L),Y(L),XS(L),YS(L),MXSL(L),MYSL(L),MXSR(L),MYSR(L
     1),SXSR(L),SYSR(L),SXSL(L),SYSL(L),THETA0,MRX(L),MRY(L),SRX(L),SRY(
     2L)
      RMDSL(L)=(MRY(L)-MYSL(L))/CT
      RMDSR(L)=(MRY(L)-MYSR(L))/CT
      RSDSL(L)=(SRY(L)-SYSL(L))/CT
      RSDSR(L)=(SRY(L)-SYSR(L))/CT
      IF(L.EQ.N)GO TO 111
      IF(RMDSR(L).GE.MPSWR)GO TO 300
      IF(RMDSL(L).LE.-MPSWL)GO TO 700
      IF(L.EQ.N)GO TO 111
      GO TO 202
  300 WRITE(6,301)
  301 FORMAT(1H0,21HRIGHT RERAY IS IN SET)
      IF(L.EQ.N)GO TO 111
      J=0
  302 J=J+1
      I=I+1
      L=L+1
      AI=-CGDT*FLOAT(I)
      DCR=CVR*DT*FLOAT(J)
      X(L)=X0+FRLC*(EXP(AI)+CGDT*FLOAT(I)-1.0)
      Y(L)=Y0+FRLS*(EXP(AI)+CGDT*FLOAT(I)-1.0)
      Y(L)=(X(L)-X0)*ST+Y0
      XS(L)=X(L)+DSP
      YS(L)=Y(L)+DCP
      MYSL(L)=YS(L)+MSST-MWCT
      MYSR(L)=YS(L)+MSST+MWCT
      SYSL(L)=YS(L)-MSST-SWCT
      SYSR(L)=YS(L)-MSST+SWCT
      MXSL(L)=XS(L)+MSCT+MWST
      MXSR(L)=XS(L)+MSCT-MWST
```

```
)*
      SXSL(L)=XS(L)-MSCT+SWST
      SXSR(L)=XS(L)-MSCT-SWST
      MRX(L)=XS(L)+0.08*CT
      SRX(L)=XS(L)-0.08*CT
      DNN=0.15*(FLOAT(M))+1.587
      IF(MRX(L).GE.DNN)GO TO 45
      IF(MRX(L).LT.DNN)GO TO 46
   45 M=M+1
      IF(M.EQ.190)GO TO 112
   46 MRY(L)=CP(M)/1000.0+EY
      SRY(L)=CP(M-1)/1000.0+EY
      RMDSR(L)=(MRY(L)-MYSR(L))/CT
      WRITE(6,108)L,X(L),Y(L),XS(L),YS(L),MXSL(L),MYSL(L),MXSR(L),MYSR(L
     1),SXSR(L),SYSR(L),SXSL(L),SYSL(L),THETA0,MRX(L),MRY(L),SRX(L),SRY(
     2L)
      IF(L.EQ.N)GO TO 111
      IF(DCR.GE.SSR)GO TO 400
      GO TO 302
  400 RMDSR0=RMDSR(L)
      WRITE(6,401)
  401 FORMAT(1H0,27HBEGINNING OF RIGHT STEERING)
      X0=X(L)
      Y0=Y(L)
      XS0=XS(L)
      YS0=YS(L)
      MYSL0=MYSL(L)
      MYSR0=MYSR(L)
      SYSL0=SYSL(L)
      SYSR0=SYSR(L)
      MXSL0=MXSL(L)
      SXSL0=SXSL(L)
      SXSR0=SXSR(L)
      J=J+1
      K=1
      ACR=AMR/CR
      AJCR=AMR*AJR/(CR*CR)
      ARC=CR/AMR
      SAT=SIN(ALPHA+THETA0)
      CAT=COS(ALPHA+THETA0)
  402 AI1=-CR*DT*FLOAT(K+NR-1)/AJR
      L=L+1
      I=I+1
      J=J+1
      THETA(K+NR-1)=(AJCR)*EXP(AI1)+ACR*DT*FLOAT(K+NR-1)-AJCR
      ATT=ALPHA+THETA(K+NR-1)+THETA0
      X(L)=X0+DGRR*(SIN(ATT)-SAT)
      Y(L)=Y0+DGRR*(CAT-COS(ATT))
      DT0=DELTA+THETA0
      DTT=DELTA+THETA0+THETA(K+NR-1)
      XS(L)=XS0+RSR*(COS(DTT)-COS(DT0))
      YS(L)=YS0-RSR*(SIN(DT0)-SIN(DTT))
      CTTRCC=COS(THETA0+THETA(K+NR-1))
      CTTRSS=SIN(THETA0+THETA(K+NR-1))
      MYSL(L)=YS(L)+MS*CTTRSS/2.0-MW*CTTRCC/2.0
      MYSR(L)=YS(L)+MS*CTTRSS/2.0+MW*CTTRCC/2.0
```

```
      SYSL(L)=YS(L)-MS*CTTRSS/2.0-SW*CTTRCC/2.0
      SYSR(L)=YS(L)-MS*CTTRSS/2.0+SW*CTTRCC/2.0
      MXSL(L)=XS(L)+MS*CTTRCC/2.0+MW*CTTRSS/2.0
      MXSR(L)=XS(L)+MS*CTTRCC/2.0-MW*CTTRSS/2.0
      SXSL(L)=XS(L)-MS*CTTRCC/2.0+SW*CTTRSS/2.0
      SXSR(L)=XS(L)-MS*CTTRCC/2.0-SW*CTTRSS/2.0
      MRX(L)=XS(L)+0.08*CTTRCC
      SRX(L)=XS(L)-0.08*CTTRCC
      DNN=0.15*(FLOAT(M))+1.587
      IF(MRX(L).GE.DNN)GO TO 80
      IF(MRX(L).LT.DNN)GO TO 81
   80 M=M+1
      IF(M.EQ.190)GO TO 112
   81 MRY(L)=CP(M)/1000.0+EY
      SRY(L)=CP(M-1)/1000.0+EY
      IR=L-J
      WRITE(6,108)L,X(L),Y(L),XS(L),YS(L),MXSL(L),MYSL(L),MXSR(L),MYSR(L
     1),SXSR(L),SYSR(L),SXSL(L),SYSL(L),THETA0,MRX(L),MRY(L),SRX(L),SRY(
     2L)
      RMDSR(L)=ABS(MYSR(L)-MYSR0)/CTTRCC
      IF(L.EQ.N)GO TO 111
      IF(RMDSR(L).GE.ABS(RMDSR0)-MPSWR)GO TO 500
      K=K+1
      GO TO 402
  500 WRITE(6,501)
  501 FORMAT(1H0,44HEND OF RIGHT STEERING BY TIME DERAY CIRCUITS)
      X0=X(L)
      Y0=Y(L)
      XS0=XS(L)
      YS0=YS(L)
      MYSL0=MYSL(L)
      MYSR0=MYSR(L)
      SYSL0=SYSL(L)
      SYSR0=SYSR(L)
      MXSL0=MXSL(L)
      MXSR0=MXSR(L)
      SXSL0=SXSL(L)
      SXSR0=SXSR(L)
      THETA0=THETA(K+NR-1)+THETA0
      GO TO 11
 1000 WRITE(6,1001)
 1001 FORMAT(1H0,49HBEGINNING OF CONTACT OF RIGHT SUBWSENSOR WITH ROW)
 1002 I=I+1
      L=L+1
      AI=-CGDT*FLOAT(I)
      X(L)=X0+FRLC*(EXP(AI)+CGDT*FLOAT(I)-1.0)
      Y(L)=Y0+FRLS*(EXP(AI)+CGDT*FLOAT(I)-1.0)
      XS(L)=X(L)+DSP
      YS(L)=Y(L)+DCP
      MYSL(L)=YS(L)+MSST-MWCT
      MYSR(L)=YS(L)+MSST+MWCT
      SYSL(L)=YS(L)-MSST-SWCT
      SYSR(L)=YS(L)-MSST+SWCT
      MXSL(L)=XS(L)+MSCT+MWST
      MXSR(L)=XS(L)+MSCT-MWST
```

```
      SXSL(L)=XS(L)-MSCT+SWST
      SXSR(L)=XS(L)-MSCT-SWST
      MRX(L)=XS(L)+0.08*CT
      SRX(L)=XS(L)-0.08*CT
      DNN=0.15*(FLOAT(M))+1.587
      IF(MRX(L).GE.DNN)GO TO 55
      IF(MRX(L).LT.DNN)GO TO 56
   55 M=M+1
      IF(M.EQ.190)GO TO 112
   56 MRY(L)=CP(M)/1000.0+EY
      SRY(L)=CP(M-1)/1000.0+EY
      WRITE(6,108)L,X(L),Y(L),XS(L),YS(L),MXSL(L),MYSL(L),MXSR(L),MYSR(L
     1),SXSR(L),SYSR(L),SXSL(L),SYSL(L),THETA0,MRX(L),MRY(L),SRX(L),SRY(
     2L)
      RMDSL(L)=(MRY(L)-MYSL(L))/CT
      RMDSR(L)=(MRY(L)-MYSR(L))/CT
      RSDSL(L)=(SRY(L)-SYSL(L))/CT
      RSDSR(L)=(SRY(L)-SYSR(L))/CT
      IF(L.EQ.N)GO TO 111
      IF(RMDSR(L).GE.MPSWR)GO TO 300
      IF(RMDSL(L).LE.-MPSWL)GO TO 700
      IF(RSDSR(L).GE.SPSWR)GO TO 1300
      IF(RSDSL(L).LE.-SPSWL)GO TO 2300
      I=I+1
      IF(L.EQ.N)GO TO 111
      GO TO 1002
 1300 WRITE(6,1301)
 1301 FORMAT(1H0,13HRMS IS IN SET)
      IF(L.EQ.N)GO TO 111
      J=0
 1302 J=J+1
      I=I+1
      L=L+1
      AI=-CGDT*FLOAT(I)
      DCR=CVR*DT*FLOAT(J)
      X(L)=X0+FRLC*(EXP(AI)+CGDT*FLOAT(I)-1.0)
      Y(L)=Y0+FRLS*(EXP(AI)+CGDT*FLOAT(I)-1.0)
      Y(L)=(X(L)-X0)*ST+Y0
      XS(L)=X(L)+DSP
      YS(L)=Y(L)+DCP
      MYSL(L)=YS(L)+MSST-MWCT
      MYSR(L)=YS(L)+MSST+MWCT
      SYSL(L)=YS(L)-MSST-SWCT
      SYSR(L)=YS(L)-MSST+SWCT
      MXSL(L)=XS(L)+MSCT+MWST
      MXSR(L)=XS(L)+MSCT-MWST
      SXSL(L)=XS(L)-MSCT+SWST
      SXSR(L)=XS(L)-MSCT-SWST
      MXSL(L)=XS(L)+MS*CTTRC/2.0+MW*CTTRS/2.0
      MXSR(L)=XS(L)+MS*CTTRC/2.0-MW*CTTRS/2.0
      SXSL(L)=XS(L)-MS*CTTRC/2.0+SW*CTTRS/2.0
      SXSR(L)=XS(L)-MS*CTTRC/2.0-SW*CTTRS/2.0
      MRX(L)=XS(L)+0.08*CT
      SRX(L)=XS(L)-0.08*CT
      DNN=0.15*(FLOAT(M))+1.587
```

```
      IF(MRX(L).GE.DNN)GO TO 50
      IF(MRX(L).LT.DNN)GO TO 51
   50 M=M+1
      IF(M.EQ.190)GO TO 112
   51 MRY(L)=CP(M)/1000.0+EY
      SRY(L)=CP(M-1)/1000.0+EY
      RMDSR(L)=(MRY(L)-MYSR(L))/CT
      RSDSR(L)=(SRY(L)-SYSR(L))/CT
      WRITE(6,108)L,X(L),Y(L),XS(L),YS(L),MXSL(L),MYSL(L),MXSR(L),MYSR(L
     1),SXSR(L),SYSR(L),SXSL(L),SYSL(L),THETA0,MRX(L),MRY(L),SRX(L),SRY(
     2L)
      IF(L.EQ.N)GO TO 111
      IF(RMDSR(L).GE.MPSWR)GO TO 400
      IF(DCR.GE.SSR)GO TO 1400
      GO TO 1302
 1400 RSDSR0=RSDSR(L)
      WRITE(6,1401)
 1401 FORMAT(1H0,27HBEGINNING OF RIGHT STEERING)
      X0=X(L)
      Y0=Y(L)
      XS0=XS(L)
      YS0=YS(L)
      MYSL0=MYSL(L)
      MYSR0=MYSR(L)
      SYSL0=SYSL(L)
      SYSR0=SYSR(L)
      MXSL0=MXSL(L)
      MXSR0=MXSR(L)
      SXSL0=SXSL(L)
      SXSR0=SXSR(L)
      J=J+1
      K=1
      ACR=AMR/CR
      AJCR=AMR*AJR/(CR*CR)
      ARC=CR/AMR
      SAT=SIN(ALPHA+THETA0)
      CAT=COS(ALPHA+THETA0)
 1402 BI1=-CR*DT*FLOAT(K)/AJR
      L=L+1
      I=I+1
      J=J+1
      THETA(K)=(AJCR)*EXP(BI1)+ACR*DT*FLOAT(K)-AJCR
      ATT=ALPHA+THETA(K)+THETA0
      X(L)=X0+DGRR*(SIN(ATT)-SAT)
      Y(L)=Y0+DGRR*(CAT-COS(ATT))
      DT0=DELTA+THETA0
      DTT=DELTA+THETA0+THETA(K)
      XS(L)=XS0+RSR*(COS(DTT)-COS(DT0))
      YS(L)=YS0-RSR*(SIN(DT0)-SIN(DTT))
      CTTRC=COS(THETA0+THETA(K))
      CTTRS=SIN(THETA0+THETA(K))
      MYSL(L)=YS(L)+MS*CTTRS/2.0-MW*CTTRC/2.0
      MYSR(L)=YS(L)+MS*CTTRS/2.0+MW*CTTRC/2.0
      SYSL(L)=YS(L)-MS*CTTRS/2.0-SW*CTTRC/2.0
      SYSR(L)=YS(L)-MS*CTTRS/2.0+SW*CTTRC/2.0
```

```
)*
      MXSL(L)=XS(L)+MS*CTTRC/2.0+MW*CTTRS/2.0
      MXSR(L)=XS(L)+MS*CTTRC/2.0-MW*CTTRS/2.0
      SXSL(L)=XS(L)-MS*CTTRC/2.0+SW*CTTRS/2.0
      SXSR(L)=XS(L)-MS*CTTRC/2.0-SW*CTTRS/2.0
      MRX(L)=XS(L)+0.08*CTTRC
      SRX(L)=XS(L)-0.08*CTTRC
      DNN=0.15*(FLOAT(M))+1.587
      IF(MRX(L).GE.DNN)GO TO 85
      IF(MRX(L).LT.DNN)GO TO 86
   85 M=M+1
      IF(M.EQ.190)GO TO 112
   86 MRY(L)=CP(M)/1000.0+EY
      SRY(L)=CP(M-1)/1000.0+EY
      IR=L-J
      WRITE(6,108)L,X(L),Y(L),XS(L),YS(L),MXSL(L),MYSL(L),MXSR(L),MYSR(L
     1),SXSR(L),SYSR(L),SXSL(L),SYSL(L),THETA0,MRX(L),MRY(L),SRX(L),SRY(
     2L)
      RSDSR(L)=ABS(SYSR(L)-SYSR0)/CTTRC
      IF(L.EQ.N)GO TO 111
      IF(RSDSR(L).GE.ABS(RSDSR0)-SPSWR)GO TO 1500
      K=K+1
      GO TO 1402
 1500 WRITE(6,1501)
 1501 FORMAT(1H0,21HEND OF RIGHT STEERING)
      X0=X(L)
      Y0=Y(L)
      XS0=XS(L)
      YS0=YS(L)
      MYSL0=MYSL(L)
      MYSR0=MYSR(L)
      SYSL0=SYSL(L)
      SYSR0=SYSL(L)
      MXSL0=MXSL(L)
      MXSR0=MXSR(L)
      SXSL0=SXSL(L)
      SXSR0=SXSR(L)
      THETA0=THETA(K)+THETA0
      IF(L.EQ.N)GO TO 111
      GO TO 11
  600 WRITE(6,601)
  601 FORMAT(1H0,49HBEGINNING OF CONTACT OF LEFT MAIN SENSOR WITH ROW)
  602 I=I+1
      L=L+1
      AI=-CGDT*FLOAT(I)
      X(L)=X0+FRLC*(EXP(AI)+CGDT*FLOAT(I)-1.0)
      Y(L)=Y0+FRLS*(EXP(AI)+CGDT*FLOAT(I)-1.0)
      XS(L)=X(L)+DSP
      YS(L)=Y(L)+DCP
      MYSL(L)=YS(L)+MSST-MWCT
      MYSR(L)=YS(L)+MSST+MWCT
      SYSL(L)=YS(L)-MSST-SWCT
      SYSR(L)=YS(L)-MSST+SWCT
      MXSL(L)=XS(L)+MSCT+MWST
      MXSR(L)=XS(L)+MSCT-MWST
      SXSL(L)=XS(L)-MSCT+SWST
```

```
)*
      SXSR(L)=XS(L)-MSCT-SWST
      MRX(L)=XS(L)+0.08*CT
      SRX(L)=XS(L)-0.08*CT
      DNN=0.15*(FLOAT(M))+1.587
      IF(MRX(L).GE.DNN)GO TO 60
      IF(MRX(L).LT.DNN)GO TO 61
   60 M=M+1
      IF(M.EQ.190)GO TO 112
   61 MRY(L)=CP(M)/1000.0+EY
      SRY(L)=CP(M-1)/1000.0+EY
      WRITE(6,108)L,X(L),Y(L),XS(L),YS(L),MXSL(L),MYSL(L),MXSR(L),MYSR(L
     1),SXSR(L),SYSR(L),SXSL(L),SYSL(L),THETA0,MRX(L),MRY(L),SRX(L),SRY(
     2L)
      RMDSL(L)=(MRY(L)-MYSL(L))*CT
      RMDSR(L)=(MRY(L)-MYSR(L))*CT
      RSDSL(L)=(SRY(L)-SYSL(L))*CT
      RSDSR(L)=(SRY(L)-SYSR(L))*CT
      IF(L.EQ.N)GO TO 111
      IF(RMDSL(L).LE.-MPSWL)GO TO 700
      IF(RMDSR(L).GE.MPSWR)GO TO 300
      IF(RSDSL(L).LE.-SPSWL)GO TO 2000
      IF(RSDSR(L).GE.SPSWR)GO TO 111
      GO TO 602
  700 WRITE(6,701)
  701 FORMAT(1H0,20HLEFT RERAY IS IN SET)
      IF(L.EQ.N)GO TO 111
      J=0
  702 J=J+1
      I=I+1
      L=L+1
      AI=-CGDT*FLOAT(I)
      DCL=CVL*DT*FLOAT(J)
      X(L)=X0+FRLC*(EXP(AI)+CGDT*FLOAT(I)-1.0)
      Y(L)=Y0+FRLS*(EXP(AI)+CGDT*FLOAT(I)-1.0)
      XS(L)=X(L)+DSP
      YS(L)=Y(L)+DCP
      MYSL(L)=YS(L)+MSST-MWCT
      MYSR(L)=YS(L)+MSST+MWCT
      SYSL(L)=YS(L)-MSST-SWCT
      SYSR(L)=YS(L)-MSST+SWCT
      MXSL(L)=XS(L)+MSCT+MWST
      MXSR(L)=XS(L)+MSCT-MWST
      SXSL(L)=XS(L)-MSCT+SWST
      SXSR(L)=XS(L)-MSCT-SWST
      MRX(L)=XS(L)+0.08*CT
      SRX(L)=XS(L)-0.08*CT
      DNN=0.15*(FLOAT(M))+1.587
      IF(MRX(L).GE.DNN)GO TO 75
      IF(MRX(L).LT.DNN)GO TO 76
   75 M=M+1
      IF(M.EQ.190)GO TO 112
   76 MRY(L)=CP(M)/1000.0+EY
      SRY(L)=CP(M-1)/1000.0+EY
      RMDSL(L)=(MRY(L)-MYSL(L))*CT
      WRITE(6,108)L,X(L),Y(L),XS(L),YS(L),MXSL(L),MYSL(L),MXSR(L),MYSR(L
```

```
)*
     1),SXSR(L),SYSR(L),SXSL(L),SYSL(L),THETA0,MRX(L),MRY(L),SRX(L),SRY(
     2L)
      IF(L.EQ.N)GO TO 111
      IF(DCL.GE.SSL)GO TO 800
      GO TO 702
  800 RMDSL0=RMDSL(L)
      WRITE(6,801)
  801 FORMAT(1H0,26HBEGINNING OF LEFT STEERING)
      X0=X(L)
      Y0=Y(L)
      XS0=XS(L)
      YS0=YS(L)
      MYSL0=MYSL(L)
      MYSR0=MYSR(L)
      SYSL0=SYSL(L)
      SYSR0=SYSL(L)
      MXSL0=MXSL(L)
      MXSR0=MXSR(L)
      SXSL0=SXSL(L)
      SXSR0=SXSR(L)
      J=J+1
      K=1
      I=I+1
      ACL=AML/CR
      AJCL=AML*AJL/(CR*CR)
      ALC=CR/AML
      SBT=SIN(BETA-THETA0)
      CBT=COS(BETA-THETA0)
  802 AI2=-CR*DT*FLOAT(K+NL-1)/AJL
      I=I+1
      L=L+1
      THETA(K+NL-1)=(AJCL)*EXP(AI2)+ACL*DT*FLOAT(K+NL-1)-AJCL
      BTT=BETA+THETA(K+NL-1)-THETA0
      X(L)=X0+DGRL*(SIN(BTT)-SBT)
      Y(L)=Y0+DGRL*(COS(BTT)-CBT)
      ALT0=ALAMDA+THETA0
      ALTT=ALAMDA+THETA0-THETA(K+NL-1)
      XS(L)=XS0+RSL*(COS(ALTT)-COS(ALT0))
      YS(L)=YS0+RSL*(SIN(ALTT)-SIN(ALT0))
      CTTLCC=COS(THETA0-THETA(K+NL-1))
      CTTLSS=SIN(THETA0-THETA(K+NL-1))
      MYSL(L)=YS(L)+MS*CTTLSS/2.0-MW*CTTLCC/2.0
      MYSR(L)=YS(L)+MS*CTTLSS/2.0+MW*CTTLCC/2.0
      SYSL(L)=YS(L)-MS*CTTLSS/2.0-SW*CTTLCC/2.0
      SYSR(L)=YS(L)-MS*CTTLSS/2.0+SW*CTTLCC/2.0
      MXSL(L)=XS(L)+MS*CTTLCC/2.0+MW*CTTLSS/2.0
      MXSR(L)=XS(L)+MS*CTTLCC/2.0-MW*CTTLSS/2.0
      SXSL(L)=XS(L)-MS*CTTLCC/2.0+SW*CTTLSS/2.0
      SXSR(L)=XS(L)-MS*CTTLCC/2.0-SW*CTTLSS/2.0
      MRX(L)=XS(L)+0.08*CTTLCC
      SRX(L)=XS(L)-0.08*CTTLCC
      DNN=0.15*(FLOAT(M))+1.587
      IF(MRX(L).GE.DNN)GO TO 92
      IF(MRX(L).LT.DNN)GO TO 91
   92 M=M+1
```

```
N  )*
      IF(M.EQ.190)GO TO 112
   91 MRY(L)=CP(M)/1000.0+EY
      SRY(L)=CP(M-1)/1000.0+EY
      IL=L-J
      WRITE(6,108)L,X(L),Y(L),XS(L),YS(L),MXSL(L),MYSL(L),MXSR(L),MYSR(L
     1),SXSR(L),SYSR(L),SXSL(L),SYSL(L),THETA0,MRX(L),MRY(L),SRX(L),SRY(
     2L)
      RMDSL(L)=ABS(MYSL(L)-MYSL0)/CTTLCC
      IF(L.EQ.N)GO TO 111
      IF(RMDSL(L).GE.ABS(RMDSL0)-MPSWL)GO TO 900
      K=K+1
      GO TO 802
  900 WRITE(6,901)
  901 FORMAT(1H0,44HEND OF LEFT  STEERING BY TIME DERAY CIRCUITS)
      X0=X(L)
      Y0=Y(L)
      XS0=XS(L)
      YS0=YS(L)
      MYSL0=MYSL(L)
      MYSR0=MYSR(L)
      SYSL0=SYSL(L)
      SYSR0=SYSR(L)
      MXSL0=MXSL(L)
      MXSR0=MXSR(L)
      SXSL0=SXSL(L)
      SXSR0=SXSR(L)
      THETA0=THETA0-THETA(K+NL-1)
      IF(L.EQ.N)GO TO 111
      GO TO 11
 2000 WRITE(6,2001)
 2001 FORMAT(1H0,48HBEGINNING OF CONTACT OF LEFT SUB SENSOR WITH ROW)
 2002 I=I+1
      L=L+1
      AI=-CGDT*FLOAT(I)
      X(L)=X0+FRLC*(EXP(AI)+CGDT*FLOAT(I)-1.0)
      Y(L)=Y0+FRLS*(EXP(AI)+CGDT*FLOAT(I)-1.0)
      XS(L)=X(L)+DSP
      YS(L)=Y(L)+DCP
      MYSL(L)=YS(L)+MSST-MWCT
      MYSR(L)=YS(L)+MSST+MWCT
      SYSL(L)=YS(L)-MSST-SWCT
      SYSR(L)=YS(L)-MSST+SWCT
      MXSL(L)=XS(L)+MSCT+MWST
      MXSR(L)=XS(L)+MSCT-MWST
      SXSL(L)=XS(L)-MSCT+SWST
      SXSR(L)=XS(L)-MSCT-SWST
      MRX(L)=XS(L)+0.08*CT
      SRX(L)=XS(L)-0.08*CT
      DNN=0.15*(FLOAT(M))+1.587
      IF(MRX(L).GE.DNN)GO TO 65
      IF(MRX(L).LT.DNN)GO TO 66
   65 M=M+1
      IF(M.EQ.190)GO TO 112
   66 MRY(L)=CP(M)/1000.0+EY
      SRY(L)=CP(M-1)/1000.0+EY
```

```
)*
      WRITE(6,108)L,X(L),Y(L),XS(L),YS(L),MXSL(L),MYSL(L),MXSR(L),MYSR(L
     1),SXSR(L),SYSR(L),SXSL(L),SYSL(L),THETAO,MRX(L),MRY(L),SRX(L),SRY(
     2L)
      RMDSL(L)=(MRY(L)-MYSL(L))*CT
      RMDSR(L)=(MRY(L)-MYSR(L))*CT
      RSDSL(L)=(SRY(L)-SYSL(L))*CT
      RSDSR(L)=(SRY(L)-SYSR(L))*CT
      IF(L.EQ.N)GO TO 111
      IF(RMDSR(L).GE.MPSWR)GO TO 300
      IF(RMDSL(L).LE.-MPSWL)GO TO 700
      IF(RSDSR(L).GE.SPSWR)GO TO 1300
      IF(RSDSL(L).LE.-SPSWL)GO TO 2300
      IF(L.EQ.N)GO TO 111
      GO TO 2002
 2300 WRITE(6,2301)
 2301 FORMAT(1H0,13HLMS IS IN SET)
      IF(L.EQ.N)GO TO 111
      J=0
 2302 J=J+1
      I=I+1
      L=L+1
      AI=-CGDT*FLOAT(I)
      DCL=CVL*DT*FLOAT(J)
      X(L)=X0+FRLC*(EXP(AI)+CGDT*FLOAT(I)-1.0)
      Y(L)=Y0+FRLS*(EXP(AI)+CGDT*FLOAT(I)-1.0)
      XS(L)=X(L)+DSP
      YS(L)=Y(L)+DCP
      MYSL(L)=YS(L)+MSST-MWCT
      MYSR(L)=YS(L)+MSST+MWCT
      SYSL(L)=YS(L)-MSST-SWCT
      SYSR(L)=YS(L)-MSST+SWCT
      MXSL(L)=XS(L)+MSCT+MWST
      MXSR(L)=XS(L)+MSCT-MWST
      SXSL(L)=XS(L)-MSCT+SWST
      SXSR(L)=XS(L)-MSCT-SWST
      MRX(L)=XS(L)+0.08*CT
      SRX(L)=XS(L)-0.08*CT
      DNN=0.15*(FLOAT(M))+1.587
      IF(MRX(L).GE.DNN)GO TO 70
      IF(MRX(L).LT.DNN)GO TO 71
   70 M=M+1
      IF(M.EQ.190)GO TO 112
   71 MRY(L)=CP(M)/1000.0+EY
      SRY(L)=CP(M-1)/1000.0+EY
      RMDSL(L)=(MRY(L)-MYSL(L))*CT
      RSDSL(L)=(SRY(L)-SYSL(L))*CT
      WRITE(6,108)L,X(L),Y(L),XS(L),YS(L),MXSL(L),MYSL(L),MXSR(L),MYSR(L
     1),SXSR(L),SYSR(L),SXSL(L),SYSL(L),THETAO,MRX(L),MRY(L),SRX(L),SRY(
     2L)
      IF(L.EQ.N)GO TO 111
      IF(ABS(RMDSL).GE.MPSWL)GO TO 800
      IF(DCL.GE.SSL)GO TO 2400
      GO TO 2302
 2400 RSDSL0=RSDSL(L)
      WRITE(6,2401)
```

```
)*
 2401 FORMAT(1H0,26HBEGINNING OF LEFT STEERING)
      X0=X(L)
      Y0=Y(L)
      XS0=XS(L)
      YS0=YS(L)
      MYSL0=MYSL(L)
      MYSR0=MYSR(L)
      SYSR0=SYSR(L)
      SYSL0=SYSL(L)
      MXSL0=MXSL(L)
      MXSR0=MXSR(L)
      SXSL0=SXSL(L)
      SXSR0=SXSR(L)
      J=J+1
      L=L+1
      I=I+1
      K=1
      ACL=AML/CR
      AJCL=AML*AJL/(CR*CR)
      ALC=CR/AML
      SBT=SIN(BETA-THETA0)
      CBT=COS(BETA-THETA0)
 2402 B12=-CR*DT*FLOAT(K)/AJL
      THETA(K)=(AJCL)*EXP(B12)+ACL*DT*FLOAT(K)-AJCL
      BTT=BETA+THETA(K)-THETA0
      X(L)=X0+DGRL*(SIN(BTT)-SBT)
      Y(L)=Y0+DGRL*(COS(BTT)-CBT)
      ALT0=ALAMDA+THETA0
      ALTT=ALAMDA+THETA0-THETA(K)
      XS(L)=XS0+RSL*(COS(ALTT)-COS(ALT0))
      YS(L)=YS0+RSL*(SIN(ALTT)-SIN(ALT0))
      CTTLC=COS(THETA0-THETA(K))
      CTTLS=SIN(THETA0-THETA(K))
      MYSL(L)=YS(L)+MS*CTTLS/2.0-MW*CTTLC/2.0
      MYSR(L)=YS(L)+MS*CTTLS/2.0+MW*CTTLC/2.0
      SYSL(L)=YS(L)-MS*CTTLS/2.0-SW*CTTLC/2.0
      SYSR(L)=YS(L)-MS*CTTLS/2.0+SW*CTTLC/2.0
      MXSL(L)=XS(L)+MS*CTTLC/2.0+MW*CTTLS/2.0
      MXSR(L)=XS(L)+MS*CTTLC/2.0-MW*CTTLS/2.0
      SXSL(L)=XS(L)-MS*CTTLC/2.0+SW*CTTLS/2.0
      SXSR(L)=XS(L)-MS*CTTLC/2.0-SW*CTTLS/2.0
      MRX(L)=XS(L)+0.08*CTTLC
      SRX(L)=XS(L)-0.08*CTTLC
      DNN=0.15*(FLOAT(M))+1.587
      IF(MRX(L).GE.DNN)GO TO 95
      IF(MRX(L).LT.DNN)GO TO 96
   95 M=M+1
      IF(M.EQ.190)GO TO 112
   96 MRY(L)=CP(M)/1000.0+EY
      SRY(L)=CP(M-1)/1000.0+EY
      IL=L-J
      WRITE(6,108)L,X(L),Y(L),XS(L),YS(L),MXSL(L),MYSL(L),MXSR(L),MYSR(L
     1),SXSR(L),SYSR(L),SXSL(L),SYSL(L),THETA0,MRX(L),MRY(L),SRX(L),SRY(
     2L)
      RSDSL(L)=ABS(SYSL(L)-SYSL0)/CTTLC
```

```
      IF(L.EQ.N)GO TO 111
      IF(RSDSL(L).GE.ABS(RSDSL0)-SPSWL)GO TO 2500
      I=I+1
      L=L+1
      K=K+1
      GO TO 2402
 2500 WRITE(6,2501)
 2501 FORMAT(1H0,20HEND OF LEFT STEERING)
      X0=X(L)
      Y0=Y(L)
      XS0=XS(L)
      YS0=YS(L)
      MYSL0=MYSL(L)
      MYSR0=MYSR(L)
      SYSL0=SYSL(L)
      SYSR0=SYSL(L)
      MXSL0=MXSL(L)
      MXSR0=MXSR(L)
      SXSL0=SXSL(L)
      SXSR0=SXSR(L)
      THETA0=THETA0-THETA(K)
      IF(L.EQ.N)GO TO 111
      GO TO 11
  112 STOP
      END
```

Appendix B Simulation Programm for Automatically Steered Combine with Sensors Detecting Row of Rice Plant from One Side of It

The constans used in this simulation programm are as follows.

N = 2000	DT = 0.05 sec	DRIVE = 0.0 rad
TR = 8.5 kg-m	AMP = 0.1 m	T = 3.6 m
PSI = 0.0 rad	CVR = 0.1575 m/sec	
RDZW = 0.035 m	RSR = 5.69 m	TL = 8.5 kg-m
GM = 76.5 kg-m^{-1}-sec^2	C = 24 kg-m^{-1}	CR = 10000 kg-m-sec
SSR = 0.017 m	AJR = 25 kg-m-sec^2	AMR = 17.6 kg-m
AMP = 0.1 m	T = 3.6 m	
PSI = 0.0 rad	CVL = 0.1175 m/sec	
FDZW = 0.02 m	RSL = 3.79 m	
SSL = 0.017 m	AJL = 25 kg-m-sec^2	AML = 17.0 kg-m

```
      REAL MS,MW,MRY,MRX,MSCT,MSST,MWCT,MWST,MDSL
      DIMENSION X(2000),Y(2000),XS(2000),YS(2000),XMF(2000),YMF(2000),XM
     1R(2000),YMR(2000),THETA(2000),MRY(2000),SRY(2000),MDSL(2000),SDSR(
     22000),RMDSL(2000),RSDSR(2000),MRX(2000),CP(200),NN(200)
  111 READ(5,100)N,KK,AMP,DT,T,MM1,AA,AAA
  100 FORMAT(2I8,3F10.0,I8,F10.0,F8.0)
      IF(KK.EQ.0)GO TO 113
      READ(5,123)PSI,DRIVE,DGS,CVR,CVL,SSR,SSL,DELTA,ALAMDA,PHI,TR,TL,GM
     1,C,AJR,AJL,CR,AMR,AML,RSR,RSL,DGRR,DGRL,FDZW,RDZW,MW,MS
  123 FORMAT(7F10.0)
      READ(5,90)(NN(M),M=1,MM1)
   90 FORMAT(12I6)
      DO 334 I=1,MM1
  334 CP(I)=FLOAT(NN(I))+AAA
      EY=AA-CP(1)/1000.0
      WRITE (6,101)
  101 FORMAT(1H1,39HSIMURATION OF AUTOMATIC STEERED COMBINE)
      WRITE(6,1)
    1 FORMAT(1H0,5X,21HRANDOM INPUT AT FIELD)
      WRITE(6,102)N,KK,DT,DRIVE,TR,TL,GM,C,CR
  102 FORMAT(1H0,2HN=I8,1X,3HKK=I8,1X,3HDT=F10.5,1X,6HDRIVE=F10.5,1X,3HT
     1R=F10.5,1X,3HTL=F10.5,1X,3HGM=F10.5,1X,2HC=F10.5,1X,3HCR=F10.5)
      WRITE(6,103)AMP,T,PSI,CVR,SSR,AJR,AMR,RDZW,RSR
  103 FORMAT(1H0,2X,4HAMP=F10.5,4X,2HT=F10.5,4X,4HPSI=F10.5,4X,4HCVR=F10
     1.5,4X,4HSSR=F10.5,4X,4HAJR=F10.5,4X,4HAMR=F10.5///,1H ,5HRDZW=F10.
     25,4X,4HRSR=F10.5)
      WRITE(6,104)AMP,T,PSI,CVL,SSL,AJL,AML,FDZW,RSL
  104 FORMAT(1H0,2X,4HAMP=F10.5,4X,2HT=F10.5,4X,4HPSI=F10.5,4X,4HCVL=F10
     1.5,4X,4HSSL=F10.5,4X,4HAJL=F10.5,4X,4HAML=F10.5///,1H ,5HFDZW=F10.
     25,4X,4HRSL=F10.5)
      WRITE(6,105)
  105 FORMAT(1H0,12X,21HLOCATION OF CENTER OF,4X,18HLOCATION OF MIDDLE,6
     1X,11HLOCATION OF,11X,11HLOCATION OF,8X,11HARGUMENT OF)
      WRITE(6,106)
  106 FORMAT(1H ,12X,7HGRAVITY,17X,9HOF SENSER,15X,12HFRONT SENSER,10X,1
     11HREAR SENSER,8X,7HCONBINE)
      WRITE(6,107)
  107 FORMAT(1H0,2X,6HNUMBER,10X,1HX,10X,1HY,8X,2HXS,8X,2HYS,9X,3HXMF,9X
     1,3HYMF,9X,3HXMR,8X,3HYMR,8X,5HTHETA,5X,3HMRY,8X,3HSRY)
      X0=0.0
      X0=0.0
      Y0=0.0
      XS0=0.0
      YS0=0.0
      THETA0=DRIVE
      L=0
      M=2
   11 I=1
      WRITE(6,204)
  204 FORMAT(1H ,31HBEGINNING OF STRAIGHT TRAVELING)
      CT=COS(THETA0)
      ST=SIN(THETA0)
      GC=GM/(C*C)
      CG=C/GM
      PT=PHI-THETA0
```

```
      DSP=DGS*SIN(PT)
      DCP=DGS*COS(PT)
      CGDT=CG*DT
      CTCG=CT*GC
      STCG=ST*GC
      MSCT=MS*CT/2.0
      MSST=MS*ST/2.0
      MWCT=MW*CT/2.0
      MWST=MW*ST/2.0
   12 CI=-2.0*FLOAT(I)
      FR=TR*(2.0*EXP(CI)+1.0)
      FL=TL*(2.0*EXP(CI)+1.0)
      FRLC=(FR+FL)*CTCG
      FRLS=(FR+FL)*STCG
      AI=-CGDT*FLOAT(I)
      L=L+1
      X(L)=X0+FRLC*(EXP(AI)+CGDT*FLOAT(I)-1.0)
      Y(L)=Y0+FRLS*(EXP(AI)+CGDT*FLOAT(I)-1.0)
      XS(L)=X(L)+DSP
      YS(L)=Y(L)+DCP
      XMF(L)=XS(L)+MSCT+MWST
      YMF(L)=YS(L)+MSST-MWCT
      XMR(L)=XS(L)-MSCT-MWST
      YMR(L)=YS(L)-MSST+MWCT
      MRX(L)=XS(L)+0.08*CT
      DNN=0.15*FLOAT(M)+1.587
      IF(MRX(L).GE.DNN)GO TO 35
      IF(MRX(L).LT.DNN)GO TO 36
   35 M=M+1
      IF(M.EQ.MM1)GO TO 112
   36 MRY(L)=CP(M)/1000.0+EY
      SRY(L)=CP(M-1)/1000.0+EY
      MDSL(L)=MRY(L)-YMF(L)
      SDSR(L)=SRY(L)-YMR(L)
      WRITE(6,108)L,X(L),Y(L),XS(L),YS(L),XMF(L),YMF(L),XMR(L),YMR(L),TH
     1ETA0,MRY(L),SRY(L)
  108 FORMAT(1H ,2X,I8,1X,11F11.6)
      IF(L.EQ.N)GO TO 111
      IF(MDSL(L).LE.0.0)GO TO 600
      IF(SDSR(L).GE.-RDZW)GO TO 1300
      I=I+1
      GO TO 12
  600 WRITE(6,601)
  601 FORMAT(1H0,45HBEGINNING OF CONTACT OF FRONT SENSER WITH ROW)
  602 I=I+1
      L=L+1
      AI=-CGDT*FLOAT(I)
      X(L)=X0+FRLC*(EXP(AI)+CGDT*FLOAT(I)-1.0)
      Y(L)=Y0+FRLS*(EXP(AI)+CGDT*FLOAT(I)-1.0)
      XS(L)=X(L)+DSP
      YS(L)=Y(L)+DCP
      XMF(L)=XS(L)+MSCT+MWST
      YMF(L)=YS(L)+MSST-MWCT
      XMR(L)=XS(L)-MSCT-MWST
      YMR(L)=YS(L)-MSST+MWCT
```

```
      MRX(L)=XS(L)+0.08*CT
      DNN=0.15*FLOAT(M)+1.587
      IF(MRX(L).GE.DNN) GO TO 60
      IF(MRX(L).LT.DNN) GO TO 61
   60 M=M+1
      IF(M.EQ.MM1)GO TO 112
   61 MRY(L)=CP(M)/1000.0+EY
      SRY(L)=CP(M-1)/1000.0+EY
      WRITE(6,108)L,X(L),Y(L),XS(L),YS(L),XMF(L),YMF(L),XMR(L),YMR(L),TH
     1ETA0,MRY(L),SRY(L)
      RMDSL(L)=(MRY(L)-YMF(L))*CT
      RSDSR(L)=(SRY(L)-YMR(L))*CT
      IF(L.EQ.N)GO TO 111
      IF(RMDSL(L).LE.-FDZW)GO TO 700
      IF(RSDSR(L).GE.-RDZW)GO TO 1300
      GO TO 602
  700 WRITE(6,701)
  701 FORMAT(1H0,22HFRONT SWITCH IS IN SET)
      IF(L.EQ.N)GO TO 111
      J=0
  702 J=J+1
      I=I+1
      L=L+1
      AI=-CGDT*FLOAT(I)
      DCL=CVL*DT*FLOAT(J)
      X(L)=X0+FRLC*(EXP(AI)+CGDT*FLOAT(I)-1.0)
      Y(L)=Y0+FRLS*(EXP(AI)+CGDT*FLOAT(I)-1.0)
      XS(L)=X(L)+DSP
      YS(L)=Y(L)+DCP
      XMF(L)=XS(L)+MSCT+MWST
      YMF(L)=YS(L)+MSST-MWCT
      XMR(L)=XS(L)-MSCT-MWST
      YMR(L)=YS(L)-MSST+MWCT
      MRX(L)=XS(L)+0.08*CT
      DNN=0.15*FLOAT(M)+1.587
      IF(MRX(L).GE.DNN)GO TO 75
      IF(MRX(L).LT.DNN)GO TO 76
   75 M=M+1
      IF(M.EQ.MM1)GO TO 112
   76 MRY(L)=CP(M)/1000.0+EY
      SRY(L)=CP(M-1)/1000.0+EY
      RMDSL(L)=(MRY(L)-YMF(L))*CT
      WRITE(6,108)L,X(L),Y(L),XS(L),YS(L),XMF(L),YMF(L),XMR(L),YMR(L),TH
     1ETA0,MRY(L),SRY(L)
      IF(L.EQ.N)GO TO 111
      IF(DCL.GE.SSL)GO TO 800
      GO TO 702
  800 WRITE(6,801)
  801 FORMAT(1H0,26HBEGINNING OF LEFT STEERING)
      X0=X(L)
      Y0=Y(L)
      XS0=XS(L)
      YS0=YS(L)
      YMF0=YMF(L)
      YMR0=YMR(L)
```

```
      J=J+1
      K=1
      I=I+1
      ACL=AML/CR
      AJCL=AML*AJL/(CR*CR)
  802 AI2=-CR*DT*FLOAT(K)/AJL
      I=I+1
      L=L+1
      THETA(K)=AJCL*EXP(AI2)+ACL*DT*FLOAT(K)-AJCL
      BTT=THETA(K)-THETA0
      X(L)=X0+DGRL*(SIN(BTT)+ST)
      Y(L)=Y0+DGRL*(COS(BTT)-CT)
      ALTT=ALAMDA+THETA0-THETA(K)
      ALT0=ALAMDA+THETA0
      XS(L)=XS0+RSL*(COS(ALTT)-COS(ALT0))
      YS(L)=YS0-RSL*(SIN(ALT0)-SIN(ALTT))
      CTTLCC=COS(THETA0-THETA(K))
      CTTLSS=SIN(THETA0-THETA(K))
      XMF(L)=XS(L)+MS*CTTLCC/2.0+MW*CTTLSS/2.0
      YMF(L)=YS(L)+MS*CTTLSS/2.0-MW*CTTLCC/2.0
      XMR(L)=XS(L)-MS*CTTLCC/2.0-MW*CTTLSS/2.0
      YMR(L)=YS(L)-MS*CTTLSS/2.0+MW*CTTLCC/2.0
      MRX(L)=XS(L)+0.08*CTTLCC
      DNN=0.15*FLOAT(M)+1.587
      IF(MRX(L).GE.DNN)GO TO 92
      IF(MRX(L).LT.DNN)GO TO 91
   92 M=M+1
      IF(M.EQ.MM1)GO TO 112
   91 MRY(L)=CP(M)/1000.0+EY
      SRY(L)=CP(M-1)/1000.0+EY
      WRITE(6,810)L,X(L),Y(L),XS(L),YS(L),XMF(L),YMF(L),XMR(L),YMR(L),TH
     1ETA(K),MRY(L),SRY(L)
  810 FORMAT(1H ,2X,I8,1X,11F11.6)
      RMDSL(L)=(YMF(L)-MRY(L))/CTTLCC
      IF(L.EQ.N)GO TO 111
      IF(RMDSL(L).LE.FDZW)GO TO 900
      K=K+1
      GO TO 802
  900 WRITE(6,901)
  901 FORMAT(1H0,20HEND OF LEFT STEERING)
      X0=X(L)
      Y0=Y(L)
      XS0=XS(L)
      YS0=YS(L)
      YMF0=YMF(L)
      YMR0=YMR(L)
      THETA0=THETA0-THETA(K)
      IF(L.EQ.N)GO TO 111
      GO TO 11
 1300 WRITE(6,1301)
 1301 FORMAT(1H0,21HREAR SWITCH IS IN SET)
      IF(L.EQ.N)GO TO 111
      J=0
 1302 J=J+1
      I=I+1
```

```
      L=L+1
      AI=-CGDT*FLOAT(I)
      DCR=CVR*DT*FLOAT(J)
      X(L)=XO+FRLC*(EXP(AI)+CGDT*FLOAT(I)-1.0)
      Y(L)=YO+FRLS*(EXP(AI)+CGDT*FLOAT(I)-1.0)
      XS(L)=X(L)+DSP
      YS(L)=Y(L)+DCP
      XMF(L)=XS(L)+MSCT+MWST
      YMF(L)=YS(L)+MSST-MWCT
      XMR(L)=XS(L)-MSCT-MWST
      YMR(L)=YS(L)-MSST+MWCT
      MRX(L)=XS(L)+0.08*CT
      DNN=0.15*FLOAT(M)+1.587
      IF(MRX(L).GE.DNN)GO TO 50
      IF(MRX(L).LT.DNN)GO TO 51
   50 M=M+1
      IF(M.EQ.MM1)GO TO 112
   51 MRY(L)=CP(M)/1000.0+EY
      SRY(L)=CP(M-1)/1000.0+EY
      RSDSR(L)=(SRY(L)-YMR(L))/CT
      WRITE(6,106)L,X(L),Y(L),XS(L),YS(L),XMF(L),YMF(L),XMR(L),YMR(L),TH
     1ETA0,MRY(L),SRY(L)
      IF(L.EQ.N)GO TO 111
      IF(DCR.GE.SSR)GO TO 1400
      GO TO 1302
 1400 WRITE(6,1401)
 1401 FORMAT(1H0,27HBEGINNING OF RIGHT STEERING)
      XO=X(L)
      YO=Y(L)
      XSO=XS(L)
      YSO=YS(L)
      YMFO=YMF(L)
      YMRO=YMR(L)
      J=J+1
      K=1
      ACR=AMR/CR
      AJCR=AMR*AJR/(CR*CR)
 1402 BI1=-CR*DT*FLOAT(K)/AJR
      L=L+1
      I=I+1
      J=J+1
      THETA(K)=AJCR*EXP(BI1)+ACR*DT*FLOAT(K)-AJCR
      ATT=THETA(K)+THETA0
      X(L)=XO+DGRR*(SIN(ATT)-ST)
      Y(L)=YO+DGRR*(CT-COS(ATT))
      DTT=DELTA+THETA0-THETA(K)
      DTO=DELTA+THETA0
      XS(L)=XSO+RSR*(COS(DTT)-COS(DTO))
      YS(L)=YSO+RSR*(SIN(DTO)-SIN(DTT))
      CTTRC=COS(THETA0+THETA(K))
      CTTRS=SIN(THETA0+THETA(K))
      XMF(L)=XS(L)+MS*CTTRC/2.0+MW*CTTRS/2.0
      YMF(L)=YS(L)+MS*CTTRS/2.0-MW*CTTRC/2.0
      XMR(L)=XS(L)-MS*CTTRC/2.0-MW*CTTRS/2.0
      YMR(L)=YS(L)-MS*CTTRS/2.0+MW*CTTRC/2.0
```

```
      MRX(L)=XS(L)+0.08*CTTRC
      DNN=0.15*FLOAT(M)+1.587
      IF(MRX(L).GE.DNN)GO TO 85
      IF(MRX(L).LT.DNN)GO TO 86
   85 M=M+1
      IF(M.EQ.MM1)GO TO 112
   86 MRY(L)=CP(M)/1000.0+EY
      SRY(L)=CP(M-1)/1000.0+EY
      WRITE(6,1403)L,X(L),Y(L),XS(L),YS(L),XMF(L),YMF(L),XMR(L),YMR(L),T
     1HETA(K),MRY(L),SRY(L)
 1403 FORMAT(1H ,2X,I8,1X,11F11.6)
      RSDSR(L)=(YMR(L)-SRY(L))/CTTRC
      IF(L.EQ.N)GO TO 111
      IF(RSDSR(L).GE.RDZW)GO TO 1500
      K=K+1
      GO TO 1402
 1500 WRITE(6,1501)
 1501 FORMAT(1H0,21HEND OF RIGHT STEERING)
      XO=X(L)
      YO=Y(L)
      XSO=XS(L)
      YSO=YS(L)
      YMFO=YMF(L)
      YMRO=YMR(L)
      THETAO=THETAO+THETA(K)
      IF(L.EQ.N)GO TO 111
      GO TO 11
  112 GO TO 111
  113 STOP
      END
```

References in Chapter 1

1) D. E. Burrough; Power Requirements of Combine drive, Agric. Engng., Vol. 35 (1954), No. 1, pp. 15 - 18

2) C. Dolling; Der Drehmoment-und Leistungsbedarf von Mähdrescher-trommeln, Grundl. Landtechn. Heft 6 (1955), pp. 27 -34

3) C. Dolling; Der Leistungsbedarf von Mähdreschern, Landtechn. Forschung, Heft 2 (1957), pp. 33 - 44

4) D. Frenzel; Einfluss der Dreschwerkeinsttelung auf die Verluste an Mähdrescher, Deutsche Agraltechnik, 17 Jg. (1967) Heft 7, pp. 299 - 300

5) N. A. Lazebnyj; Kornbewegung auf Mähdreschersieben (translated from Russian Literature, Mechnizacija i Electrifikacija, 1967 - 8, pp. 17 - 19), Landtechn. Forschung, 17 (1967) Heft 6, pp. 194 - 196

6) N. V. Filatov and P. G. Chavrad; Verstarkung der Körnerabscheidung auf Horden-Strohschüttern (translated from Russian Literature, Mehanizacija i Electrifikacija, 1967 - 6, pp. 22 - 26), Landtechn. Forschung 17 (1967) Heft 6, pp. 196 - 200

7) N. V. Tudel' and V. E. Poedinok; Verojatnostnoe Predstavlenie Usilij v Molotil'nom Apparate Kombajna SK-4 (in Russian) (Probabilistic Representation of Forces in Threshing Device of Combine SK-4), Traktory i Sel'hozmasiny, 1968, Nr.12, pp. 22 - 25

8) A. F. Kononenko ; Verojatnostno-statisticeskij Analiz Raboty Zernouborocny k Kombajnov (in Russian) (Probabilistic and Statistical Analysis of Operation of Grain Harvesting Combine) Mehanizacija i Elektrifikacija, 1970-3, pp.44 - 49

9) A. B. Lur'e and Ju. A. Vantjusov ; Statisticeskie Ocenki

Pokazatelej Raboty Zernoyborocnogo Kombajna (in Russian) (Statistical Evaluation Index of Operation of Grain Harvesting Combine), Mehanizacija i Elektrificacija, 1970-6, pp. 53 -56

10) Z. Undirbaev ; Sirokozahvatnaja Zatka na Vborke Risa (in Russion) (Wide-span Harvester on Rice Harvesting), Mehanizacija i Elektrifikacija, 1970-9, pp. 56 - 57

11) I. Yokoyama, I. Doihara, H. Kadowaki, M. Tomita and S. Owa ; Studies on HS61-A Combine (A Trial Manufacture of a Rice Combine) (in Japanese) J. of SAM, Vol. 25 (1963), No. 1, pp. 43 - 46

12) S. Umeda, Y. Shibano, K. Moori, T. Ichikawa and H. Oba ; Performance of Small Header Combine (I - Power Requirements) (in Japanese) J. of SAM, Japan, Vol. 28 (1966), No. 3, pp. 157 - 161

13) S. Umeda, H. Takigawa, M. Otsuka and M. Kusunose ; Performance of Small Header Combine (II - Separation Characteristics) (in Japanese) J. of SAM, Japan, Vol. 28 (1967), No. 4, pp. 223-226

14) N. Kawamura, R. Yamashita, M. Nakatani and Y. Ikeda; Functional Studies of Combine (Part 1) - The Properties of the Power Requirements of Combine (in Japanese) -, J. of SAM, Japan, Vol.28(1967), No.4, pp.217-222

15) N. Kawamura, R. Yamashita, M. Nakatani and Y. Ikeda; Functional Studies of Combine (Part 2 & 3) - Characteristics of the Fluctuating Torques of the Combine Elements (in Japanese) -, J. SAM, Japan, Vol.29(1967), No.2, pp. 73-76

16) H. Ezaki, K. Miura and S. Imazono; Load Characteristics

of a Two-Cylindered Rice Combine (I) (in Japanese), J. of SAM, Japan, Vol. 32 (1970), No. 3, pp. 203-210

17) N. Kawamura, R. Yamashita, K. Namikawa and Y. Ikeda; Functional Studies of the Small Combine with Self-feeding Type Thresher (Part 1) - The Power Requirements of the Functional Elements of the Thresher (in Japanese) -, J. SAM, Japan, Vol.30(1968), No. 1, pp. 19-23

18) Y. Ikeda, N. Kawamura, R. Yamashita and K. Namikawa; Functional Studies of the Small Combine with Self-feeding Type Thresher (Part 2) - The Dynamic Characteristics of Fluctuating Torques of the Functional Elements of the Thresher (in Japanese) -, J. of SAM, Japan , Vol.32 (1970), No. 3, pp. 198-202

19) N. Kawamura, R. Yamashita, K. Namikawa, Y. Ikeda and M. Yukueda;Studies of Small Rice Combine of Head Feeding Type, Memoirs of the College of Agriculture, Kyoto Univ., No. 99, March 1971, Kyoto, Japan, pp.101-126

20) H. Ezaki, K. Miura and S. Imazono;Load Characteristics of Head-Feeding Combine (II) (in Japanese), J. of SAM, Japan, Vol. 32 (1971), No. 4, pp. 284-288

21) I. F. Reed; Measurement of Foeces of Track-Type Tractor Shoes, Transacs. ASAE, Vol. 1 (1958), No. 1, pp. 15-18

22) A. P. Sofijan and Ye. I. Maximenko; The Distribution of Pressure under a Tracklaying Vehicle, J. Terramechanics, Vol. 2 (1965), No. 3, pp. 11-16

23) A. I. Brusencev ; Issledavanie Tjagavoj Harakteristiki Traktora s Bul'dozerom (in Russian) (Study of Characteristics of Propulsion of Tractor with Bulldozer),Traktory i

Sel'hozmasiny, 1966-11, pp. 18 - 20

24)Y. Yasuda and J. Doi ; On Measurement of Soil Pressure under Tracklayer of Combine on Sand, Preprint of the 27th Annual Meeting og SAM,Japan (Tokyo), 1968, p.9

25)W. Söhne ; Stand des Wissens auf Gebiet der Fahrzeugschwingen unter besonderer Berücksichtgung landwirtschaftlicher Fahrzeug, Grundl.Landtechn. Bd. 15 (1965) Nr. 1, pp. 11 - 22

26)Ju. V. Grin'kov ; Issledavanie Vibracii Kombajna SK-4 (in Russian) (Study of Vibration of Combine SK-4), Traktory i Selihozmasiny, 1965-2, pp. 24 - 26

27)L. M. Grosev ; Clucajnye Kolebanija pri Dvizenii Zernouborocnogo Kombajna (in Russian) (Random Vibration in Moving of Combine), Mehanizacija i Elektrifikacija, 1969-5, pp. 38 - 39

28)L.A. Liljedahl and J. Strait ; Automatic Tractor Steering, Agric. Engng. June 1962, pp. 332 - 335, 349

29)M. A. Grovum and G. C. Zoerb ; An Automatic Guidance System for Farm Tractor, Transaca. ASAE, 1970, pp. 565 - 576

30)Lal. N. Shukla, C. E. Goering and C. L. Day ; Effect of Tractor Parameters on Automatic Steering, Transacs. ASAE, 1970, pp. 678 - 681

31)A. P. Julian ; Design and Performance of a Steering Control System for Agricultural Tractor, J. agric. Engng. Res. (1971) 16 (3), pp. 324 - 336

32)M. G. R. Wanner and G. O. Harris ; An Ultrasonic Guidance System for Driverless Tractors, J. agric. Engng. Res. (1972), pp. 1 - 9

33)M. B. Widden and J. R. Blair ; A New-Automatic Tractor Guidance

System, J. agric. Engng. Res. (1972) 17 (1), pp. 10 - 21

34)R. L. Parish and C. E. Goering ; Developing an Automatic Steering System for a Hydrostatic Vehicle, Transacs. ASAE, 1970, pp. 523 - 527

35)R. L. Parish and C. E. Goering ; Simulation of an Automatic Steering System for a Hydrostatic Vehicle, Transacs. ASAE, 1971, pp. 450 - 454

36)N. Kawamura, Y. Ikeda and N. Nagasawa ; Fundamental Experiments on the Automatic Steering System of the Head-feeding Type Combine (in Japanese), J. of SAM, Kansai, No. 30 (1971) June, pp. 40-42

37)N. Kawamura, Y. Ikeda, H. Kuroda and K. Matsushima ; Studies of the Automatic Steering Systems of the Head-feeding Type Combine (in Japanese), J. SAM, Kansai, No. 32 (1972) June, pp. 58-60

38)N.Kawamura, Y.Ikeda and Y. Hayashi ; Studies of the Automatic Steering Systems of the Head-feeding Type Combine (Continued) (in Japanese), J. SAM, Kansai, No. 34 (1973) June, pp. 65-68

39)Y. Ikeda and N. Kawamura ; Studies of Automatic Steering System of Combine (in Japanese), (Being contributed to J. SAM)

40)Y. Yasuda H. Kishida I. Tada and T. Oda ; Electro-hydraulic Control of Combine (Part 4 , Automatic Steering System for Head-feeding Type Combine) (in Japanese), Preprint of the 32nd Annual Meeting of SAM, Japan (Yamagata), 1973, p. 29

References in Chapter 2

1) D. E. Burrough ; Power Requirements of Combine Drive, Agric. Engng., Vol. 35 (1954), No. 1, pp. 15 - 18

2) C. Dolling ; Der Drehmoment-und Leistungsbedarf von Mähdrescher-trommeln, Grundl. Landtechn., Heft 6 (1955), pp. 27 - 34

3) C. Dolling ; Der Leistungsbedarf von Mähdreschern, Landtechn. Forschung, Heft 2 (1957), pp. 33 - 44

4) C. Kanafojski ; Theorie, Berechnung und Konstruktion der Landmaschine - 2 Halmfruchterntemaschinen

5) F. Shoji and Z. Yoshida ; Studies on the Distribution of Threshed Materials under the Concave-Sieve of a Threshing Machine with Self-Feeder, J. of SAM, Japan, Vol. 19 (1962), No. 3, pp. 117 - 120

6) F. Shoji and F. Sano ; An Analytical Example on Threshing Process of Threshing Cylinder by High-Speed Camera, J. of SAM, Vol. 19 (1963), No. 4, pp. 167 - 173

*) N. Kawamura, R. Yamashita, M. Nakatani and Y. Ikeda ; Functional Studies of Combine (Part 1) - The Properties of the Power Requirements of Combine - , J. of SAM, Vol.28 (1967), No. 4, pp. 217 - 222

**) N. Kawamura, R. Yamashita, K. Namikawa and Y. Ikeda ; Functional Studies of the Small Combine with Self-feeding Type Thresher (Part 1) - The Power Requirements of the Functional Elements of the Thresher -, J. of SAM, Japan, Vol. 30 (1968), No. 1, pp. 19 - 23

***) N. Kawamura, R. Yamashita, K. Namikawa, Y. Ikeda and M. Yukueda ; Studies on Small Rice Combine of Head Feeding Type, Memoirs of the College of Agric., Kyoto Univ.

No. 99 (1971), pp. 101 - 126

References in Chapter 3

1) H. H. Coenenberg ; Die Belastung von Motor, Fahrgetriebe und Zapfwelle bei Ackerschleppern, Grundl. Landtechn. 16 (1963) pp. 16 - 30

2) V. V. Solodofnikov and A. S. Uskov ; Statisticeskij Analiz Obektov Regulirovanija (Statistical Analysis of Control System) (translated in Japanese) 1960

3) J. S. Bendat and A. G. Piersal ; Measurement and Analysis of Random Data, John Wiley & Sons, 1968

4) G. M. Jenkins and D. G. Watts ; Spectral Analysis and its Application, Holden-Day, 1969

5) M. Eimer ; Möglichkeiten einer festigkeitsgerechten Bewertung von Belastungsaufzeichnungen, Landtechn. Forschung, 2 (1966) pp. 56 - 62

6) J. L. Holloway, Jr. ; Smoothing and Filtering of Time Series and Space Field, pp. 351 - 389

7) A. Horikawa ; Analysis of Random Variation (in Japanese), Kyoritsu Press, 1966

8) C. Dolling ; Der Drehmoment- und Leistungsbedarf von Mähdrescher-trommeln in Feldbetrieb, Grund. Landtechn. 6 (1955), pp.27-34

9) C. Dolling ; Der Leistungsbedarf von Mähdrescher, Landtechn. Forschung, 2 (1957), pp. 33 - 40

*) N. Kawamura, R. Yamashita, M. Nakatani and Y. Ikeda ; Functional Studies of Combine (Part 1) - The Properties of the Power Requirements of Combine - , J. of SAM, Japan, Vol. 28 (1967), No. 4, pp. 217 - 222

**) N. Kawamura, R. Yamashita, M. Nakatani and Y. Ikeda ; Functional Studies of Combine (Part 2 & 3) - Characte-

ristics of the Fluctuating Torques of the Combine Elements and the Ground Contact Pressure Distribution of its Track -, J. of SAM, Japan, Vol. 29 (1967), No. 2, pp. 73 - 76

***) Y. Ikeda, N. Kawamura, R. Yamashita and K. Namikawa ; Functional Studies of the Small Combine with Self-feeding Type Thresher (Part 2) - The Dynamic Characteristics of the Fluctuating Torques of the Functional Elements of the Thresher -, J. of SAM, Japan, Vol.32 (1970) , No. 3, pp. 198 - 202

****) N. Kawamura, R. Yamashita, K. Namikawa, Y. Ikeda and M. Yukueda ; Studies on Small Rice Combine of Head Feeding Type, Memoirs of the College of Agric., Kyoto Univ. No. 99 (1971), pp. 101 - 126

References in Chapter 4

1) I. F. Reed ; Measurement of Forces on Track-Type Tractor Shoes, Transacs. ASAE, 1958, Vol. 1, No. 1, pp. 15 - 18

2) A. S. Sofijan and Ye. I. Maximenko ; The Distribution of Pressure under a Tracklaying Vehicle, J. of Terramecha. 1965, Vol. 2, No. 3, pp. 11 - 16

3) R. Yonekura ; The Contact Pressure Distribution under a Bulldozer, (in Japanese) Excavation Industry, No. 63,1955 pp. 30 - 33

4) V. Guskov ; The Effect of Drawbar Pull on the Rolling Resistance of Track-Laying Tractor, J. of Terramechan.1968 Vol.5, No. 4, pp. 27 - 32

5) G. G. Kolobov ; Soil Pressure Measurements beneath Tractor Tyres, J. of Terramechan. 1966, Vol. 3, No.4, pp. 9 - 15

6) V. V. Kocigin and V. V. Guskov ; The Basic of Tractor Performance Theory, J. of Terramechan. 1968, Vol. 5, No. 3 , pp. 44 - 66

7) D. M. Mitropan, G. I. Shepelenko, A. D. Levitanus and L. T. Tchervonyi ; Issledovanije Davlenya Dvighitelei Kolsnogo i Gusenitchnogo Traktora Klasa 3 Ton na Vlazhnyh Potchvah (in Russian) (Ground Pressure Study of Wheeled and Tracked Tractor of 3 ton Class), Traktory i Sel'khozmashiny, 1966 No. 6, pp. 13 - 15

8) M. G. Bekker ; Introduction to Terrain-Vehicle Systems,The University of Michigan Press (1969), p. 488

9) P. W. Rowe ; A Soil Pressure Gauge for Laboratory Model Research, Proc. ASCE, 569 (1954)

10) O. Kitani ; Fundamental Studies on Tillage Machinery (II),

Soil Stress Meters and Their Faculty and Performance (in Japanese), J. of SAM, Japan, 4 (4),1963, pp. 163 - 170

11)T. Ballstenius and W. Bergau ; Investgation of Soil Pressure Measuring by Means of Cells, Royal Swedish Geotechnical Institute Proceedings, 12 (1956)(requotation from Y. Noziri ; Reliability Improvement on Kyowa Garlson Type Instrument, Kyowa Engng. News, 115, pp. 723 - 726 (1967))

11)'A. I. Brusencev ; Issledovanie Tjagavoj Harakteriictiki Traktora s Bul'dozerom (in Russian) (Study of Traction Characteristics of Track-Type Tractor with Bulldozer), Traktory i Sel'hozmasiny, 1966, pp. 18 - 20

12)E. D. Lwow ; Theorie des Schleppers, 91 VEB Verlag Technik, Berlin, (translated from Russian by W. Stocker) 1954

13)S. Woelk ; Kinematics and Dynamics of a Track Chain, J. Agric. Engng. Res., 13(3), 1968, pp. 168 - 186

14)Hokkaido Prefecture, 1963 ; Report on the Characteristics of Tractor, 55, Hokkaido Prefecture, Sapporo

15)C. M. Harris and C. E. Crede, Shock and Vibration Handbook, MacGraw Hill, 1969

16)G. M. Jenkins and D. G. Watts ; Spectral Analysis and its Application, Holden-Day, 1969

17)J. S. Bendat and A. G. Piersal ; Measurement and Analysis of Random Data, John Wiley & Sons, 1966

18)M. Oshima ; Vibration and Human Body (in Japanese), p.57 Tokyo University Press, 1969

19)J. Mattkews ; Ride Comfort for Tractor Operator, J.Agric. Engng. Res., 1964 (Vol. 9), No. 1, pp. 3 - 31

20)J. O. Wendeborn ; Mechanische Schwingungen auf Ackerschleppern

und ihre Wirkung auf den Fahrer, Grundl. Landtechn. Bd. 19 (1969), Nr. 2, pp. 47 - 55

21) H. Dilg ; Modelbildung und Schwingungsberechnung an Landmaschinen, Arch. für Landtechn. Bd. 8, 1969, Heft 2/3, pp. 81 - 102

22) W. F. Lins ; Vehicle Vibration Analysis Using Frequency Domain Techniques, Transacs. ASME, J. of Engng. for Industry, 1969-11, pp. 1057 - 1086

*) N. Kawamura, R. Yamashita, M. Nakatani and Y. Ikeda ; Functional Studies of Combine (Part 2 & 3) - Characteristics of the Fluctuating Torques of the Combine Elements and the Ground Contact Pressure Distribution of its Track - , J. SAM. Japan, Vol. 29 (1967), No. 2, pp. 73 - 76

**) N. Kawamura, R. Yamashita, N. Namikawa, Y. Ikeda and M. Yukueda ; Studies on Small Rice Combine of Head Feeding Type, Memoirs of the College of Agric., Kyotu Univ., No. 99 (1971), pp. 101 - 126

References in Chapter 5

1) L. A. Liljedahl and J. Strait ; Automatic Tractor Steering, Agric. Engng., June, 1962, pp. 332 - 335, 349

2) M. A. Grovum and G. C. Zoerb ; An Automatic Guidance System for Farm Tractor, Transacs. ASAE, 1970, pp. 565 - 573, 576

3) R. L. Parish and C. E. Goering ; Developing an Automatic Steering System for a Hydraulic Vehicle, Transacs. ASAE, 1970, pp. 523 - 527

4) A. P. Julian ; Design and Performance of a Steering Control System for Agricultural Tractors, J. Agric. Engng. Res., 1971, 16 (3), pp. 323 - 336

5) M.G.R. Warner and G. O. Harris ; An Ultrasonic Guidance System for Driverless Tractor, J. Agric. Engng. Res.,1972, 17(1), pp. 1 - 9

6) M. B. Widden and J. R. Blair ; A New Automatic Tractor Guidance System, J. Agric. Engng. Res., 1972, 17 (1), pp. 10 - 21

7) J. E. Gibson ; Nonlinear Automatic Control, McGraw-Hill, 1963, pp. 355 - 372

8) L. N. Shukla, C. E. Goering and C. L. Day ; Effect of Tractor Parameter on Automatic Steering, Transacs. ASAE, 1970, pp. 678 - 681

9) R. L. Parish and C. E. Goering ; Simulation of an Automatic Steering System for Hydrostatic Vehicle, Transacs. ASAE, 1971, pp. 450 - 456

10) N. Wlener ; Extrapolation, Interpolation and Smoothing of Stationary Time Series, The M.I.T. Press, 1966

11) J. J. Stoker ; Nonlinear Vibrations in Mechanical and Electri-

cal System, Interscience Publishers, 1950

12)C. M. Ludeke ; Nonlinear Phenomena, Transacs. ASME, 1957-4, pp. 439 - 444

13)C. M. Harris and C. E. Crede ; Shock and Vibration Handbook, McGraw Hill

*)N. Kawamura,Y. Ikeda, H. Kuroda and K. Matsushima ; Studies of the Automatic Steering Systems of the Head-feeding Type Combine , J. of SAM,Kansai, No. 30 (1972) June, pp. 58 - 60

**)N. Kawamura, Y. Ikeda and Y. Hayashi ; Studies of the Automatic Steering Systems of the Head-feeding Type Combine (Continued), J. of SAM, Kansai, No. 34 (1973) June, pp. 65 -68

***)Y. Ikeda and N. Kawamura ; Studies of the Automatic Steering System of Combine , J. SAM. Japan,Vol.35(1974), No.4, pp. 368-377

References in Chapter 6

1) R. L. Parish and C. E. Goering ; Simulation of an Automatic Steering System for a Hydrostatic Vehicle, Transacs. ASAE, 1971 pp. 450 - 454

2) I. I. Vodyanik ; The Motion of a Tracked Vehicles on Deformable Ground ; J. of Terramechan., 1966, Vol.3, No. 1, pp.7 - 11

3) F. A. Opejko ; Issledovanie Povorota Gucenitsnogo Samokhoda, (in Russian) (Study on the Steering of Tracked Vehicle) Voprosy Sel'skokhozjajstbennoj Mekhanika, 1970, Tom. 18, pp. 3 - 41

4) A. V. Marav'ev ; Voprosy Teorii Povorota Gusenicn'h Trele-vocnyh Traktorov (in Russian) (Problems of Theories of Skidding Tracked Tractor), Traktory i Sel'hozmasiny, No. 5, 1969, pp. 19 - 21

5) M. Kakikura, K. Sato and M. Yamaguchi ; On the Control of an Industrial Robot with Tactile Sensors (in Japanese), Transacs. SICE, Vol. 7 (1971), No. 1, pp. 31 - 38

*) N. Kawamura, Y. Ikeda, H. Kuroda and K. Matsushima; Studies of the Automatic Steering Systems of the Head-feeding Type Combine, J. of SAM, Kansai, No. 30 (1972) June, pp. 58 - 60

**) N. Kawamura , Y. Ikeda and Y. Hayashi ; Studies of the Automatic Steering Systems of the Head-feeding Type Combine (Continued), J. of SAM, Kansai, No. 34 (1973)

***) Y. Ikeda and N. Kawamura ; Studies of the Automatic Steering Systems of Combine , J. SAM. Japan,Vol.35 (1974), No.4, pp. 368-377